JOHN ALEXANDER VERGARA TORRES

SYNTHESIS AND EVALUATION OF NIOBIUM OR VANADIUM – DOPED HETEROPOLYACID CATALYSTS IN OXIDATION AND ACETALIZATION REACTIONS OF ALCOHOLS AND ALDEHYDES DERIVATED OF BIOMASS

Dissertation submitted to the Agrochemistry Graduate Program of the Universidade Federal de Viçosa in partial fulfillment of the requirements for the degree of *Magister Scientiae*.

Adviser: Márcio José da Silva

VIÇOSA - MINAS GERAIS
2022

Ficha catalográfica elaborada pela Biblioteca Central da Universidade Federal de Viçosa - Campus Viçosa

T
V494s
2022

Vergara Torres, John Alexander, 1997-
Synthesis and evaluation of Niobium or Vanadium – doped heteropolyacidcatalysts in oxidation and acetalization reactions of alcohols and aldehydesderivated of biomass / John Alexander Vergara Torres. – Viçosa, MG, 2022.
1 dissertação eletrônica (132 f.): il. (algumas color.).

Texto em inglês.
Inclui anexos.
Orientador: Márcio José da Silva.
Dissertação (mestrado) - Universidade Federal de Viçosa, Departamento de Química, 2022.
Referências bibliográficas: f. 104-125.
DOI: https://doi.org/10.47328/ufvbbt.2022.138
Modo de acesso: World Wide Web.

1. Furaldeido. 2. Terpenos. 3. Esterificação. 4. Oxidação. I. Silva, Márcio José da, 1965-. II. Universidade Federal de Viçosa. Departamento de Química. Programa de Pós-Graduação em Agroquímica. III. Título.

CDD 22. ed. 547.27

Bibliotecário(a) responsável: Renata de Fátima Alves CRB6/2578

JOHN ALEXANDER VERGARA TORRES

SYNTHESIS AND EVALUATION OF REPLACED HETEROPOLYACIDS WITH NIÓBIUM AND VANADIUM IN OXIDATION AND ACETALIZATION REACTIONS OF ALCOHOLS AND ALDEHYDES DERIVATES OF BIOMASS

Dissertation presented to the Federal University of Viçosa, as part of requirements of the Agrochemistry Postgraduate Program, to obtain the Magister Scientiae title.

APROVED: February 18, 2022.

Assent:

John Alexander Vergara Torres
Author

Márcio José da Silva
Advisor

“For everyone who believed in me and didn't, "Everything is possible if you believe in yourself"

ACKNOWLEDGEMENT

I want to thank God for taking me by the hand on this path.

I thank my mom, grandmother and other angels in heaven for keeping me by the hand on this path

I thank my advisor Márcio Jóse da Silva for having welcomed me, for having been an excellent guide, for having shared his knowledge with me, for having become a guide. Colleague and friend for my life.

I thank Professor Natalia for being the one who believed in me to start this process, and for being the manager of my professional and personal progress.

. I thank my father for being my support and my motivation for continuous professional and personal growth.

To my brother Camilo for always being there when advice, a hug from a distance, or any kind of help was needed, to him and Jessica for giving me the best energy and motivation over the years, Salvador.

To my sister Maria for her constant support and accompaniment during my ups and downs during this process, and for my second niece Dulce.

To the Torres family, especially my uncle Alex, my aunt ledy and my grandmother, for always giving me a home, a safe place, a refuge and for always being my support and company. And for giving me my goddaughter Ivanna.

To the Vergara for taking care of my dad while I couldn't, for giving him love and company, helping him, is giving me love.

I thank love for knocking on my door in an inexplicable way, and staying to watch me grow.

I thank my laboratory colleagues, especially Paloma, Alana, Xuxu, Daniel and Claudio for becoming friends and for their constant help throughout this time.

To my colleagues and friends Debora, Ueslei, Adriane and others for the love, help and experiences during this time.

To my friends in viçosa, especially Bruno, Diego, Larissa and other who came along the way, for making my days calmer and accompanying me to grow and enjoy life.

To my best friends Rafa and Karen for always being there, in every possible way, for so many years

I thank the evaluators bank for agreeing to be my evaluator and for the knowledge shared during this experience.

To the Federal University of Viçosa, for the opportunity to complete the postgraduate course.

This study was financed in part by the Coordenação de Aperfeiçoamento de Pessoal de Nível Superior – Brasil (CAPES) – Finance Code 10611275854.

To the Conselho Nacional de Desenvolvimento Científico e Tecnológico (CNPq), for granting the scholarship.

To the Fundação de Amparo à Pesquisa do Estado de Minas Gerais (FAPEMIG), for granting the scholarship.

To the Coordenação de Aperfeiçoamento de Pessoal de Nível Superior (CAPES), to granting the scholarship.

“The only place success comes before work is in the dictionary”

(Albert Einstein)

ABSTRACT

VERGARA,Torres John Alexander, M.Sc., Universidade Federal de Viçosa, February, 2022. **Synthesis and evaluation of Niobium or Vanadium – doped heteropolyacid catalysts in oxidation and acetalization reactions of alcohols and aldehydes derivated of biomass**. Adviser: Marcio Jose da Silva.

Aldehydes derived from biomass and terpene alcohols are abundant raw materials, of plant origin, and of interest for production of fine chemicals products, such as fragrances, pharmaceuticals and agrochemicals. Recently, for economic and environmental reasons, catalytic processes have been developed to transform these renewable resources into chemical products with higher added value. In this work, heteropolyacids (HAPs) obtained from phosphomolybdic acid doped with 1, 2, and 3 mol of Niobium (i.e., $H_4PMo_{11}Nb_1O_{40}$, $H_5PMo_{10}Nb_2O_{40}$ and $H_6PMo_9Nb_3O_{40}$) were synthesized and evaluated as catalysts in oxidation and acetalization reactions of aldehydes present in the biomass. Niobium- doped HAPs were synthesized from different precursors: MoO_3, Nb_2O_5, H_3PO_4. Furthermore, HAPs obtained from the doping of phosphomolybdic acid with Vanadium were applied in oxidation reactions of terpene alcohols by hydrogen peroxide in acetonitrile solutions. The synthesis procedures used proved to be efficient, since the catalyst were obtained with satisfactory yields. All synthesized acids were characterized by infrared spectroscopy analysis, ultraviolet-visible spectroscopy, thermal analysis, surface area and porosimetry, X-ray diffraction, and potentiometric titration. The catalytic activity of HAPs was evaluated in different oxidation and acetalization reactions. The Nb-doped HAPs were evaluated in oxidative esterification reaction of furfural, chosen as a model substrate due to its reactivity and industrial interest. In addition, they were also evaluated in acetalization reaction. In this reaction, the amount of Nb does not seem to have produced a significant difference in terms of conversion and selectivity. Furthermore, most of the catalytic tests were performed with $H_6PMo_9Nb_3O_{40}$ obtaining conversion of approximately 50% and 2-furfuraldehyde-methylacetal as the only product. The concentration of 0.0312 mol % of catalyst presents the best catalytic activity. Finally, the reaction was extended to benzaldehyde, obtaining similar results. Tests performed with Vanadium-doped catalysts showed that $H_4PMo_{11}VO_{40}$ was the most active and selective in the oxidation of geraniol (the substrate chosen as model

terpene alcohol) toward geraldehyde, mono and diepoxide, with epoxide being the major product. Conversion greater than 94% was obtained with selectivity between 80 and 85% for epoxide geraniol. $H_4PMo_{11}VO_{40}$ has also been tested in the oxidation of other terpene alcohols, and has been shown to be active in the oxidation of nerol.

Keywords: Furfural. Terpene alcohols. Keggin Heteropolyacids. Oxidative esterification

RESUMO

VERGARA,Torres John Alexander, M.Sc., Universidade Federal de Viçosa, fevereiro de 2022. **Synthesis and evaluation of Niobium or Vanadium – doped heteropolyacid catalysts in oxidation and acetalization reactions of alcohols and aldehydes derivated of biomass**. Orientador: Marcio José da Silva.

Aldeídos derivados da biomassa e álcoois terpênicos são matérias-primas abundantes, de origem vegetal, e de interesse para a síntese de produtos da química fina, como fragrâncias, fármacos e agroquímicos. Recentemente, por razões econômicas e ambientais, processos catalíticos têm sido desenvolvidos visando transformar esses recursos renováveis em produtos químicos de maior valor agregado. Neste trabalho, heteropoliácidos (HPAs) obtidos a partir do ácido fosfomolíbdico dopado com 1, 2 e 3 mols de Nióbio (i.e., $H_4PMo_{11}Nb_1O_{40}$, $H_5PMo_{10}Nb_2O_{40}$ e $H_6PMo_9Nb_3O_{40}$) foram sintetizados e avaliados como catalisadores em reações de oxidação e acetalização de aldeídos presentes na biomassa. Os HPAs de Nióbio foram sintetizados a partir de diferentes precursores: MoO_3, Nb_2O_5, H_3PO_4. Além disso, HPAs obtidos a partir da dopagem do ácido fosfomolíbdico com Vanádio foram aplicados em reações de oxidação de álcoois terpênicos por peróxido de hidrogênio em soluções de acetonitrila. Os procedimentos de síntese utilizados mostraram-se eficientes, uma vez que os catalisadores foram obtidos com rendimentos satisfatórios. Todos os ácidos sintetizados foram caracterizados por análises de espetroscopia no infravermelho, na região do ultravioleta-visível, análises térmicas, de área superficial e porosimetria, difração de raios-X, e titulação potenciométrica. A atividade catalítica dos HPAs foi avaliada em diferentes reações de oxidação e acetalização. Os HPAs dopados com diferentes quantidades de Nb foram avaliados em reações de esterificação oxidativa do furfural, escolhido como substrato modelo devido à sua reatividade e interesse industrial. Além disso, eles foram também avaliados em reações de acetalizaçao. Nessa reação a quantidade de Nb parece não ter produzido diferença significativa em termos de conversão e seletividade. Ademais, a maior parte dos testes catalíticos foram realizados com $H_6PMo_9Nb_3O_{40}$ obtendo aproximadamente 50 % de conversão e 2-furfuraldeído-metilaceta como único produto. A concentração de 0.0312 mol % de catalisador apresento a melhor atividade catalítica. Finalmente, a reação foi estendida a benzaldeído obtendo resultados similares. Os testes realizados com os catalisadores

dopados com Vanádio mostraram que $H_4PMo_{11}VO_{40}$ foi o mais ativo e seletivo na oxidação do geraniol (substrato escolhido como álcool terpênico modelo) para geraldeído, mono e diepóxido, sendo o epóxido o produto majoritário. Foi obtida conversa maior a 94% com seletividade entre 80 e 85 % para o geraniol epoxido. O $H_4PMo_{11}VO_{40}$ também foi testado na oxidação de outros álcoois terpênicos, e mostrou-se ativo na oxidação de nerol.

Palavras-chave: Furfural. Álcoois terpênicos. Heteropoliácidos de Keggin. Oxidação esterificativa.

LIST OF ILLUSTRATIONS

LIST OF TABLES

LIST OF ACRONYMS AND ABBREVIATIONS

POMs = Polyoxometalates

HAPs = Heteropolyacids

FT-IR = Fourier transform infrared spectroscopy

ATR = Attenuated total reflectance technique

SMSI = Strong metal-support interaction

STA = Simultaneous Thermal Analyzer

BET = Brunauer, Emmet and Teller method

TG = Thermogravimetry

UV-Vis = Ultraviolet visible spectroscopy

XDR = X-rays diffraction

CG = Gas chromatography

MS = Mass Spectrometer

FID = Flame ionization detector

Ea = Activation energy

$\bar{V}_{ass}$ = Asymmetric stretch

PTSA = *p*-toluenosufonic acid

PND = Products not detected by GC analysis

FMD = 2-furfuraldehyde-methylacetal

5-HMF = 5-hidroximethyl-furfural

LMTC = Ligand to Metal Charge Transfer Transitions

SUMMARY

1. GENERAL INTRODUCTION

1.1 Catalysis basics concepts

Catalysis is a process in which chemical reactions are accelerated by using small amounts of substances called “catalysts”. A catalyst can enhance the speed of a thermodynamically feasible reaction but cannot affect the thermodynamic equilibrium position (KNÖZINGER; KOCHLOEFL, 2003). For chemical reactions to take place, the molecules must collide with each other, in suitable orientations allowing the breaking of existing bonds and the formation of new bonds. These collisions must have an equal to or greater energy than the minimum necessary energy to initiate the chemical reaction (Activation energy (Ea))(ATKINS, DE PAULA, 2012). The activation energy is the barrier energy between the reagents and the transition state.

The catalytic reactions are cyclical processes, in which the reactants are converted to products with the participation of a catalyst, passing through an activated complex, regenerating the catalyst at the end of the process. The presence of catalyst provides a reaction pathway in which the energy required for the reactant to be converted to a product is lower than that will be necessary without its presence.

Figure 1 shows that the difference of energy between reagents and products is the same in the catalyzed and not catalyzed processes (Gibbs free energy). It means that the catalysts affect the reaction kinetic but not thermodynamical equilibrium (SCHOBERT, 2010;ATKINS,DE PAULA,2012).

The catalytic processes are classified as homogeneous, in which the reactants and catalyst are in the same phase, and heterogeneous, where catalyst and reactants are in distinct phases.

Figure 1 - Typical diagram for catalyzed and uncatalyzed exothermic reactions.

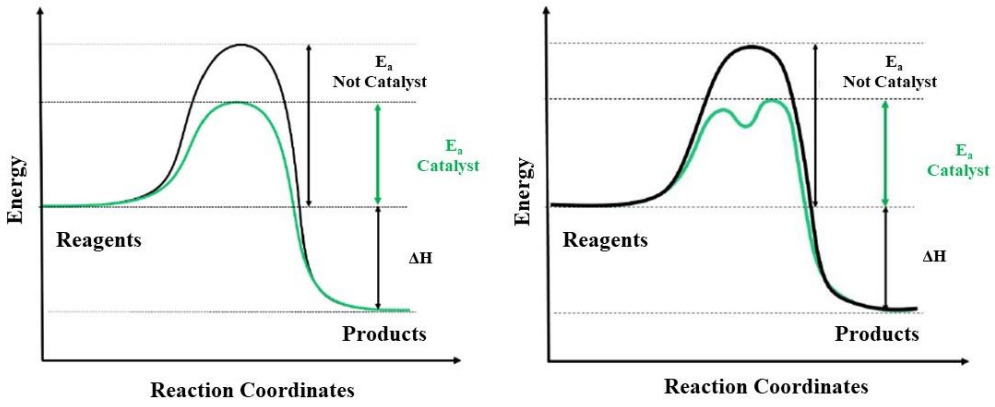

Adapted from: ATKINS, DE PAULA, 2012

More than 90 % of industrial chemical processes are catalytic, showing the importance of catalysis in different industries such as petrochemical, biochemical, polymers, agrochemical, and pharmaceutics ones (BERNARDO-GUSMÃO; PERGHER; DOS SANTOS, 2017). Due to their possible reusability heterogeneous catalyst embrace almost 74 % of the industry. However, homogeneous catalysts are used to generate value-added products in different sectors of fine chemicals.

The increase in the use of catalytic processes in different chemicals industries, on which the advancement of our humanity depends, shows the importance of the study and development of new catalysts, and the challenges to obtaining greater reliability and profitability in their applications(TONIATO; VAUCHER, 2021).

Exist a great variety of catalysts with different structures, proprieties, and industrial applications. Ones of the most studied and that has attracted significant

attention are the polyoxometalates (POMs), due to their versatility, acidic properties, easy synthesis, well know characterization, and various applications (GARCÍA-LÓPEZ et al., 2019; CORONEL; DA SILVA, 2018; DA SILVA et al., 2016).

1.2 Polyoxometalates

The application of POMs in catalysis has been goal studied in several works. POMs are metal-Oxygen clusters with great versatility that combines redox and acid catalytic proprieties (KOZHEVNIKOV, 1998). POMs are classified into two classes; the first, isopolyoxometalates, containing only transition metal cations and oxide anions, and the second one, heteropolyoxometalates, having p or d block elements. This late classification includes heteropolyacids (HPAs), which are the goal of this present work (LONG; TSUNASHIMA; CRONIN, 2010).

The general structural formula of POMs is $[X_xM_mOy]^{q-}$, where X^n is a heteroatom normally of the group 14 or 15 (example: Si^{4+} , Ge^{5+}, P^{5+},As^{5+}), M is an atom of metal usually from d block in the periodic table (example: V^{+4}, V^{+5}, Nb^{+5}, Mo^{+6} or W^{+6}) and q represent the anion charge, where q = 8-n, and n is the heteroatom valence X. The different classic types or POMs are shown in Figure 2.

Figure 2 - polyoxometalates (POMs) classic structure.

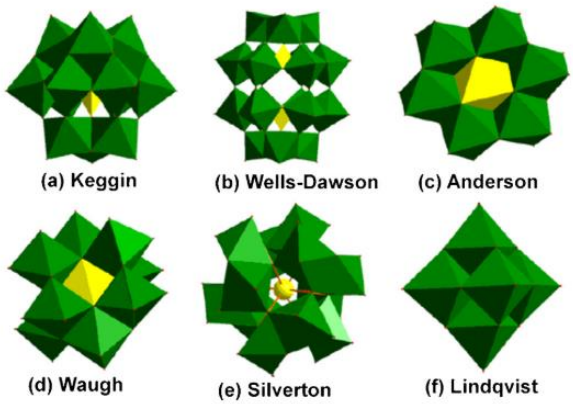

Source: adapted from OMWOMA et al., 2015.

1.3 Keggin heteropolyacids

Heteropolyacids (HPAs) are attractive catalysts due to their great thermal stability, combined with their extensively flexible molecular proprieties. Furthermore, they are easily synthesized, and their acidity proprieties are easily adjustable through structural changes. It modifies their physical properties, allowing that they can be used as catalysts in homogeneous or heterogeneous phases (HILL; PROSSER-MCCARTHA, 1995).

One of the most studied and well-characterized types of HPAs are those with Keggin structure anion, which are stable, versatile, and have strong Brønsted acid proprieties (J. DA SILVA; A. LIBERTO, 2015). The strength of acidity of the HPAs acidity can be modified by the protons exchanging in their structure, or by the replacement of addenda atoms present in the Keggin anion (i.e., W, Mo, V) (VILLABRILLE et al., 2004).

Their basic structure is shown in Figure 3. The Keggin HPAs structure $(XM_{12}O_{40})^{n-}$ is formed by one tetrahedral (XO_4) containing a heteroatom X (X = P^{+5}, Si^{+5}), which is surrounded by twelve edge- and corner-sharing metal-oxygen octahedral (MO_6. M= W^{+6}, Mo^{+6}).

Figure 3 - Primary and secondary structure of Keggin HAPs.

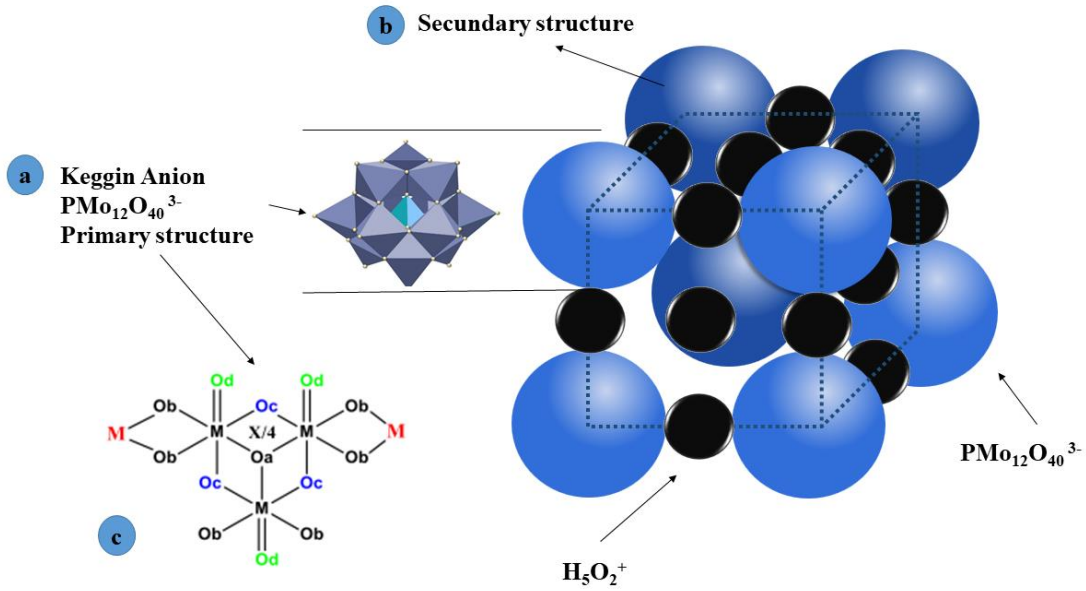

Source: adapted from (DA SILVA et al., 2016).

The MO_6 octahedral are attached in four groups M_3O_{13} and connected by common edges and vertices of the central tetrahedron (NARKHEDE; SINGH; PATEL, 2015; MIZUNO, 2009).

The primary structure (i.e., Figure 3a) is formed by the heteropoly anion, which is the fundamental unit of HPAs. These units are linked to each other forming the secondary structures (Figure 3b). Besides that, in the secondary structure, hydrogen bonding connects the dihydrogen cation ($H_5O_2^+$) to terminal Oxygen atoms. It means the amount of hydration and/or counteractions water affects the crystallographic structure of Keggin anions (DA SILVA; DE OLIVEIRA, 2017a; PAQUIN et al., 2015; MICEK-ILNICKA, 2009)

Secondary structure is described for differences Oxygen atoms, classified in four different types, with equivalent symmetry. In Figure 3c, the Oxygens called Oa are internal Oxygens linked to the central tetrahedron with four triads of octahedrons MO_6.

Oxygen Ob binding the Mo_3O_{13} groups through the vertices, Oxygen O_c binding the octahedra across the edges to form triads and the terminal oxygens O_d. In addition, protons distribution and physical proprieties like particle size, texture and uniformity porous and chemical properties depend on the tertiary structure (DA SILVA; DE OLIVEIRA, 2017b).

HPAs have attracted great interest in catalysis due to their large variety of composition, electronic properties, and structure, which make them versatile catalysts in different types of reactions (PATEL et al., 2016). Due to their high Brønsted acidity, they have been used mainly in acid-catalyzed reactions. However, Keggin HPAs have interesting redox properties that also allows their use like oxidation reaction catalysts (FARSANI et al., 2014). Some examples are of acid-catalyzed reactions that are effectively promoted by Keggin catalysts are esterification and transesterification (ALSALME; KOZHEVNIKOVA; KOZHEVNIKOV, 2008), hydrolysis (GARCÍA-LÓPEZ et al., 2019), acylation and alkylation of Friedel-Crafts (KABA; SONG; BARTEAU, 1997). Conversely, various substrates are effectively oxidized in the presence of HPA catalysts, such as alkanes, aromatics, alcohols and olefins, mainly using hydrogen peroxide as an oxidant (CORONEL et al., 2019; VILANCULO et al., 2019).

HPAs are thermally stable, another important characteristic to be highlighted because it allows that they can be used as solid catalysts in reactions carried out at vapour-phase, and reactions in liquid phase conducted at high temperatures (SCHLÖGL, 2015). Nevertheless, HPAs are solids with low surface area (1 to 5 m^2g^{-1}). Moreover, they are soluble in water, alkyl alcohols and other polar compounds (LEE; LEE, 2014)

Keggin HPAs and their derivatives can be easily obtained through various synthesis processes. Modifications in the structure of HPAs like switching the protons

by cations with large ionic radium or even organic cation (KNÖZINGER; KOCHLOEFL, 2003), change properties of the catalyst such as surface area, thermal stability, and solubility. Furthermore, allowing the catalyst to go from homogeneous to heterogeneous phase (J. DA SILVA; A. LIBERTO, 2015).

HPAs are acids formed by the combination of heteropoly anions and protons, the negative charge of the heteropoly anion is distributed over the atoms that make it up, this generates a low density of charge on the spheric surface. The presence of M=O bonds polarizes the negative charge in the Oxygen, for the positive metal atoms inside the structure, allowing a better delocalization of charge over the anion surface. This charge delocalization in the heteropoly anions, makes the heteropoly acids have high Brønsted acidity, normally greater than sulfuric acid (ROMANELLI et al., 2005).

Perhaps the most important property of the HPAs is the acidity strength, which is the principal factor in the acid-catalysts reaction. There are different techniques to measure the HPAs acidity strength (REDDY et al., 2006). Timofeeva (TIMOFEEVA, 2003) obtained the pKa values of the HPAs in different solvents by potentiometric titration curves.

The following trend $H_3PW_{12}O_{40}$ > $H_3PMo_{12}O_{40}$ > $H_4SiW_{12}O_{40}$ was always observed no matter the changes in the chemical composition of the HPAs, although the pKa values depended on the solved employed (HU et al., 1993).

The development of catalysts at the molecular or at an atomic level has long been pursued, due to the multifunctional catalysts with precise design are desirable for many applications. Nevertheless, the development of catalysts at this level is a difficult goal in many instances (MISONO, 2001). Despite their easy synthesis of HPAS allows building catalysts with multicenter sites that improve their performance, for the

reliability of the procedures, both precursors and catalysts must be well characterized (NOMIYA et al., 2000).

One of the advantages of the HPAs is that their catalytic proprieties can be tuned easily by changing the identity of the centra heteroatom, counter cation and framework addenda atoms (SCHLÖGL, 2015).

1.4 Keggin HPAs derivate compounds

1.4.1. Vanadium HPAs compounds

Among the HPAs varieties, phosphomolybdic acid ($H_3PMo_{12}O_{40}$) has been widely used, due to its strong acid strength and oxidation potential (SHEN et al., 2012). The substitution effect of one or more Mo units by atoms like V or Nb, which increases the catalytic activity of HPA and modified their acidity and thermal stability, has widely studied and reported in the literature (ROCCHICCIOLI-DELTCHEFF; FOURNIER, 1991; SUN et al., 2008; COLOMBO MIGLIORERO et al., 2021). This partial substitution could be localized in two different positions: cationic (counter ions) or anionic (inside the heteropolyanion) (NOMIYA et al., 2000) (Figure 4).

Figure 4 - Scheme of the heteroatom localization in the heteropolyacids partial substitution.

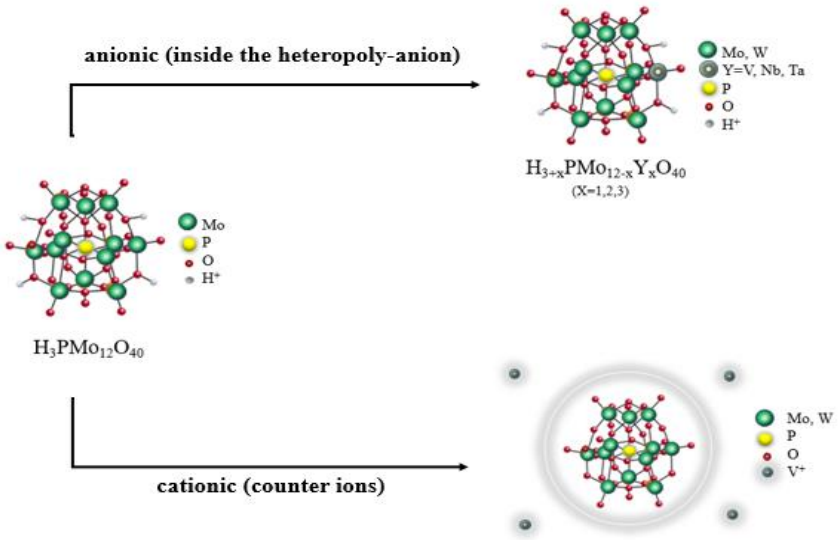

Source: Own authorship.

It has been reported that the introduction of Vanadium enhances the oxidation catalysts of the HPAs, the bi-functional character of molybdophosphoric acids substituted with Vanadium ($H_4PMo_{12}VO_{40}$) show unique catalytic features for oxidation, due to the redox nature of Vanadium and de acid and oxidation character of $H_3PMo_{12}O_{40}$ (PALERMO et al., 2011). The energy of the lowest unoccupied molecular orbital (LUMO) that involves the binding Oxygen and the *d*-Orbitals of the framework metals, may be changed by metal substitution. The *d*-Orbitals of Vanadium have been assumed to be more stable than *d*-orbitals of Molybdenum and Tungsten, for this reason, the LUMO is stabilized by the substitution of Vanadium into the Molybdenum framework (PARK et al., 2010a).

Supported polyvanadates, monovanadates and V_2O_5 were studied in the oxidation reaction of furfural to maleic acid in the gas phase; those authors verified that the polyvanadates were more actives than the other catalysts (ALONSO-FAGÚNDEZ et al., 2012).

Molybdo(vanado)phosphoric HPAs supported on oxides of Si, Ti and Al were used in oxidation reactions of ethane to acetic acid in high temperatures and was verified that with an introduction of Vanadium into the HPAs the oxidation activity was improved. However, the conversion decreased when the vanadyl groups occupied the cationic positions (HERAVI; VAZIN FARD; FAGHIHI, 2013). Another oxidation reaction was the conversion of benzene to phenol by Vanadium-substituted phosphomolybdic acid (TANG; ZHANG, 2006), which was carried out in the liquid phase in presence of H_2O_2 oxidant (ARICHI; ETERNOT; LOUIS, 2008). Thus, it can be inferred that metals (V, Nb, Ta)-containing HPAs would be excellent catalysts in oxidation reactions.

1.4.2. Niobium HPAs compounds

Niobium is a metal that has been used for the preparation of different types of catalytic materials, being widely studied in homogeneous and heterogeneous oxidation reactions (ZIOLEK; SOBCZAK, 2017; TANABE, 2003; ZIOLEK, 2003). In addition, Nb compounds exhibit specific properties that their neighbouring elements in the periodic table do not show. The most important is the stability of strong metal-support interaction (SMSI), which is important for a good quality catalyst (ZIOLEK, 2003). Another relevant factor of the Nb is its location in the periodic table belongings to the same period as Mo and to V group, indicative that radium and other chemical properties should be similar.

A wide variety of catalytic studies has been developed with the use of Nb as catalysts. Oxidative dehydration reactions of propane and ethane as olefin production routes using mixed oxides composed of M-O-V doped with Nb obtained good results(BAROI; GAFFNEY; FUSHIMI, 2017) are a good example. A similar effect was observed for VOx supported in NiO and doped with Nb, showing that the incorporation of Nb increases the catalytic activity (BOTELLA et al., 2009). Ce-Nb-Ti catalysts were also synthesized for selective catalytic reduction of NO with ammonia, achieving catalytic improvements with Nb incorporation (MA et al., 2021). Nb catalysts ($NbCl_5$, $Nb(OEt)_5$), mesoporous Niobium silicate, $Nb(Cp)_2Cl_2$ on silica) were used in oxidations of alkenes (IVANCHIKOVA et al., 2015) and sulfides (KIRIHARA et al., 2009) with hydrogen peroxide. Finally, some studies show that Nb_2O_5 is mainly used as support for HAPs (DA CONCEIÇÃO et al., 2017).

Recently, Yang et al. (YANG et al., 2019) prepared multilayer POMs ($HNbMo_6$) by calcining stoichiometric amounts of Li_2Co_3, Nb_2O_5 and MoO_3 using the acid catalyst for 5-hidroxymethylfurfural esterification. Keggin and Wells-Danson HPAs were replaced with a member from group 5 (V = V, Nb, Ta) of the periodic table to prove their catalytic capacity in acetic acid esterification with ethanol in the vapour phase, showing catalytic activity increases with acidity increasing (PARK et al., 2010b). Okumura et al. (OKUMURA et al., 2007) showed that in the formation processes of their mixed acid catalyst H_3PO_4-WO_3-Nb_2O_5 there was a spontaneous formation of Keggin- type mixed heteropolyacid $H_4PNbW_{11}O_{40}$, demonstrating good catalytic activity in the Friedel-crafts acylation of anisole with carboxylic acids.

Redox properties and catalytic oxidation activities of $H_{3+n}PW_{12-n}M_nO_{40}$ substituted with different poly-atoms (M= V, Nb, Ta, and W; n = 0, 1, 2 or 3) were examined by electrochemical methods and measurements in UV-Vis spectroscopy. It

was observed a reduction potential catalysts increase and UV-vis absorption edge energies decrease with decreasing electronegativity in the poly-atom (PARK et al., 2009). Catalysts made from $NaHPO_4$, Na_2WO_4, $NbCl_5$ with later acidification, were tested in the oxidation of benzyl alcohol to benzaldehyde in the vapour phase, showing an increase in the yield for benzaldehyde formation with the increasing of reduction potencies and decrease in the absorption at the edges energies of HAPs (PARK et al., 2010a). Park et al (PARK et al., 2011) prepared $H_{3+x}PW_{12}Nb_xO_{40}$ HPAs catalysts with different amounts (x= 1, 2 and 3) of Niobium showing that this type of catalyst has a preference for oxidation reactions obtaining better activities and that the mono-substituted Nb catalyst is more stable.

In this work, HPAs derived from phosphomolybdic acid were synthesized containing Nb or V as dopant, characterized, and evaluated in reactions of oxidation of terpene alcohols, acetalization of furfural and benzaldehyde.

1.5 Catalysts and Biomass

Organic substance coming from the photosynthesis process is considered biomass, more generally, biomass could be considered a combination of naturally derived materials, coming from plants, as well as all the materials composed of the organic matrix, except plastics. The most important biomass sources are animals residues, agricultural residues and aquatic crops (TURSI, 2019) (Figure. 5).

Figure 5 - Most important biomass sources.

Source: adapted from (TURSI, 2019).

The biomass composition is diverse, depending on its origin. However, the cellulosic biomass composition can be mainly described by cellulose (38 % - 50 %), hemicellulose (23 % - 32 %), and lignin (15 % - 25 %). Into the hemicellulose is find a large number of polysaccharides, which are used as raw materials in different processes in the chemical industry (MCKENDRY, 2002).

Environmental concerns, proposals for sustainable growth and the trend towards depletion of fossil fuels, are some of the reasons that searching for alternatives to the production of energy and renewable fuels is important (AXELSSON et al., 2012).

Residues and derived of the biomass transformation process have achieved great attention in recent years, it due to that they generate alternatives with good potential to produce fine chemical derivatives and renewable fuels, which are options for not use of fossil oil. Besides that, they constitute a raw natural renewable material with low cost, after the chemical transformation process or in their natural form (CORMA CANOS; IBORRA; VELTY, 2007). One of the most important catalysts applications is biomass transformation into higher value-add products.

1.6 Terpene alcohols

Monoterpenes are naturally occurring, abundant and renewable compounds in nature, making them a low-cost raw material, it is present in most plants, being one of the main components of essential oils. it generally has a pleasant smell; Besides that, monoterpenes are also by-products of cellulose production, mainly α and β-pinene (YOO; DAY, 2002). These characteristics make them attractive for the fine chemical and pharmaceutical industry (GALLEZOT, 2007).

Monoterpenoids, derivatives of oxygenated monoterpenes, are important for the industry. (DA SILVA et al., 2013). Terpene alcohols are functionalized products derived from terpenes, which are classified according to the number of carbons in their structure (DEGENHARDT; KÖLLNER; GERSHENZON, 2009; SANCHEZ-MARTINEZ et al., 2021). Especially, terpene alcohols such as nerol, geraniol, and β-citronellol, are valuable raw materials in the agrochemical, perfume and pharmaceutic industries (DA SILVA; JULIO; DOS SANTOS, 2015).

The main source of terpene alcohols in nature is in wood and plants extractions, they are ones of the main essential oil's constituents, being essentially responsible for the characteristic smell, into their characteristics are the high viscosity, volatility, water immiscibility, in addition, most of them are liquid at room temperature. Figure 6 show the terpene alcohols (BELSITO et al., 2008).

Figure 6 - Terpene alcohols.

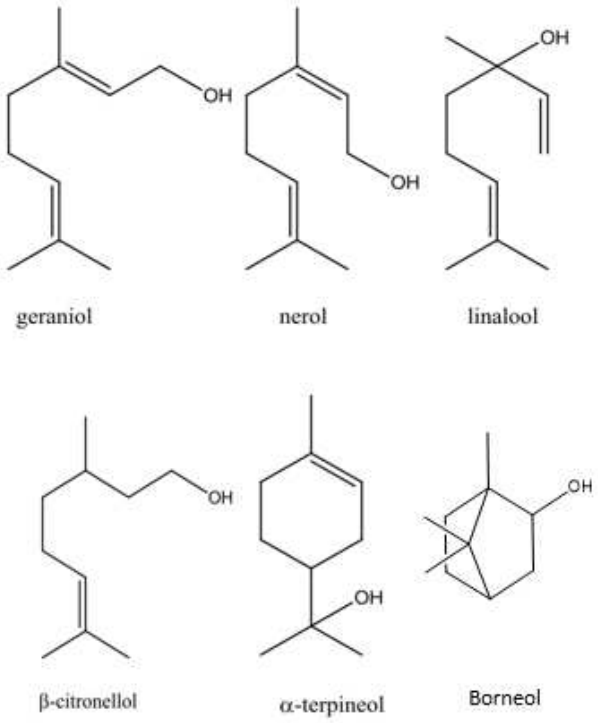

Source: Own authorship.

Terpene alcohols are principally used in flavour ingredients and the perfume industry, in addition, they can be found in cosmetics, shampoos, household cleaners (BELSITO et al., 2008). Finally, it is important to say, that Brazil is one of the main exporters of essential oils in the world, being one of the largest exporters of its citrus derivatives, and having a great variety of studies on the extraction process and its use (BIZZO; ANA MARIA; REZENDE, 2009; LINDE et al., 2016).

1.6.1 Terpene alcohols and oxidation reactions

Oxidation reactions of terpene alcohols are widely used in laboratories and industry, due to their carbonylic derivatives which have important organoleptic proprieties, making them an ingredient to fragrance and perfumes (DA SILVA; CARARI; MANOEL DA SILVA, 2015). In addition, Epoxides are a key intermediate in the manufacture of different value-added products (DUSI; MALLAT; BAIKER, 2000).

The selectivity control of the terpene alcohols oxidations is one of the main challenges, mainly why the substrate can react in different ways. The hydroxyl group and its double bond could be oxidate, depending on the oxidation attack mode, resulting in both oxidation cleavage and epoxidation (CÁNEPA et al., 2013).

Another problem is that oxidants are used in stoichiometric quantities, these oxidants are normally toxic and corrosives, they often need a separation step to isolate the product to the solvent. Furthermore, many studies are described involving the use of palladium, platinum, and ruthenium catalyst, these types of catalysts are expensive and environmentally aggressive (VIANA; DA SILVA; DA SILVA, 2018; DA SILVA; TEIXEIRA; CARARI, 2009; DENICOURT-NOWICKI et al., 2019).

In this work hydrogen peroxide was used as a green oxidant, due to its secondary reaction product is water, heteropoly acids were investigated like a catalyst and the terpene alcohols oxidations reactions were studied due to terpene alcohols being selective substrates, all these alcohols have double bonds which could be functionalized through epoxidation.

1.7 Furfural

Biomass is an important resource of carbon structures, that can be considered raw material. Among the different types of biomasses, monomers of lignocellulosic biomass have received important attention because it can generate platform-molecules such as furfural and 5-HMF (Figure 7), which are desired products to replace numerous chemicals fine in the biorefinery industry (STEPAN et al., 2018). These products are synthesized by dehydration reactions of sugar residues (CORMA CANOS; IBORRA; VELTY, 2007). However, furfural is more attractive because it is principally obtained on large scale from agriculture waste while HMF is only produced on small scales from sugar dehydration (LI et al., 2017b; PELETEIRO et al., 2016)

Figure 7 - Structural form of furfural and 5-hydroxymethylfurfural.

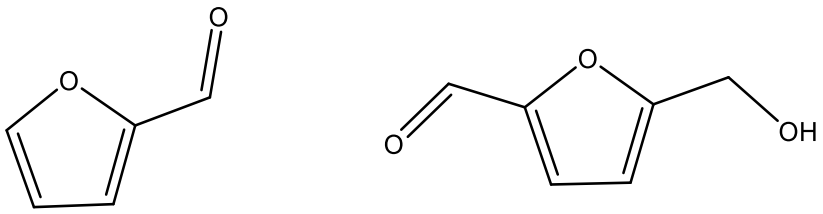

furfural 5-hydroxymethylfurfural

Source: Own authorship

Furfural is obtained from xylans presents in the hemicellulose through the acid-catalyzed reactions. Xylenes undergo acid hydrolysis to form xylose, whose cyclodehydration gives rise to furfural Figure 8 (AXELSSON et al., 2012). Furfural is principally used for the production of polymers, for the refining of diesel fuels, agrochemical, and as a chemical intermediate in the production of methyl tetrahydrofuran and tetrahydrofuran, which are used as solvents (BIZZI et al., 2019).

These characteristics and its variety of applications in the chemical industry make furfural an attractive compound to be studied.

Figure 8 - Obtention of furfural from hemicellulose.

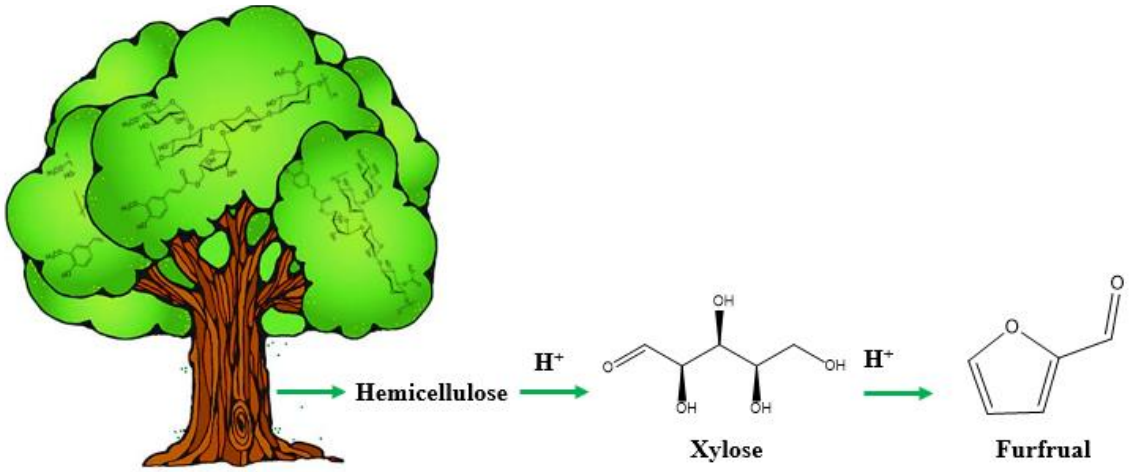

Source: Own authorship.

1.7.1 Furfural reactions.

Due to the aldehyde present within the furfural structure, this compound exhibits all the typical aldehyde reactions like acylation, acetylation, aldol, reductions, decarboxylation, oxidation to carboxylic acids. Besides that, alkylation, oxidation, hydrogenation and other reactions can be carried out in the furan ring (REED; KWOK, 2014).

Among all the possible reactions that can be carried out with furfural, acetalization reactions have received high attention because furfural acetals are useful as bioadditives and in the synthesis of perfumes, pharmaceuticals, solvents, flavours and polymers (WEINGARTEN et al., 2010). Normally, acids such as H_2SO_4 and HCl are used as a catalyst in the acetalization reactions, although, these acids show good

catalytic performance on these reactions, they need neutralizations steps, product purification and they are corrosive, which make them not environment friendly (LI; LIANG, 2017; CLARK, 2002).

Consequently, one of the biggest challenges is creating acid catalysts with high catalytic activity and being environmentally friendly. In this sense, heteropolyacids have attracted great interest for their characteristics such as easy synthesis and well-known characterization (ODYAKOV et al., 2015). In addition, their acidic Brønsted and lewis properties and high catalytic activities (DA SILVA et al., 2016; VILLABRILLE et al., 2002; MISONO, 2001), make them active in different reactions including aldehyde acetalization reaction (LI; LIANG, 2017; RUIZ et al., 2010).

Keggin HPAs $H_3PW_{12}O_{40}$ and $H_3PMo_{12}O_{40}$ were evaluated by (TEIXEIRA; NATALINO; DA SILVA, 2020a) in acetalization reaction of furfural with alkyl alcohols (Figure 9). Furfural acetals were synthesized from condensations of furfural with methanol at room temperature. The HPAs activity was compared with HCl, H_2SO_4 and p-toluenesulfonic acid, showing the following sequence in catalytic activities terms $H_3PW1_2O_{40} \geq H_3PMo_{12}O_{40} > H_2SO_4 >$ HCl > p-toluenesulfonic acid.

Another important reaction is the oxidation process of the furfural to their acyclic acid derivatives like fumaric and maleic acid, these products are intermediates used for the manufacture of unsaturated polyester resins, pharmaceuticals and other important products for the fine chemistry industry (ALONSO-FAGÚNDEZ et al., 2012; ALONSO-FAGÚNDEZ et al., 2014). Nevertheless, due to polymerization of the substrate not always high efficiency has been achieved in the conversations reactions (LOU et al., 2020).

Figure 9 - General scheme of furfural acetalization with alkyl alcohols.

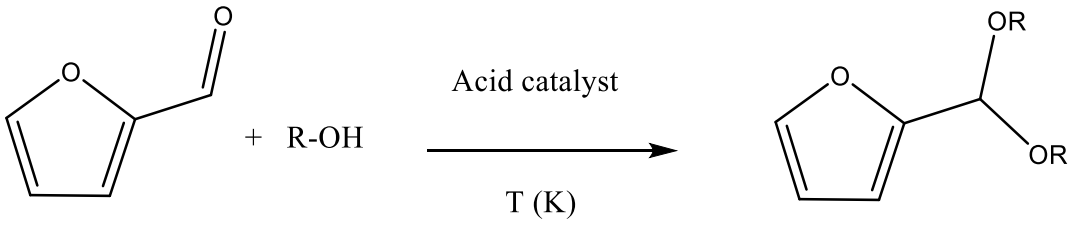

Source: Own authorship.

Oxidative esterification of furfural with alkyl alcohols (Figure 10), in a solid-catalyzed process such as gold-based catalyst (MENEGAZZO et al., 2014) which produces alkyl furoates, derivatives added to liquid fuels, is another important conversion reaction of furfural in value-add products. Besides that, furoates production from xyloses present in biomass as feedstocks, make them economically attractive, and the oxidation esterification in one pot using solid catalysts and hydrogen peroxide as green oxidant is an alternative to the traditional process that implements sulfuric acid and metal salts (WANG; YANG, 2015).

Silicontugstic acid salts were evaluated by (DA SILVA; RODRIGUES, 2020) as catalysts in oxidative esterification of furfural with hydrogen peroxide as oxidant using alkyl alcohols, obtained as main products furoic acid, alkyl furoate and 2-furfural dimethyl acetal, high conversion and ester selectivity in mild conditions was successfully achieved.

Figure 10 - General scheme of oxidative esterification of furfural.

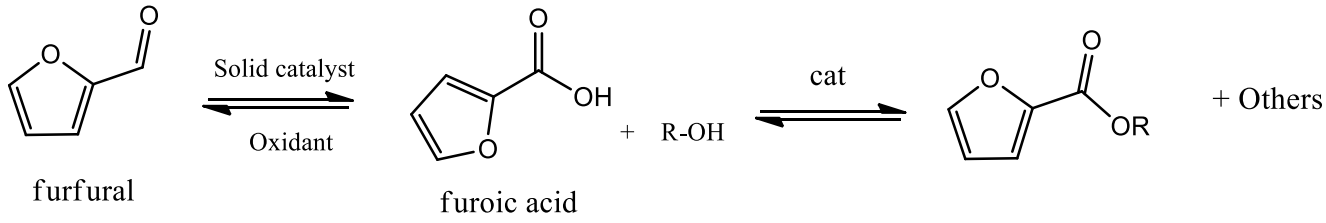

Source: Own authorship

Studies carried out on furfural and its derivatization reactions suggest that there is still much to be done to obtain a more viable, economical, and eco-friendly process.

1.8 Benzaldehyde

Primary alcohols oxidation to the corresponding aldehydes is an important reaction to obtain carbonylic compounds (YUE et al., 2017; LI et al., 2017a; SCHULTZ et al., 2005), aldehydes are important in perfumery, pharmaceutical and agrochemical industries (CHOUDHARY; DUMBRE; BHARGAVA, 2009). Besides that, benzaldehyde is one of the aromatic compost most used in perfumeries and flavour industry after vanillin (DELLA PINA; FALLETTA; ROSSI, 2008).

Benzaldehyde is conventionally synthesized by hydrolysis of benzyl chloride and is like a by-product in the oxidation route of toluene to benzoic acid, but in this process the presence of contaminants is chlorides or benzoic acid are limiting factors (NDOLOMINGO; MEIJBOOM, 2017). As an option, catalytic oxidation of benzyl alcohol to benzaldehyde in liquid phase reaction is exceptionally investigated, because it furnishes chlorides-free benzaldehyde, and avoid carbon oxides formation (KUMAR et al., 2016; RAVAT et al., 2013; CHOUDHARY et al., 2005).

1.8.1 Benzaldehyde derivative reactions

As aldehyde, benzaldehyde exhibits typical aldehyde reactions like furfural. The acid and esters of benzaldehyde are organic products with great importance for pharmaceutic, cosmetic, plasticizers, flavours (DEVARAJAN et al., 2016;TEJEDOR et al., 2016; WEN et al., 2017).

Conventionally the oxidation reaction of aldehydes to carboxylic acids is carried out with stoichiometric metallic oxidants like Mn and Cr salts(DASH; PATEL; MISHRA, 2009) organic oxidants are like N-iodosuccinimide are used too (BARLUENGA et al., 2004), and after that aldehyde, esters can be obtained by alcoholic esterification(LEE; KIM; LEE, 2016),. However, these conventional routes are not sure, the oxidant agents are toxics, not ecofriendly and generate unwanted by-products(AGRAWAL; ADIMURTHY; GHOSH, 2012; CHAVAN et al., 2002).

As an alternative to these traditional synthesis routes, which are not economically viable or environmentally friendly, Oxidative esterification reactions of aldehydes like benzaldehyde (Figure 11a) in an alcoholic medium, using solid catalysts, with oxidants such as hydrogen peroxide and molecular oxygen are being highly reported (LIU et al., 2004; MILLER; HOERRNER, 2003; GOPINATH; PATEL, 2000). In addition, these reactions are normally selective, and water is obtained as by-products.

Reactions with hydrogen peroxide are efficient. However, it is necessary to use catalysts such as transition metals for the peroxide activation (WU, 2012; DA SILVA et al., 2020). Among the catalysts used, HAPs are attracted great attention, due to their low toxicity and other characteristics already discussed (MATKOVIC; VALLE; BRIAND, 2005).

Figure 11 - General (a) oxidative esterification reaction of benzaldehyde (b) and acetalization reaction.

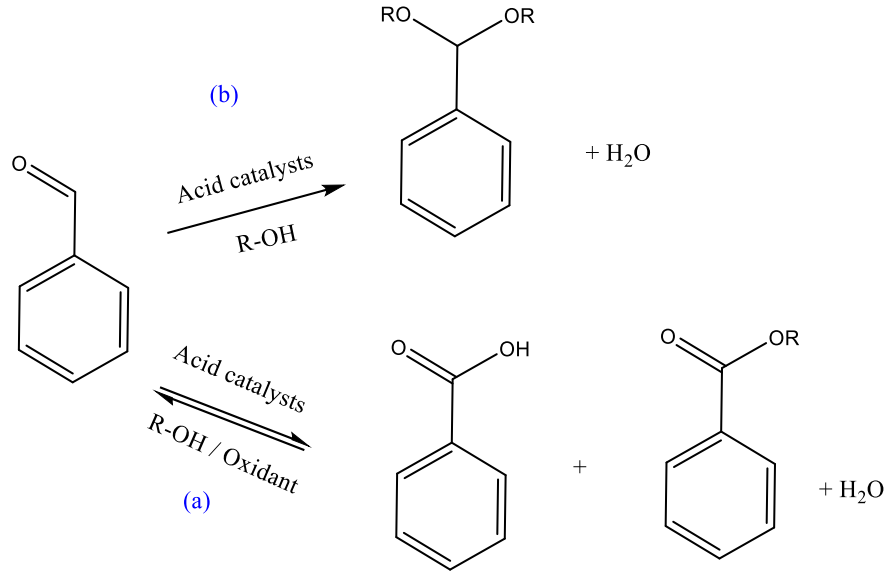

Source: Own authorship

Another important reaction of derivatization of benzaldehyde is the acetalization (Figure 11b). These reactions are normally carried out with alkyl alcohols and using acid catalysts as H_2SO_4 or H_3PO_4 (YUSUF; SITEPU, 2017). Nevertheless, homogeneous acid catalysts present a series of problems in catalyst recovery and in products separation, due to their corrosive nature. As option catalysts with better qualities HPAs have been studied (RABINDRAN JERMY; PANDURANGAN, 2006; BAO et al., 2009).

In this work, both reactions were tested using substituted HPA, like possible solid catalyst, and hydrogen peroxide as oxidant, looking for the reaction conditions improvement

2. OBJECTIVES

2.1 General Objective

Synthesize, characterize Niobium substituted phopshomolydic acids, and evaluate their activity and activity of Vanadium substituted phopshomolydic acids in oxidation and acetalization reactions of alcohols and aldehydes derived of biomass.

2.2 Specific Objectives

- Synthesize Niobium substituted heteropolyacids $H_{3+x}PMo_{12-x}Nb_xO_{40}$ (x= 1,2,3) derivatives of $H_3PMo_{12}O_{40}$ (phosphomolybdic acid).
- Characterizate the Niobium-substituted acids by infrared spectroscopy analysis, powder X-ray diffraction pattern analysis, potentiometric titration, nitrogen adsorption/desorption analysis and thermogravimetric analysis.
- Evaluate the activity of Vanadium substituted acids $H_{3+x}PMo_{12-x}V_xO_{40}$ (x= 1,2,3) as catalysts previously synthesize and characterized in our research group in oxidation reactions of terpene alcohols derived from biomass.
- Evaluate the activity of Niobium substituted acids ($H_4PMo_{11}Nb_1O_{40}$, $H_5PMo_{10}Nb_2O_{40}$ and $H_6PMo_9Nb_3O_{40}$), as catalysts in oxidative esterification and acetalization reactions of furfural.
- Evaluate the activity of Niobium substituted acids ($H_4PMo_{11}Nb_1O_{40}$, $H_5PMo_{10}Nb_2O_{40}$ and $H_6PMo_9Nb_3O_{40}$), as catalysts in benzaldehyde acetalization reactions with alkyl alcohols.

- Evaluate the effect of the relationship variables on the conversion and selectivity of the different substrates.
- Evaluated de reactions Kinetics in the absence and presence of catalysts.

3. EXPERIMENTAL

3.1 Reagents

Reagents were purchased from commercial sources with analytic grade and used without purification treatment exceed for furfural, which was previous treated due to its self-oxidation process. For this distillation process, furfural, and Sodium carbonate (7% by mass), were added in a distillation flask, and kept in stirring at room temperature for one hour. Finally, the distillation was conducted in a Vigreux column, and the distilled furfural, was stored in an amber flask under refrigeration.

Table 1 - Reagents, substrates, and solvents used in the catalyst synthesis and catalytic runs.

Reagent	Brand	Purity
$H_3PMo_{12}O_{40}$	Sigma-Aldrich	99.9 %
Nb_2O_5	Sigma-Aldrich	99.9 %
MoO_3	Sigma-Aldrich	99.5 %
H_3PO_4	Sigma-Aldrich	85%
H_2SO_4	Dinâmica.	98%
H_2O_2	Alphatec	35%
CH_3OH	Alphatec	99.8%
CH_3CN	Sigma-Aldrich	99%
Toluene	Sigma-Aldrich	99.8%
Geraniol	Sigma-Aldrich	99%
Nerol	Sigma-Aldrich	99%
Linalool	Sigma-Aldrich	99%

β-citronellol	Sigma-Aldrich	95%
Borneol	Sigma-Aldrich	97%
α-Terpineol	Sigma-Aldrich	96%
Furfural	Sigma-Aldrich	99%
Benzaldehyde	Sigma-Aldrich	99%
$H_4PMo_{11}VO_{40}$	LaCat-UFV[1]	-
$H_5PMo_{10}V_2O_{40}$	LaCat-UFV[1]	-
$H_6PMo_9V_3O_{40}$	LaCat-UFV[1]	-

1- Previously synthesized and characterized in the catalysis Laboratory of the Univerdade Federal de Viçosa by Vilanculo, Castelo

3.2. Catalyst synthesis

$H_{3+x}PMo_{12-x}Nb_xO_{40}$ (x= 1,2,3) acids were prepared by a hydrothermal synthesis method described in the literature (COLOMBO MIGLIORERO et al., 2020; VILLABRILLE et al., 2004) with some modifications. To prepare $H_4PMo_{11}Nb_1O_{40}$ was used a stoichiometric mixture of MoO_3 (54.01 mmol), Nb_2O_5 (2.47 mmol), H_3PO_4 85% (w/w) (0.240mL) suspended in distilled water (100 mL), the mixture was magnetically stirred for 6 h at 75-80 °C, then, it was cooled to room temperature, and the insoluble molybdates and niobates was removed by vacuum filtration. The solution was evaporated and dried at 85 °C for 12h, and finally a dark green solid ($H_4PMo_{11}Nb_1O_{40}$) was obtained. The $H_5PMo_{10}Nb_2O_{40}$ and $H_6PMo_9Nb_3O_{40}$ were synthesized following the same hydrothermal procedure but with modification stoichiometric relation (Figure 12) (ARICHI; ETERNOT; LOUIS, 2008). The catalyst was named $HPMoNb_{(x)}$ were (X=1,2,3).

Figure 12 - Scheme of stochiometric reaction conditions of catalyst synthesis.

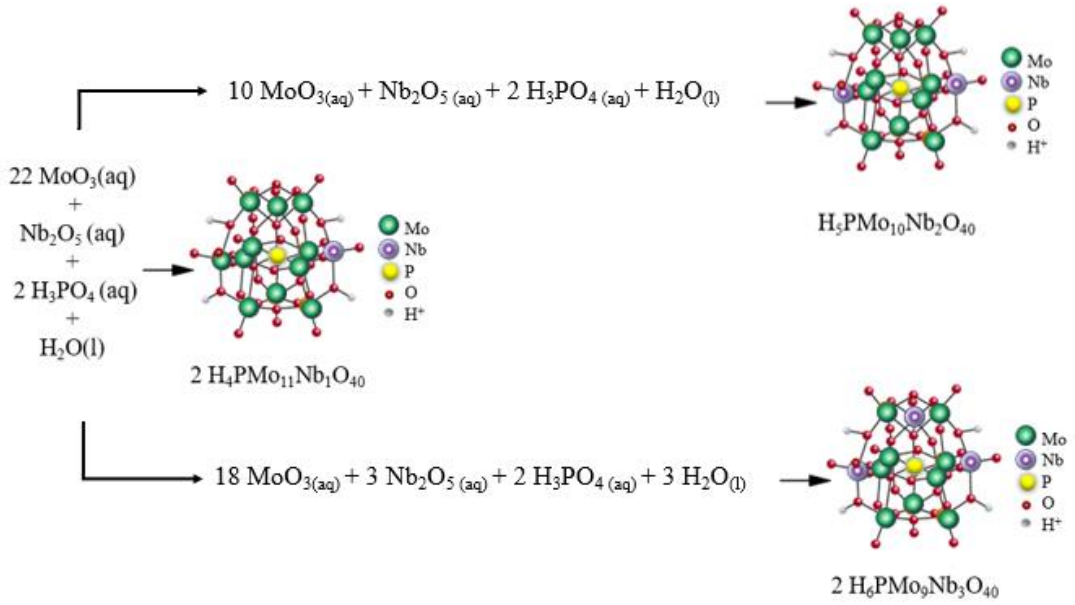

3.3 Characterization Techniques

3.3.1 Fourier transform infrared spectroscopy couple with the attenuated total reflectance technique FT-IR/ATR

Fourier transform infrared spectra FT-IR/ATR using the attenuated total reflectance technique of the substitute heteropolyacid catalysts were recorded on an FT-IR Varian 660 spectrometer from PIKE company, in the spectral range from 400 to 1700 cm^{-1}, for the analysis 2 mg of each catalyst was used.

3.3.2 Thermal analysis

To perform the thermogravimetric analysis, a simultaneous Thermal Analyzer (STA) 6000, Perkin Elmer, From the DEQ in the Laboratory of Homogeneous and Heterogeneous Catalysts was used. The sample were weighed, each aliquot

containing between 10-50 mg, and subjected to heating rate of 10°C min^{-1} in a range that varied from 30-700°C. The technique allows verifying mass loss at different temperatures and define the catalysts hydration water on the catalysts.

3.3.3 Potentiometric titration with n-butylamine

Potentiometric titration was used to determine the acidity of the synthesized catalysts, according to (PIZZIO et al., 2003). The variation of the electrode potential was measured in a Bel potentiometer, model W3B.

Typically, a solution containing 50mg of the catalyst ($H_3PMo_{12}O_{40}$ or $H_{3+x}PMo_{12-x}Nb_xO_{40}$ (x=1,2,3)) was dissolved in acetonitrile, under stirring for 3h and was titrated with a solution of n-butylamine in acetonitrile (0.025 mol. L^{-1}), dripping 0.10mL/min. Potentiometric measurements made possible to evaluate the acid strength. Based on the potentiometric titration, it was possible to estimate the acid strength of the substituted heteropolyacids. The analysis was performed in the homogeneous and heterogeneous catalysis laboratory of the chemistry department at UFV.

3.3.4 Specific surface and pore structure analysis

The gas physisorption technique is one of the techniques used for the analysis solid study. in these characteristics such as porosity (size and volume of the pore) and surface area are studied. This consists in put a surface of a solid (catalyst) in contact with a gas (N_2) result in an equilibrium between the adsorbed molecules and molecules in the gas phase that depends on the pressure and temperature of the gas.

Through the adsorption isotherms, the relation between the volume of the adsorbed molecules and the pressure at constant temperature is shown. These isotherms are classified by UIPAC (Figure 13) between types I to VI, each type of isotherm shows the differences in the interaction energy between the adsorbent and adsorbate and the solid porosity.

Figure 13 - Types of physisorption isotherms.

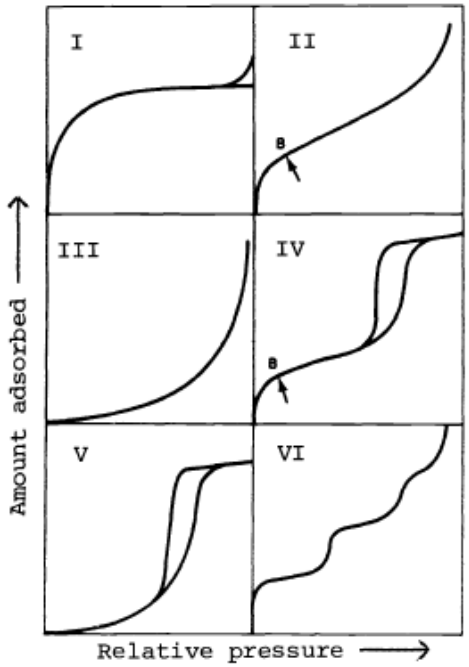

From. (SING, 1982).

BET (SING, 1982; TEIXEIRA; COUTINHO; GOMES, 2001) is a technique to measure the surface area and porosity distribution through the measuring of adsorbed gas necessary to cover the adsorbate-free surface, with a layer of thickness of one molecule (monolayer volume (V_m)). The surface area equals Vm times the area covered per unit volume of the gas.

The synthesized catalysts were characterized by physisorption of N_2 to 77K to the determination of the specific area by BET method. Poros diameter was measure by

DMF method. The volumeter machines NOVA 1200e and pore analyzer Quantachrome were used. 150 mg of sample was degassed for 5h at 200°C with relative pressure between 0.01 and 1.00 P/P_0. The analysis was performed in the homogeneous and heterogeneous catalysis laboratory of the chemistry department at UFV.

3.3.5 Molecular absorption analysis (UV-Vis)

UV–visible spectra of aqueous solutions containing undoped or Niobium doped phosphomolybdic acids in quartz cuvettes were measured at room temperature with an AJX-6100 PC double bean Micronal spectrometer, fitted with Tungsten and Deuterium lamps and between 190 and 110 nm to provide visible and UV wavelengths, respectively.

3.3.6 Powder X-Rays diffraction patterns

Powder diffraction patterns of salts and phosphomolybdic acids with or without Niobium were analyzed by X-rays diffraction (XRD) spectroscopy using a XRD-ray Diffraction System model D8-Discover Bruker using Ni filtered Cu-kα radiation (λ = 1.5418 Å), working at 40 kV and 40 mA, with a counting time 1.0 s in the diffraction angle (2θ) ranging from 5 to 80 degrees

3.4 Catalytic Runs

3.4.1 Geraniol oxidation reactions

Catalytic runs were carried out in a 25 mL three-necked glass reactor, equipped with a reflux condenser and sampling system, under magnetic stirring, and in controlled temperature (Figure 14)

Figure 14 - Assembly scheme for catalytic reactions

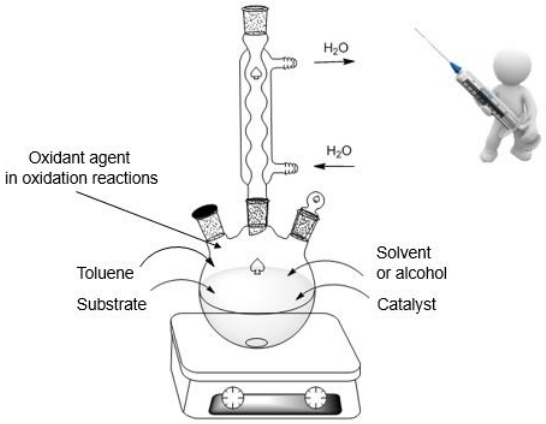

To carry out the oxidation reactions, a known quantity of geraniol the model substrate and hydrogen peroxide was added to the reactor, totaling the volume to 10 mL with acetonitrile, and using toluene as internal stander. Finally, a specific mass of catalyst (i.e $H_3PMo_{12}O_{40}$, $H_4PMo_{11}VO_{40}$, $H_5PMo_{10}V_2O_{40}$, $H_6PMo_9V_3O_{40}$) were added

The reactions were monitoring during 8 h. To do it, samples were periodically collected (1,2,4,6, and 8h) and analyzed by gas chromatography (Shimadzu 2010) couple with Flame Ionization Detector (FID). Target reactions were carried out in the same conditions but without catalyst.

The solvent free-oxidation of geraniol and nerol reactions were carried out using 13,75 mmol of substrate, 13,75 mmol of hydrogen peroxide and 0.33 mol % of

$H_4PMo_{11}VO_{40}$ as catalyst, on controlled temperature, using the same equipment for the reaction and analysis.

3.4.2 Furfural oxidative esterification reactions

Catalytic runs were carried out in a 25 mL three-necked glass reactor, equipped with a reflux condenser and sampling system, under magnetic stirring, and in controlled temperature as is shown in Figure 14. Typically, a known quantity of furfural and hydrogen peroxide was added to the reactor, totaling the volume to 10 mL with methanol, and using toluene as internal stander. Finally, a specific mass of catalyst (i.e $H_3PMo_{12}O_{40}$, $H_4PMo_{11}NbO_{40}$, $H_5PMo_{10}Nb_2O_{40}$, $H_6PMo_9Nb_3O_{40}$) were added.

The reactions were monitoring during for certain time. To do it, samples were periodically collected and analyzed by gas chromatography (Shimadzu 2010) couple with Flame Ionization Detector (FID). Target reactions were carried out in the same conditions but without catalyst.

3.4.3 Furfural acetalization reactions

Catalytic runs were carried out in a 25 mL three-necked glass reactor, equipped with a reflux condenser and sampling system, under magnetic stirring, and in controlled temperature as shown in Figure 14 but without oxidant agent.

To carried out the acetalization reactions, a known quantity of furfural was added to the reactor, totaling the volume to 10 mL with methanol, and using toluene as internal stander. Finally, a specific mass of catalyst (i.e $H_3PMo_{12}O_{40}$, $H_4PMo_{11}VO_{40}$, $H_5PMo_{10}V_2O_{40}$, $H_6PMo_9V_3O_{40}$) were added.

The reactions were monitoring during 180 min. To do it, samples were periodically collected (15, 30, 60, 90, 120 and 180 min) and analyzed by gas chromatography (Shimadzu 2010) couple with Mass Spectrometer Shimadzu MS-QP 2010 ultra. Target reactions were carried out in the same conditions but without catalyst.

For comparison with furfural as modal substrate, a catalytic test was carried out with benzaldehyde using the optimized parameters obtained in the acetalization reaction of furfural, through the same procedure.

3.5 Reaction monitoring and product identification.

To perform the quantitative analyses, reactions aliquots were injected in a Gas Chromatograph (GC) model Shimadzu GC-2010 Plus, equipped with an auto-injector, flame ionization detector (FID) and RTX-Wax capillary column (30m x 0.25mm ID x 0.25µm). The method conditions used were: column initial temperature 80°C maintained for 3 min, heating rate of 10 K/min, up to 230 °C, (total of 18 min); injector (250 °C); detector (250 °C); H2 carrier gas at 1.2 mL / min. Some reactions like furfural acetalization were carried out using a mass spectrometer (MS) to quantify the reactions product. The main chromatograms are present in the attachments section (Geraniol oxidation reaction attachment 1, Furfural oxidative reaction attachment 2, Furfural acetalization reaction attachment 3 and Benzaldehyde acetalization reaction attachment 4)

For products identification, the mass spectrums obtained in a mass spectrometer (MS) model Shimadzu MS-QP 2010 ultra, couple to a Gas Chromatograph (GC) Shimadzu GC-2010 (Tokyo, Japon), with a carbowax 20M capillary column (30 m x 0.25µm) using Helium as the carrier gas (flow 1.6 mL min^{-1})

were used. The injection process was manual. The interface temperature of the GC-MS the detector was 260 and 270 °C respectively, which operated in electron impact mode at 70 eV. Mass scanning was carried out in the range of 50-400 m/z. The mass spectrum of the different products is present in the attachment section (geraniol mass spectrum and their reaction products attachment 1.1 to 1.4, furfural mass spectrum and their reaction products attachment 3.1 and 3.2 and benzaldehyde mass spectrum and their reaction products attachment 4.1 and 4.2).

3.6 Quantitative analysis

As one of the most important parameters to know of the catalyst is being efficient in the reaction process, the reaction conversions were calculated through Equation 1, comparing the GC peak area of substrate in each reaction (Ai) with the initial area (A_0).

$$\% \textbf{Conversion} = \mathbf{100\ x\ \frac{A_0 - Ai}{A_0}} \qquad \textbf{Equation 1}$$

Selectivity is a parameter used to study the catalyst efficiency in the main product formation, it was calculated from Equation 2, where the corrected area of GC peak of each product (Ap) was compared to the A_0 x 100

$$\% \ \textbf{selectivity} = \mathbf{100\ x\ \frac{A_p}{\sum A}} \qquad \textbf{Equation 2}$$

The selectivity of terpene alcohols peroxide, which is an undetected product by GC analysis, was calculated using (Equation 3.)

$$\%\ \textbf{Terpene alcohols peroxide selectivity} = \frac{[(\text{consumed area of substrate GC peak} - \sum \text{GC peak corrected area of products})\ X100}{\text{consumed area of substrate GC peak}}$$ **Equation 3**

The oligomers were quantified through mass balance of reactions, comparing the sum of the GC peak areas of the products with the GC peak area of the substrate consume (Equation 4)

$$\%\ \text{oligomers} = ((A_0 - A_i) - \sum A_p) \times 100$$ **Equation 4**

A0 = GC peak area of furfural (time = t_0);

Ai = GC peak area of furfural (time = t);

$\sum$Ap = total sum of GC peak areas of the products after the correction by the response factor, which was determined comparing the GC peak of the pure products with the GC peak of furfural at the same concentrations

4. RESULTS AND DISCUSSION

4.1 Catalyst Characterization

4.1.1 Fourier transform infrared spectroscopy couple with the attenuated total reflectance technique FT-IR/ATR

The characteristic absorption bands present in the infrared spectrum of Keggin heteropoly anion are present between of wavenumber from 600 to 1400 cm^{-1} (i.e., fingerprint region). (Figure 15) shows the FT-IR spectra of undoped and Niobium doped phosphomolybdic acids. As a reference, dashed lines centered at the main absorption bands were added to it infrared spectra of pristine phosphomolybdic acid.

Spectrum of FT-IR of the $H_3PMo_{12}O_{40}$ heteropolyacid especially the fingerprint region shows four characteristic bands: 1064 cm^{-1} (P-O_a) where Oa connects the central tetrahedral P with Mo atoms, 962 cm^{-1} (Mo - O_d) corresponding to terminal oxygen , 871 cm^{-1} (Mo-O_b-Mo) related to the intra-bridge oxygen, between edge-sharing MoO_6 octahedra, 780 cm^{-1} (Mo-O_c-Mo) related to inter-bridge oxygen, between corner- sharing MoO_6 octahedral (WU et al., 2009).

Figure 15 - FT-IR spectra of Niobium substituted HAPs and $H_3PMo_{12}O_{40}$

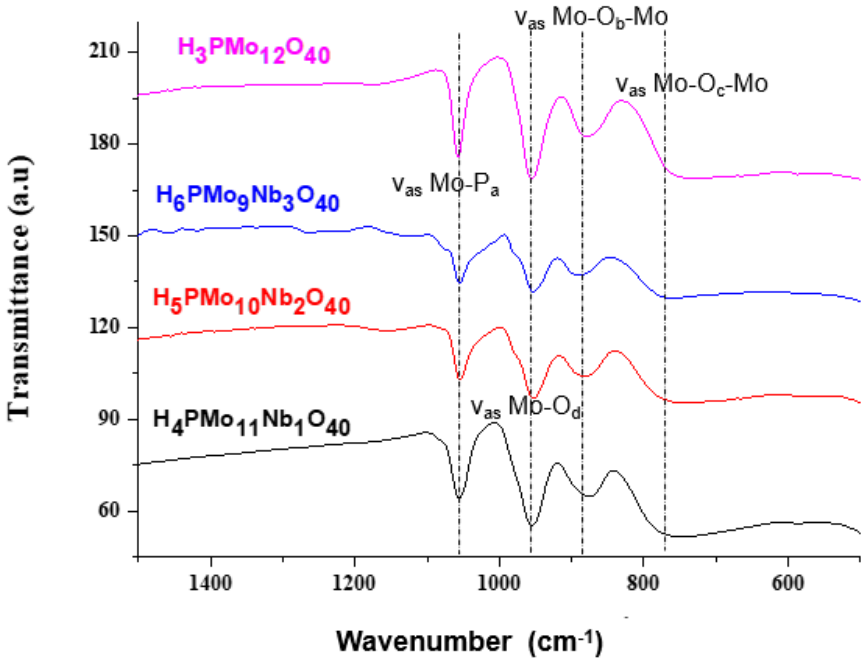

The FT-IR spectra of the $HPMoNb_{(X)}$ (x=1,2,3) catalysts (Figure 15) presents four bands at 1057 cm^{-1}, 955 cm^{-1}, 877 cm^{-1}, and 766 cm^{-1}, which are in agreement with the characteristics bands of Keggin structure (COLOMBO MIGLIORERO et al., 2020). This confirms that the synthesized $HPMoNb_{(x)}$ (x=1,2,3) presents primary kegging structure. Figure 14 shows that the characteristic bands shifts to lower wavenumbers with the increase of Nb, it can suggesting the incorporation of Nb in the kegging structure, which form Mo-O-Nb linkages by replacing Mo from Mo-O-Mo bonds of phosphomolybdic acid (YANG et al., 2021).Nevertheless, when the shift to lower wavenumbers is not observed, it's possible that has occurred the elimination of the transition metal from the primary keggin structure toward the secondary structure in the thermal treatment (EVTUSHOK et al., 2020).

4.1.2 Thermal analysis

Through the thermograms (TG) was possible determine the number of water molecules present in the compounds (Table 2). For this, the initial mass was considered as 100%, considering the loss of mass occurred to estimate the amount of water, the molecular mass of each compound was considered as MM+ n H_2O, with this estimate was possible to calculate the amount of water in each compound.

Figure 16 - TG and DTA analysis of different synthesized catalyst and $H_3PMo_{12}O_{40}$.

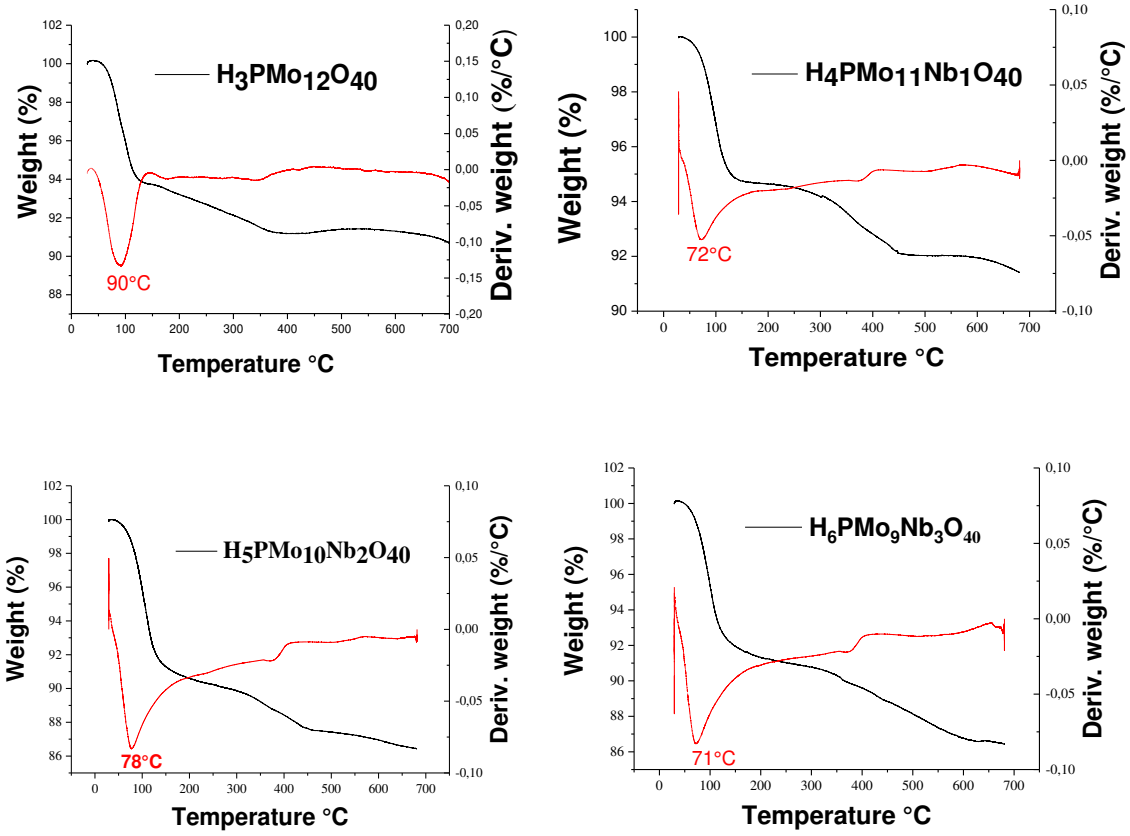

Using $H_3PMo_{12}O_{40}.nH_20$ as an example, the calculations were performed as follows:

First weight loss percent was 6,33 % in the temperature between 80 °C and 125 °C

$$H_3PMo_{12}O_{40}.n\ H_2O = 1825,25\ g.mol^{-1}$$

$$(1825,25 + 18.n)\ g.mol^{-1} \quad \text{--------} \quad 100\ \%$$

$$18.n\ g.mol^{-1} \quad \text{---------} \quad 6,33\ \%$$

$$1800.n = 11553,83 + 113,94.n$$

$$n = 6,85 \approx 7\ H_2O$$

Table 2 - Measurement of number water molecules into the Nb substituted HAPs.

Catalyst	T(°C) of Weight loss	Number of water molecules	Total water molecules	Molecular Formula
$H_3PMo_{12}O_{40}$	80-125	7	8	**$H_3PMo_{12}O_{40}.8H_2O$**
	125-250	1		
	250-400	2*		
$H_4PMo_{11}Nb_1O_{40}$	80-125	5	6	**$H_4PMo_{11}Nb_1O_{40}.6H_2O$**
	125-250	1		
	250-450	3*		
$H_5PMo_{10}Nb_2O_{40}$	80-125	9	11	**$H_5PMo_{10}Nb_2O_{40}.11H_2O$**
	125-250	2		
	250-450	3*		
$H_6PMo_9Nb_3O_{40}$	80-125	8	10	**$H_6PMo_9Nb_3O_{40}.10H_2O$**
	125-250	2		

	250-450	2*		

***Constitution water**

Thermogravimetric curves TG (Figure 16) obtained to the different catalysts and the precursor $H_3PMo_{12}O_{40}$ allow to identify which are characteristic degradations events for the heteropoly acid.

Figure 17 - TG and DSC analysis of different Niobium substituted catalysts and $H_3PMo_{12}O_{40}$.

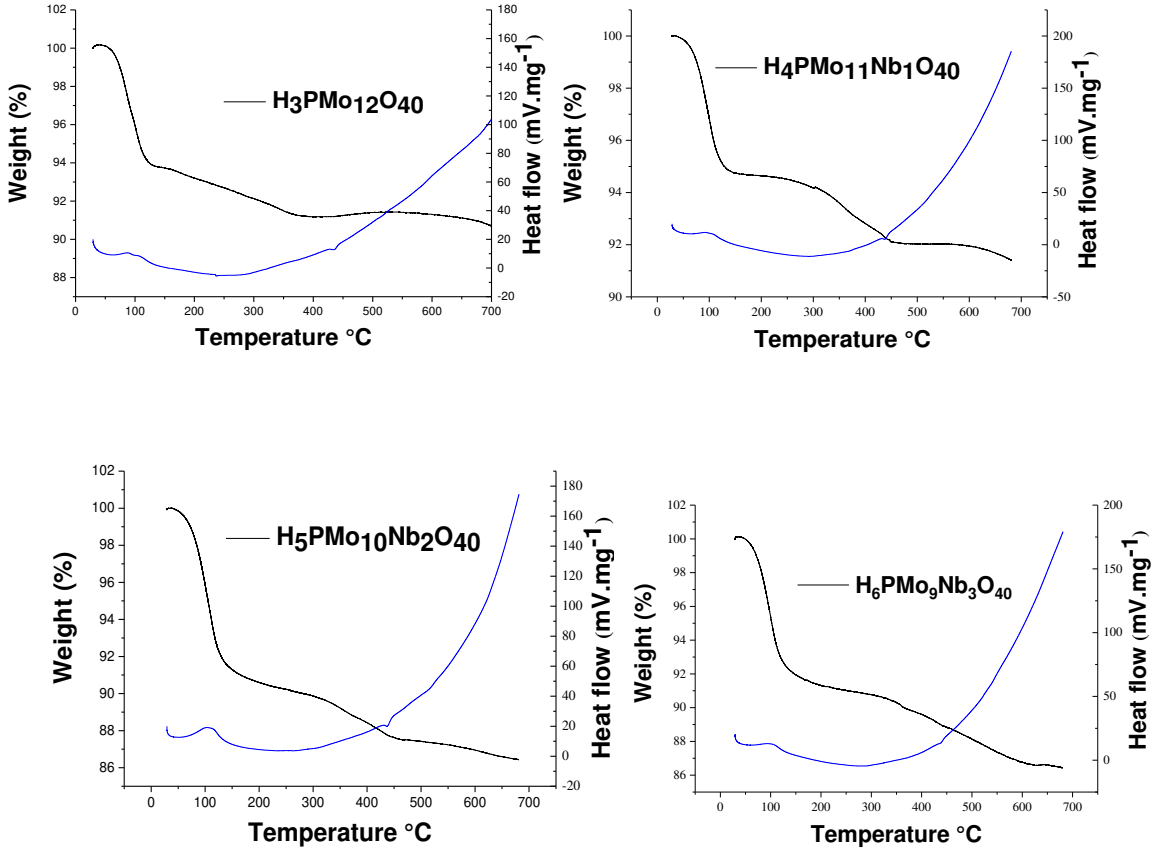

The mass lose events were calculated using the first derived from the thermogravimetric curve (DTA) and by means of the differential exploratory calorimetry (DSC) (Figure 17), the different endothermic and exothermic peaks were determined.

The DTA curve allow to differentiate the types of water that are lost in each event. It is possible to notice that two events occur before 250°C, which can be attributed to the loss of water adsorbed by the material, followed by coordination water molecules that make up the secondary structure of the kegging anion (MICEK-ILNICKA, 2009), these events can be confirmed by DSC, in which two endothermic peaks must appear, one of them before 100°C and a second one endothermic peak between 100°C-250°C. It should be noted that the amount of water of a heteropoly acid is not easy to be controlled, it depends on the species and the condition of preparation of an acid.(XIAN-E et al., 1997).

From 250°C and 450°C another event occurs, there is a small weight loss for all materials, this event corresponds to the evolution of protonic water, the so-called constitution water (COLOMBO MIGLIORERO et al., 2020). A final event can be observed after 450°C, which corresponds to the decomposition of the keggin lattice, this decomposition is marked by the appearance of exothermic peaks in the DSC curves around 450°C, and is possible observed by DTA that the catalyst decompose in a mixture of oxides (VILLABRILLE et al., 2004).

In the Table 2 is possible to observe the temperature ranges in which the different events occur of the catalysts and the molecular formula for each of them. Due to the water is part of the secondary structure of the keggin anion, it can affect the acidity and the sorption properties as well the crystalline structure of the HAPs, influencing the catalytic activity, allowing the reaction to take place or not (BARDIN et al., 1998).

4.1.3 Potentiometric titration with n-butylamine

Potentiometric titration is one of the methods applied to determine the acid properties of heteropoly acid and their derived salts, due to it allows the number of acid sites of the catalysts as well as the acid strength to be measured(DA SILVA et al., 2019).

Figure 18 - Potentiometric titration of acid catalysts (a) $H_4PMo_{11}Nb_1O_{40}$, $H_5PMo_{10}Nb_2O_{40}$, $H_6PMo_9Nb_3O_{40}$ (b) $H_3PMo1_2O_{40}$.

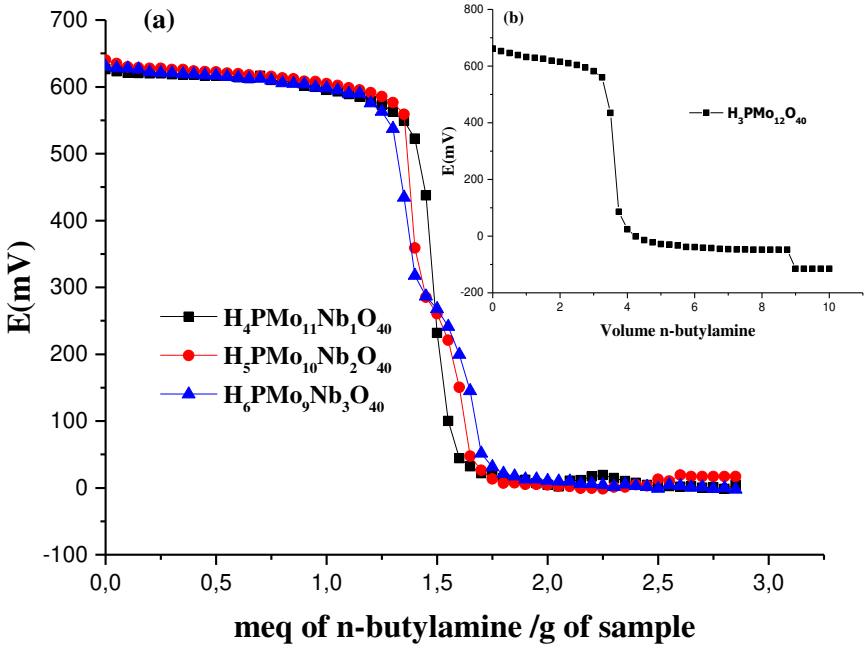

The initial electrode potential (E_i) in the potentiometric titration, indicates the maximum acid strength of the surface sites. The acid strength of surface sites can be assigned according to the following ranges: very strong site, $E_i > 100mV$; strong site, $0 < E_i < 100mV$; weak site, $-100 < E_i < 0mV$ and very weak site, $E_i < -100mV$ (PIZZIO et al., 2003). In addition, the number of acidic sites present in the catalyst can

be determined by means of the volume of n-butylamine consumed per gram of sample (milliequivalent (meq) n-butylamine/ g sample) (REDDY et al., 2006).

Figure 18a shows that the three heteropoly acids substituted with Nb_x (X=1,2,3) have very strong acid sites and for that reason their protons were fully titrated with n-butylamine. However, the variation in acidity between them it is not very significant and de acidic proprieties of the catalysts are like the acidity of the $H_3PMo_{12}O_{40}$ Figure 18b. The trend in the acid strength of the catalysts follows the following order $H_4PMo_{11}Nb_1O_{40}$ (626.5mV) ≈ < $H_6PMo_9Nb_3O_{40}$ (630,2 mV) < $H_5PMo_{10}Nb_2O_{40}$ (640,3mV). < $H_3PMo_{12}O_{40}$ (662mV).

The small initial variations observed in the potential values obtained in the titration can be explained because the heteropoly acids are not deprotonated when they are hydrated, in the hydrated phase the protons reside in the bridging water remains forming $H_5O_2^+$ (BARDIN et al., 1998).

Generally, the titration curves of the catalysts only present an inflection because the protons are titrated simultaneously, the curve of the catalysts $H_5PMo_{10}Nb_2O_{40}$ and $H_6PMo_9Nb_3O_{40}$ in the Figure 18 shows two inflections which may suggest that the metal reacts with the titrant n-butylamine and can form complex (CHAVES et al., 2019)

4.1.4 Specific surface and pore structure analysis

Adsorption isotherms in the Figure 19 show the same profile, suggesting that all the catalysts reflect the same type of porosity (type IV according to IUPAC classification).

The isotherms type IV are characteristics for solids non-porous or mesoporosity, another important characteristic feature it's the hysteresis loop, which is related with the limiting uptake over a range of high p/p° and the capillary condensation

taking place in mesopores. The first part of the isotherm is associate with monolayer-multilayer adsorption since it follows the same path of the isotherms type II (SING, 1982)(TEIXEIRA; COUTINHO; GOMES, 2001). The hysteresis loops indicate the irreversibility of the adsorption-desorption isotherm.

Figure 19 - Adsorption/ Desorption isotherms and Graphs of pore distribution of $H_3PMo_{12}O_{40}$ and $H_{3+x}PMo_{12-x}Nb_xO_{40}$ (x=1,2,3).

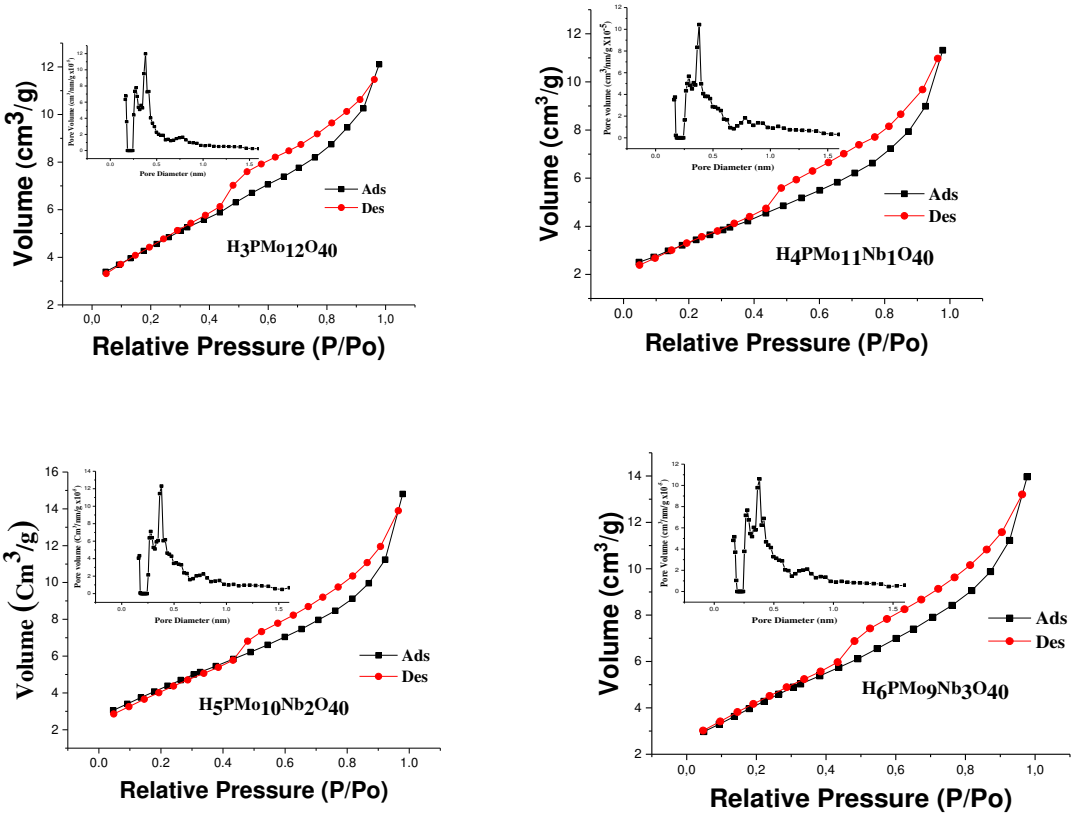

Adsorption hysteresis takes place when the adsorption and desorption deviate from one another, and they are classified between H1 to H4. The isotherms in Figure 19 show hysteresis with behavior between type H3 and H4,in the type H3 the hysteresis have a relation with isotherms type II, the loops on this are given by non-rigid aggregates of plate-like particles, and the H4 hysteresis is a composite of Type I

and II, where the more pronounced uptake at low P/P^o is associated with the filling of micropores, furthermore, H4 loops are often found in micro-mesoporous structures (THOMMES et al., 2015).

The Table 3 show the texture parameters of the Nb-substitute kegging HAPs, the BET surface area of the catalysts were 10 m^2/g on overage, in good agreement with other investigations (ARICHI; ETERNOT; LOUIS, 2008), in addition, it can be observed that with the incorporation of Nb in the kegging HAP structure, a decrease in the surface area take place, increasing as more Nb units are incorporated, the same behavior is related by Park et al (PARK et al., 2011).

Table 3 - Textural properties of $H_3PMo_{12}O_{40}$ and Nb substituted HAPs.

Catalyst	Surface Area S_{BET} (m^2/g)	Pore Volume (cm_3/g)	Pore Size Å	Pore size (nm)
$H_3PMo_{12}O_{40}$	11.74	0.01660	18.97	1.897
$H_4PMo_{11}Nb_1O_{40}$	8.90	0.01596	18.97	1.897
$H_5PMo_{10}Nb_2O_{40}$	10.87	0.02407	18.97	1.897
$H_6PMo_9Nb_3O_{40}$	11.03	0.01916	18.97	1.897

*DTF method
Pore size not exceeding 2 nm are called micropores

The pore size of all catalysts was 1.897 nm, this size allows the structures to be characterized as microporous, However, due to the proximity between the values obtained for the heteropoly acids and the range of characterization (2 nm microporous – exceeding 2 nm mesoporous), is difficult to be secure that the behavior of the catalysts is only as microporous, besides that the existence of hysteresis loop in the adsorption-desorption isotherm for this solid is consistent with the onset of

mesoporosity (MOFFAT, 1989). These limits are to some arbitrary due to the filling mechanism dependent on the pore shape and the proprieties of the adsorptive and the adsorbent -adsorbate interactions.

4.1.5 Molecular absorption analysis (UV-Vis)

UV–visible spectra of aqueous solutions containing undoped or Niobium doped phosphomolybdic acids in quartz cuvettes were measured at room temperature with an AJX-6100 PC double bean Micronal spectrometer, fitted with Tungsten and Deuterium lamps and between 190 and 110 nm to provide visible and UV wavelengths, respectively.

Figure 20 - UV-Vis spectra of undoped and doped phosphomolybdic catalysts.

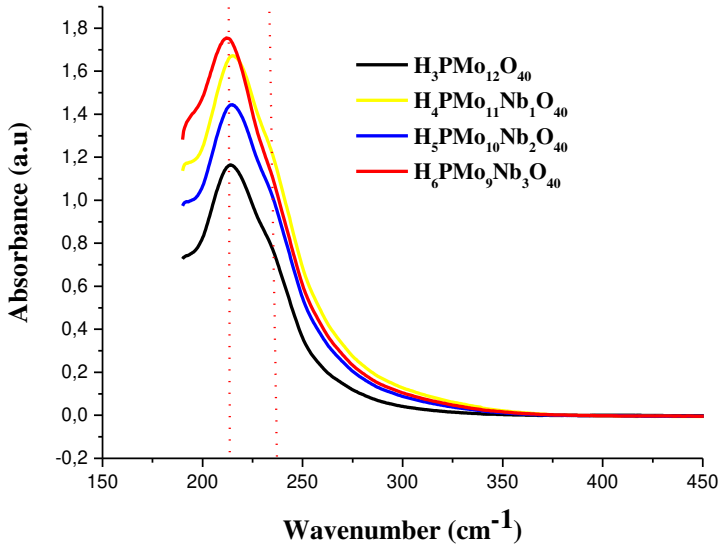

The UV-vis spectrum of the undoped and Niobium doped phosphomolybdic acid is shown in (Figure 20), in this spectrum the first band 210-260 is assigned to oxygen-metal transfers , it band is clear showed for all the spectrums, another band with weak intensity at 240-500 nm can be seen, in this case the band is assigned to octahedral

Mo into kegging structure (COLOMBO MIGLIORERO et al., 2020;MOTHÉ-ESTEVES et al., 2010). Furthermore, these characteristic bands allow to confirm the presence of the keggin structure in the catalysts.

UV-vis spectroscopy in solution is also important to evaluate the potential activity of the heteropoly acids as oxidation catalysts in liquid phase. From these spectrum is possible calculate the absorption edge energy (BARTEAU et al., 2006), which can be correlated with the reduction potential of the HAPs catalysts, as is show by (PARK et al., 2011) with HAPs catalysts containing Niobium,

The absorption edge in the UV-Vis spectra is used to measure the energy necessary for “d-d” transitions, it transitions involves transference of an electron from the (HOMO) Highest Occupied Molecular Orbital to (LUMO) the Lowest Unoccupied Molecular Orbital, besides that, Ligand to Metal Charge Transfer Transitions (LMTC) (BARTEAU et al., 2006). The incorporation of a heteropoly-anion in the kegging structure, substituting one or more Mo atoms by Nb, modifies the absorption edge, this reflects changes in the LUMO energy. The LUMO energy is principally affected due to that the LUMO involve the bridging oxygen atoms and the d-orbitals of the framework metals (MAESTRE et al., 2001).

4.1.6. Powder X-Rays diffraction patterns

X-rays diffraction is important to assess at the secondary structure of the keggin heteropoly anion, it is important due to the presence of hydration water or metal cations may affect the structure, through of modifications in the symmetry and the arrange of unitary cell of the HAPs (FOURNIER et al., 1992; ILLINGWORTH. J. W 1935). This measurement is a qualitative one.

Figure 21 - (a) Powder XRD of Niobium-substituted phosphomolybdate acids and (b) first peak positions in the range between 5° to 10 °.

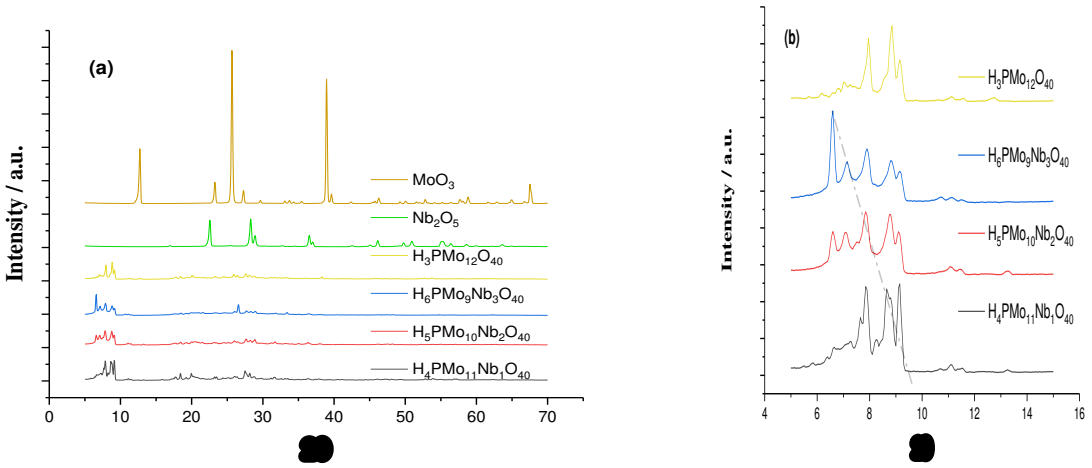

The successful synthesis of the different Niobium- doped phosphomolybdate acids was examined through the crystal structure of HAPs. As shown in the Figure 21a, the XDR patterns present the most significant diffraction peaks to phosphomolybdic acid, this were observed at 2Θ values of (5.0-10.0)°, (18.0-23.0)°, and (25.0-30.0)° counts, which is in good agreement with reported literature and suggest cubic crystalline structure(TANG; ZHANG, 2006).

Niobium- doped heteropoly acids present the mains characteristic peaks for $H_3PMo_{12}O_{40}$, indicating the successful synthesis of the catalysts, and allows to verifying the dominant crystal unit structure of the initial phosphomolybdate acid(YANG et al., 2019).for comparison, Nb_2O_5 pattern is included in the (Figure 21).In addition, the flexibility of replacing Nb and Mo cations allows to maintain the structure without important deforming. However, exceed addition of Niobium or Molybdenum resulted in some impurity weak diffraction peaks indicating the presence of heterogeneous phase crystal structure like Nb_2O_5 or Mo_2O_3 (TAGUSAGAWA et al., 2009).

For the samples after proton exchange the XDR diffractograms show (Figure 21b), that the first peak positions in the range between 5° to 10 ° were shifted to lower angles with increasing Niobium content, it means that the interlayer space increase with Nb content. Furthermore, the expansion of the interlayer spacing probably resulted from an increase in the proton density in the proton interlayer and hydration degree of interlayer protons, which so compensated for the negative charge of the Nb-Mo Oxide sheets (TAGUSAGAWA et al., 2009; TAGUSAGAWA et al., 2008).

Finally, it is reported in previous work that the $H_3PMo_{12}O_{40}$ and $H_4PVMo_{11}O_{40}$ exhibit similar XDR patterns, consistent with tricyclic lattice(FOURNIER et al., 1992; SUN et al., 2008; MAROSI et al., 2000), by comparison with the patterns obtained to the $H_4PMo_{11}Nb_1O_{40}$ in this work, its expected the same type of lattice.

4.2 Vanadium-Substituted Phosphomolybdate Acids as Catalysts for Geraniol Oxidation with Hydrogen Peroxide

4.2.1 Effect of Vanadium doping on the conversion and selectivity of phosphomolybdic acid-catalyzed geraniol oxidation reactions with hydrogen peroxide

To research the efficiency of Vanadium-doped phosphomolybdic acids as catalysts, they were used in the geraniol oxidation reactions and compared with the pristine HPA. The main results are summarized in the (Figure 22). The reaction conditions were chosen base on previous works in our research group, reported by (VILANCULO et al., 2021).

The kinetic curves show that reactions carried out with undoped or monosubstituted phosphomolybdic acids have similar profile, achieving a conversion of 94% within 2 first hours of reaction, while the di or trisubstituted-vanadium reached 76 and 65% of conversion after 8h, respectively (Figure 22a)

It's possible to see, that the highest selectivity toward geraniol epoxide was achieved when $H_4PMo_{11}VO_{40}$ was used as catalyst (Figure 22b). the epoxide selectivity in presence of disubstituted acid has been slightly lower than monosubstituted. However, the conversion was visible lower. In addition, the worst performance of trisubstituted acid is another evidence that a high Vanadium load was not beneficial, either in terms of conversion or selectivity (Figure 22).

Figure 22 - Effect of Vanadium doping on the activity of phosphomolybdic acid catalysts on the geraniol oxidation reactions with H_2O_2: kinetic curves (a), conversion, and products selectivity after 8 h (b)[a]

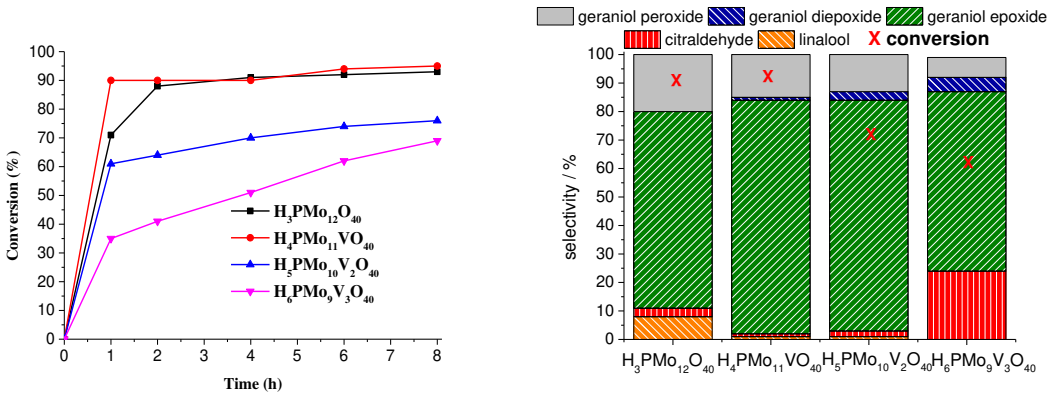

(a) (b)

[a]Reaction conditions: geraniol (2.75 mmol), H_2O_2 (2.75 mmol), toluene (internal stander), catalyst (0.66 mol %), temperature (60°C), CH_3CN (10 mL).

The main explication of these results can be done through the reduction potentials of these catalysts, as higher was the potential (see Table 4), more efficient was the catalyst, realizing greater conversion and selectivity respecting geraniol epoxide.

These reduction potentials were measured through the UV-Vis spectra of the undoped and Vanadium-doped HAPs, (reported in submitted article by Da Silva.M , Vergara. J and Vilanculo. C.). It was taken Barteau et al. as a reference, due to they demonstrated that the level of vanadium doping in the pristine phosphomolybdic HAP can be correlated with the absorption edge in UV-Vis spectra, and the reduction potential of these HAPs can be measured(SONG; BARTEAU, 2004). They show that the edge energy and the reduction potential of $H_4PMo_{11}VO_{40}$ acid is higher than the

$H_3PMo_{12}O_{40}$ precursor acid. Besides that, they demonstrated that an increase in the Vanadium load, reduce the edge energy and reduction potential.

Table 4 - Absorption edge energies and reduction potentials of phosphomolybdic catalysts.[a]

Catalyst	Solution edge (nm)	Edge energy[a] (eV)	Reduction potential Ag/ AgCl (Volts)
$H_3PMo_{12}O_{40}$	468	2.65	-0.082
$H_4PMo_{11}VO_{40}$	526	2.36	0.261
$H_5PMo_{10}V_2O_{40}$	532	2.33	0.233
$H_6PMo_9V_3O_{40}$	536	2.32	0.168

[a]Edge energy (E) was calculated from the absorption edge wavelength (k) by $E = hc/\lambda$, where *h* is Planck's constant and *c* is the speed of light.
adapted from: (SONG; BARTEAU, 2004)).

Different products can be obtained by the oxidation reaction of geraniol (Figure 23). However, anyway of catalyst nature, geraniol epoxide (1b) was always the major product, being the secondary products geraniol diepoxide (1c) and aldehyde (i.e., citral 1d). The literature describes that peroxide (i.e., geraniol peroxide, 1a) is the most probable intermediate in these reactions, which are non-detected products by GC-FID analysis, but were quantified through the mass balance of reactions (VILANCULO et al., 2021; VILANCULO; DA SILVA, 2021).

Figure 23 - Scheme 1, of the main products of geraniol oxidation with H_2O_2 in the presence of Vanadium-doped phosphomolybdate catalysts in CH_3CN solutions.

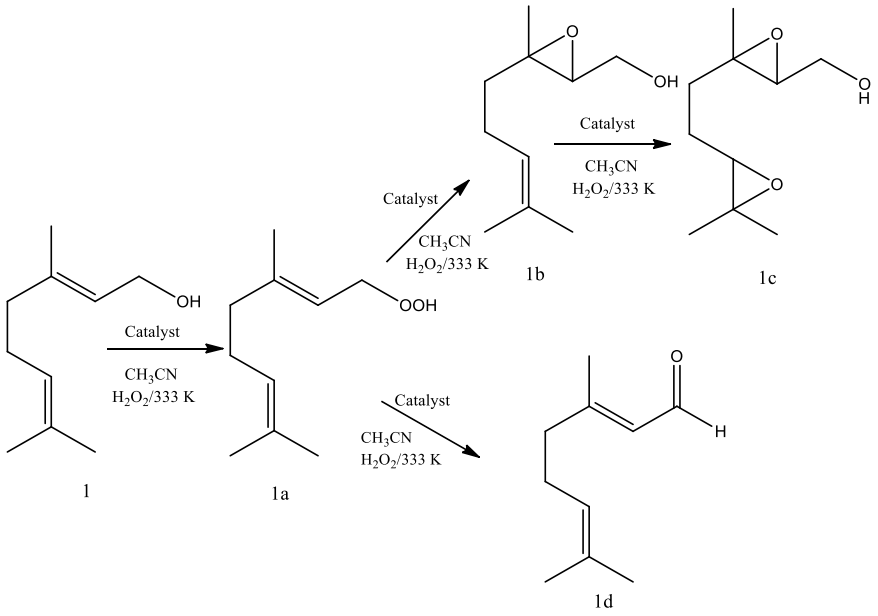

Although sometimes the reactions had reached the maximum conversion within the initial period, the reaction selectivity can be modified throughout the time according with reports, to research this effect, we have monitored the reactions during the reactions during the runs and displayed the main results in Figure 24.

Regardless the catalyst in all the runs, it was display that throughout the reactions the geraniol peroxide is converted to geraniol epoxide, demonstrating that these are consecutive reactions, such as proposed in Figure 23. Nevertheless, among the catalyst tested, the $H_4PMo_{11}VO_{40}$ acid was the most efficient realizing the highest conversion and selectivity toward geraniol epoxide.

Figure 24 - Monitoring of conversion and selectivity of geraniol oxidation reactions by H_2O_2 in the presence of phosphomolybdic acid or their Vanadium doped derivatives.[a]

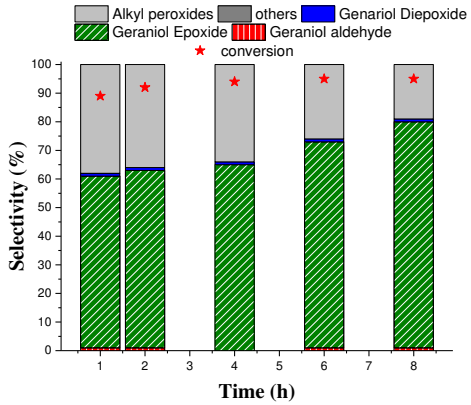

(a) $H_3PMo_{12}O_{40}$

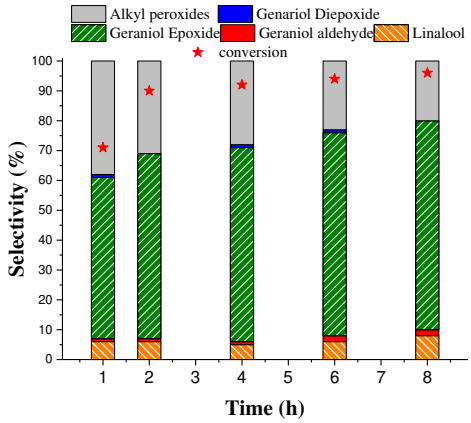

(b) $H_4PMo_{11}VO_{40}$

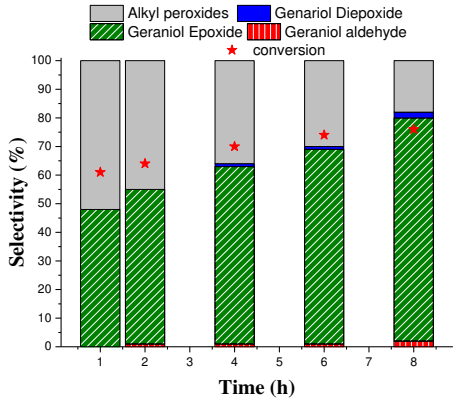

(c) $H_5PMo_{10}V_2O_{40}$

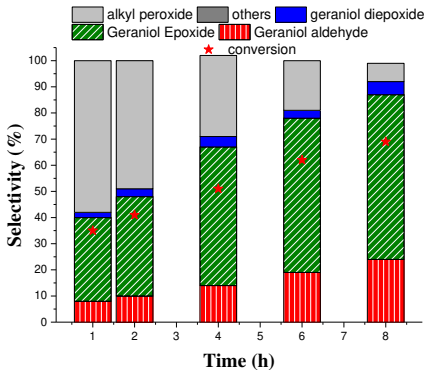

(d) $H_6PMo_9V_3O_{40}$

[a]Reaction conditions: geraniol (2.75 mmol), H_2O_2 (2.75 mmol), toluene (internal stander), temperature (60 °C), CH_3CN (9.3 mL), Catalyst load (0.66 mol %).

Besides the potential reduction, acid properties can be useful to explain the behavior of the Vanadium- doped phosphomolybdic acids in oxidations reactions of geraniol, Like Weinstock et al. reported, Keggin- type (Mo-V-P) HAPs possess strong Brønsted acidity, which is beneficial to the oxidative catalytic transformations of

biomass derived (WEINSTOCK; SCHREIBER; NEUMANN, 2018). In effect, previous research has described that the formation of the peroxo-metal intermediated between the peroxide and the HAP catalyst (i.e., V, Mo or W HPA) is bountied with the Vanadium atom presence (CASARINI et al., 1993; RAO et al., 2015; PALERMO et al., 2016; PALERMO et al., 2015).

The reaction in absence of Vanadium, when phosphomolybdic acid was used as catalyst achieved high conversion, nevertheless, in this case, the conversion can be attributed to the existence of higher Brønsted acidity strength, which means into better catalytic performance, as in phosphomolybdic acid catalyst (Figure 24) (VILANCULO et al., 2021). Recently, Vilanculo et al. evaluate different Brønsted acids and their performance in oxidation reactions of nerol with hydrogen peroxide, and demonstrated that the acidity of $H_3PMo_{12}O_{40}$ higher than other HAPs (i.e., $H_3PW_{12}O_{40}$ and $H_4SiW_{12}O_{40}$), and then the other typical Brønsted acids (i.e., H_2SO_4 and P-toluenesulfonic acid) (VILANCULO; DA SILVA, 2021). Arcoria et al. confirmed that protonic species can accelerated the epoxidation rate of a simple olefin, likely through hydrogen bonding of the peroxide oxygen in the transition state(ARCORIA et al., 1986)

It proposes to the geraniol epoxidation, that both Lewis´s acid sites (i.e., Vanadium sites, $H_4PMo_{11}VO_{40}$), and Brønsted (i.e., H_3O^+ ions, $H_3PMo_{12}O_{40}$), seems to play a key role. The reaction mechanism involving a peroxide intermediate bonded to keggin Vanadophosphomolybdate anion was suggested using (VILANCULO et al., 2021) as a reference.

In addition, with increasing in the Vanadium load (i.e., V_2 and V_3 catalysts), the catalysts go through a decreasing in performance, justified by an increment in the energy barrier between HOMO and LUMO orbitals, which difficult the reducibility of the

$H_5PMo_{10}V_2O_{40}$ and $H_6PMo_9V_3O_{40}$ heteropolyanions (MAESTRE et al., 2001; PILLAI; SAHLE-DEMESSIE, 2004).

Another aspect that characterized the performance of Vanadium doped phosphomolybdic acids is the highest selectivity toward geraniol aldehyde (i.e., citral 1d, Figure 23), accomplished in the $H_6PMo_9V_3O_{40}$ – catalyzed reaction. This geraniol aldehyde is obtained by decomposition of peroxide geraniol intermediated(VILANCULO et al., 2021). Previous research describes that this composition to a carbonylic compound (geraniol aldehyde) is more favourable when the catalyst is easily oxidable, it means, through a fast interconversion of one electron (i.e., V^{+4}/V^{+5}), which in this case is promoted by high Vanadium load (RAO et al., 2015)(PALERMO et al., 2016; PALERMO et al., 2015; PILLAI; SAHLE-DEMESSIE, 2004). Same results were observed when Sodium salt of this acid (i.e., $Na_6PMo_9V_3O_{40}$) was used in oxidation reactions of nerol (VILANCULO et al., 2021).

4.2.2. Effect of $H_4PMo_{11}VO_{40}$ concentration on geraniol oxidation with hydrogen peroxide

To evaluate the catalytic activity of $H_4PMo_{11}VO_{40}$, the catalyst concentration was studied, the main results are displayed in Figure 25. It shown that the initial rate of reactions is improved with an increase in the catalyst load, Nevertheless, the kinetic curves present almost the same profile, attaining the maximum conversion within the initial period.

Although independent of the catalyst load, geraniol peroxide remained as the principal product, a decrease in the concentration of catalyst, changed the selectivity favoring the aldehyde (i.e., citral 1d, Scheme 1) formation.

Figure 25 - Effect of $H_4PMo_{11}VO_{40}$ catalyst load on the kinetic curves (a), conversion, and products selectivity after 8 h (b) of geraniol oxidation reactions with H_2O_2.[a]

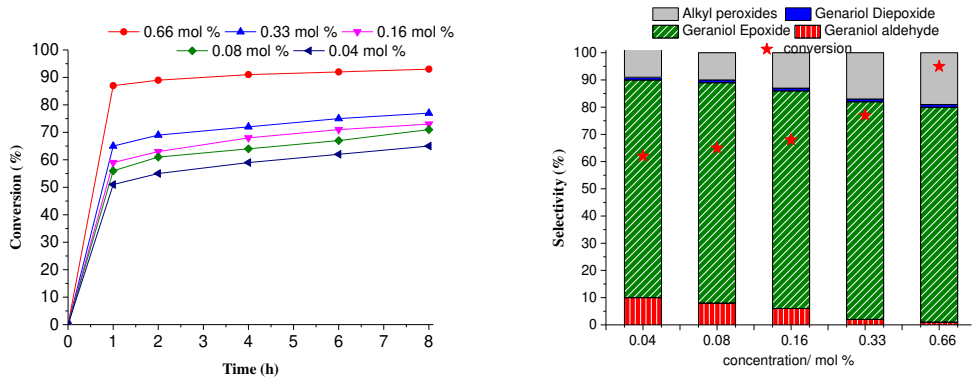

(a) **(b)**

[a]Reaction conditions: Geraniol (2.75 mmol), H_2O_2 (2.75 mmol), toluene (internal stander), temperature (60 °C), CH_3CN (10 mL).

4.2.3. Effect of temperature on the $H_4PMo_{11}VO_{40}$-catalyzed oxidation of geraniol with H_2O_2

The effect of the temperature on the catalytic performance of the $H_4PMo_{11}VO_{40}$ acid was studied, the kinetic curves are shown in the Figure 26. These curves shown that with a higher temperature, the reactions became faster, which can be explained due to a higher number of effective collisions, this effect was much more visible at 60 °C.

Figure 26 - Impacts of temperature on the kinetic curves of $H_4PMo_{11}VO_{40}$-catalyzed geraniol oxidation reaction with H_2O_2.[a]

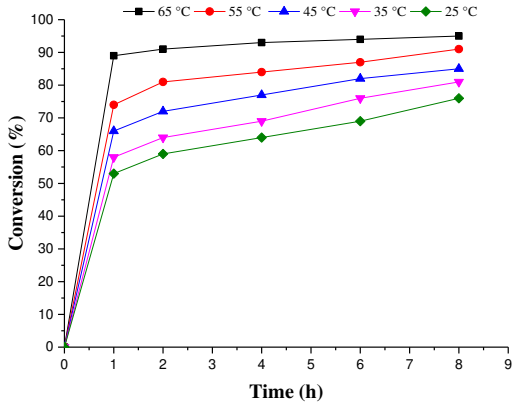

[a]Reaction conditions: nerol (2.75 mmol), H_2O_2 (2.75 mmol), toluene (internal stander), catalyst (0.66 mol %), CH_3CN (10 mL).

In all the runs, geraniol epoxide was always the main product, it means, no significant change was shown in the reaction selectivity when the reactions were carried out at different temperatures.

4.2.4. Effect of oxidant load on the conversion and selectivity $H_4PMo_{11}VO_{40}$-catalyzed oxidation with H_2O_2

The effect of the hydrogen peroxide was evaluated, and the main results are present in the Figure 27, a greater quantity of oxidant could affect the reaction performance, especial the substrate conversion and the products selectivity, largely due to the higher presence of water in the reaction medium.

A higher amount of peroxide had different impacts on the reaction and in the selectivity of products. Although omitted herein, it was revelated through the kinetic

monitoring of reaction, that independently of the molar ratio used, the reactions accomplish the maximum conversion within the first hour of the run, furthermore, the conversions were almost the same.

Figure 27 - Effect of oxidant substrate molar ratio on the conversion and reaction selectivity of $H_4PMo_{11}VO^{40}$-catalyzed geraniol oxidation reactions with H_2O_2.[a]

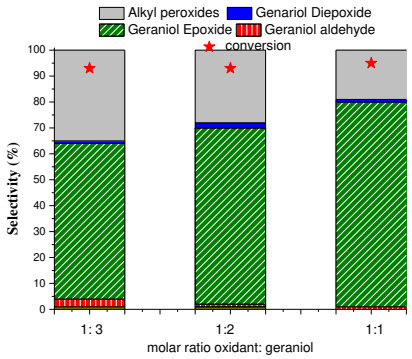

[a]Reaction conditions: geraniol (2.75 mmol), catalyst (0.66 mol %), temperature (60 °C), CH_3CN (10 mL).

Nevertheless, a high excess of oxidant, make the selectivity toward geraniol epoxide lower, due to the large formation of alkyl peroxides.

4.2.5 $H_4PMo_{11}VO_{40}$-catalyzed oxidation reactions with H_2O_2: effect of the substrate

Different alcohols were selected as substrates, this with the object of evaluate how electronic and steric affects may affect the conversion and selectivity; moreover geraniol, nerol that is a geometric isomer (i.e., allylic alcohol), β-citronellol (i.e., primary alcohol), linalool (i.e., tertiary alcohol) were tested in the conditions previously established (Figures 26-28).

Geraniol and nerol are (Z) and (E) geometric isomers respectively. It was asserted that the catalytic performance of $H_4PMo_{11}VO_{40}$ in their oxidation reactions with hydrogen peroxide was almost the same; almost 95% of conversion and epoxide selectivity close to 80% were achieved within 2 first hours of reaction (Figure 28).

Figure 28 - Scheme 2, $H_4PMo_{11}VO40$-catalyzed nerol oxidation reactions with H_2O_2.[a]

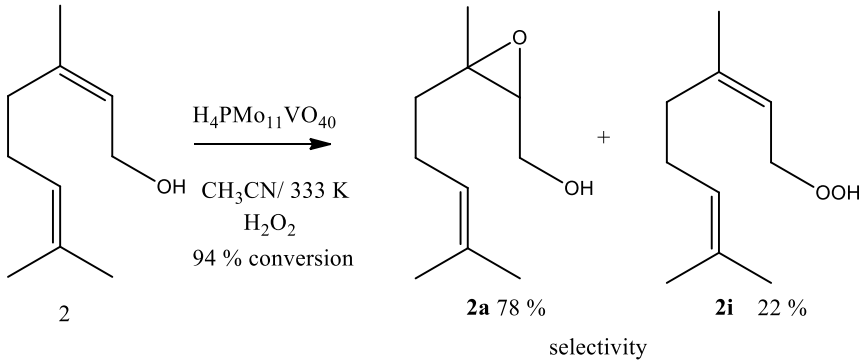

[a]Reaction conditions: nerol (2.75 mmol), catalyst (0.66 mol %), temperature (60 °C), reaction time 8 h, CH_3CN (10 mL).

The probable reaction intermediate, alkyl peroxides, was a secondary product in both cases. The same performance was perceived in the presence of their metal catalysts, Tungsten, Niobium oxides or metal substituted heteropolyacid catalysts (CAVANI; BALLARINI; LUCIANI, 2009; WANG; YANG, 2015; DA SILVA; DA SILVA ANDRADE; SAMPAIO, 2021). In all the cases, different authors ascribed that the epoxidation of these alcohols is a hydroxy group assisted reaction (BECK; MALLAT; BAIKER, 2003).

A tertiary allylic alcohol, Linalool was other substrate evaluated, for this alcohol the epoxide selectivity was lower than that reached (Figure 29) in geraniol and nerol oxidations (Figure 28), even though, its structure has a terminal double bond, which could be more easily epoxidized. This can be explained due to steric effects, the step

of Oxygen atom transfers from peroxide intermediate to double bond, which is promoted by the presence of Vanadium doped catalyst may be less favoured with the structure conformation.

Figure 29 - Scheme 3, $H_4PMo_{11}VO_{40}$-catalyzed linalool oxidation reactions with H_2O_2.[a]

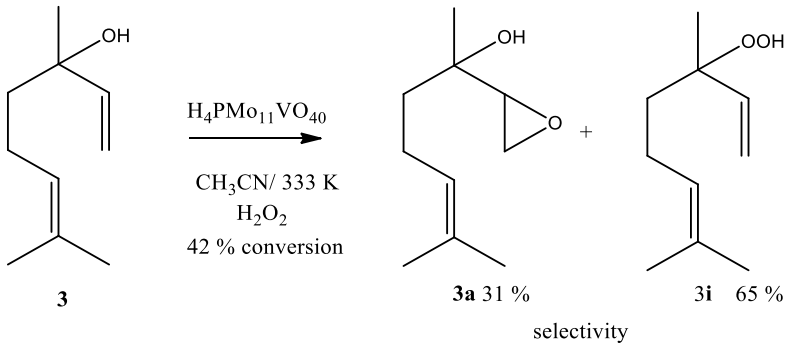

[a]Reaction conditions: linalool (2.75 mmol), catalyst (0.66 mol %), reaction time (8 h), temperature (60°C), CH_3CN (10 mL).

Despite the different performance, it is suggested that the hydroxyl group plays an essential role in these epoxidation reactions, this due to these three terpene alcohols remained with a double bond almost untouched after the oxidation reactions.

Figure 30 - Scheme 4, $H_4PMo_{11}VO_{40}$-catalyzed β-citronellol oxidation reactions with H_2O_2.[a]

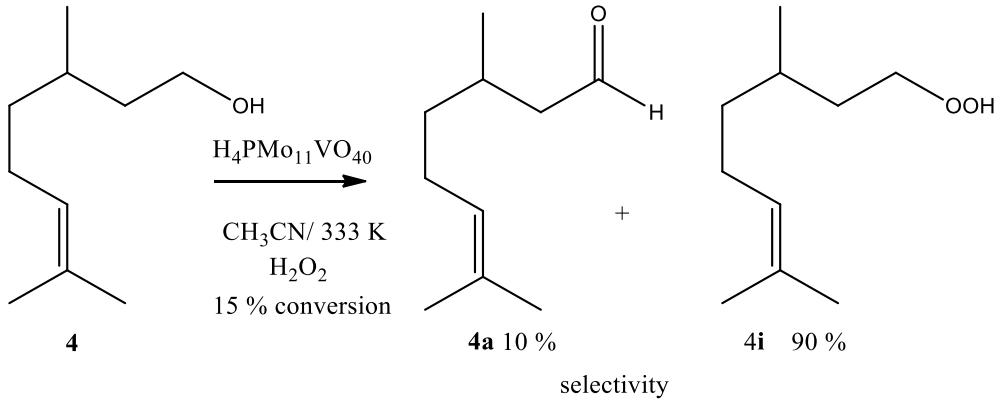

[a]Reaction conditions: β-citronellol (2.75 mmol), catalyst (0.66 mol %), reaction time (8 h), temperature (60°C), CH_3CN (10 mL).

When β-citronellol oxidation reaction was carried out, the main products were alkyl peroxide and β-citronella, this demonstrated that in default of an allylic hydroxyl group, epoxidation is overlooked by the oxidation of hydroxyl carbon to the carbonyl group (Figure 30). Nevertheless, since that β-citronellol is a primary alcohol, under these reaction conditions which are limited by the boiling point of the solvent, only a poor conversion was achieved (ca. 15%, Figure 30).

4.3. Niobium-Doped Phosphomolybdate Acids as Catalysts for Furfural Oxidation with Hydrogen Peroxide in Methyl Alcohol Solutions.

4.3.1 Effect of Niobium doping on the conversion and selectivity of phosphomolybdic acid-catalyzed Furfural oxidative esterification with hydrogen peroxide.

To research the efficiency of Niobium-doped phosphomolybdic acids as catalysts, they were used in the furfural oxidative esterification reactions with hydrogen peroxide and compared with the pristine HPA, the main results are summarized in the (Figure 32). The reaction conditions were chosen base on previous works in our research group, reported by (DA SILVA; RODRIGUES, 2020).

The furfural oxidation reaction can occur without or with rupture of the aromatic ring, the main products commonly obtained in furfural oxidation reactions over heterogeneous catalyst are maleic or succinic acids (LI; HO; ZHANG, 2016; CHOUDHARY; NISHIMURA; EBITANI, 2013). Conversely, in this case is waited that the furfural esterification reactions provided products where the aromatic ring of furfural was preserved (Figure 31), furoic acid, methyl furoate ester, and 2-fufuraldehyde-dimethyl acetal were the main products expects and subsequently identified by GC-MS analyses.

Figure 31 - Scheme 5, main products of Nb-doped phosphomolybdic acid -catalyzed furfural oxidation with H_2O_2.

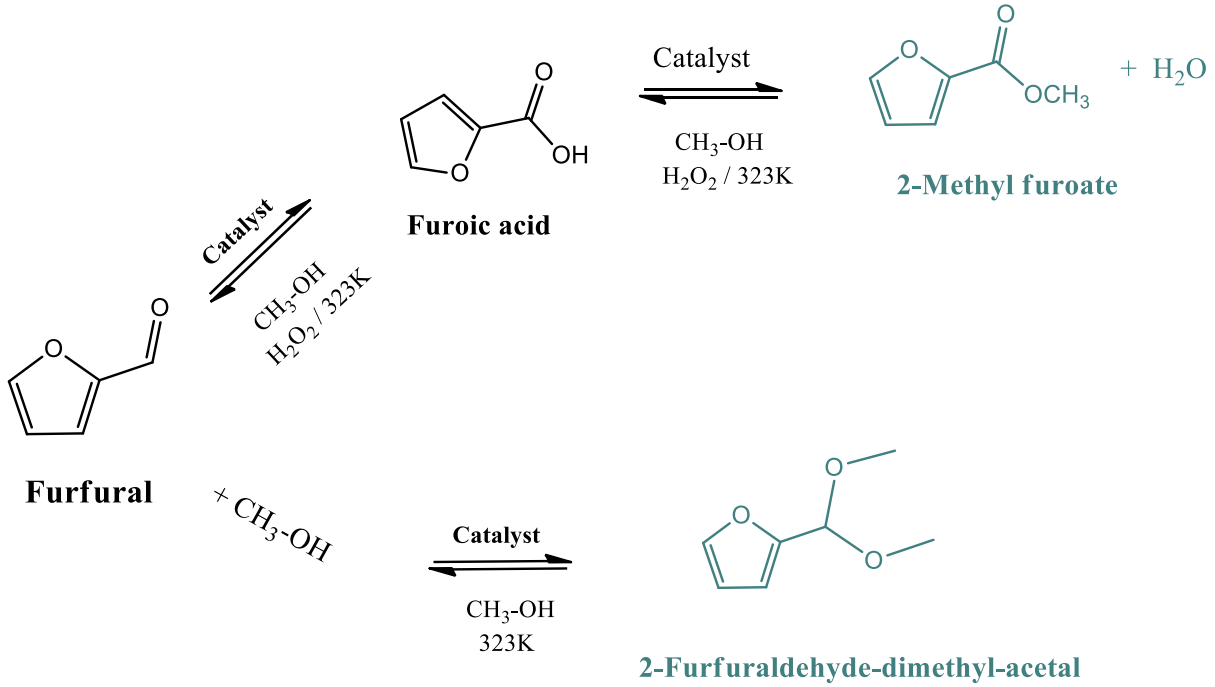

Others products that can be also obtained in the metal-catalyzed oxidation reaction of furfural with hydrogen peroxide, according with the literature, are products with a high molar weight (i.e.., oligomers), these are not detected in gas chromatography analysis. Herein, these products were quantified through the mass balance of reactions, (Equation 4, experimental section), using the comparison between the sum of the GC peak areas of the products with the GC peak area of furfural consume.

Figure 32 shows the reaction conversion and the Figure 33 shown the reaction selectivity of furfural esterification reaction using Nb-doped phosphomolybdic acids as catalyst.

Figure 32 - Effect of the catalyst on the conversion versus time of oxidation reactions of Furfural with H_2O_2.[a]

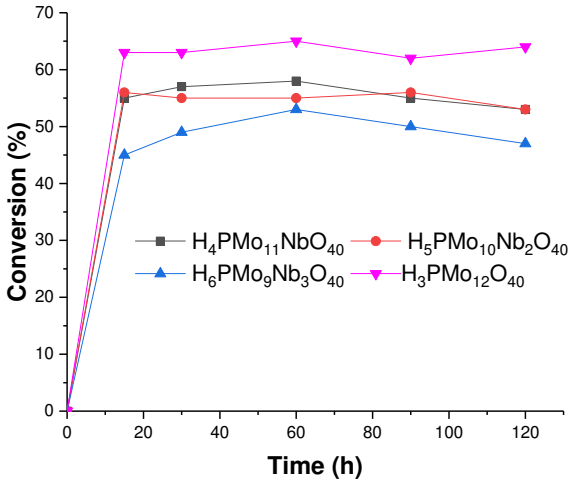

[a] Reaction conditions: (1:2) Furfural (2.5 mmol) and H_2O_2 (5 mmol), MeOH (9.37 mL), Toluene (internal stander), catalysts (1 mol%), temperature (60°C).

Although, the graph is omitted here, the reaction without catalyst was perfumed, in this, almost 30 % of conversion was achieved, it could be explained due to the furfural is a substrate with high reactivity that can react with the atmosphere oxygen and the oxygen present in the hydrogen peroxide.

In the catalyzed reactions (Figure 32), it is shown that the best performance was achieved for the phosphomolybdic acid without Niobium. Besides that, with the increase in the Niobium amount, the conversion decreased. These best efficient of phosphomolybdic acid can be explained by the highest acidity (Figure 18) than the other catalyst, we suppose the Brønsted acid character of this catalyst is a key factor in the oxidation and esterification reactions.

Figure 33a present the selectivity and conversion obtained when the reaction was carried out without catalyst, a lowest conversion was achieved and the main

products were the intermediated alkyl peroxides and acetal, with almost nothing of oxidation product detected.

Figure 33 - Effect of the Nb-catalyst on the selectivity versus time in the oxidation reactions of Furfural with H_2O_2.[a]

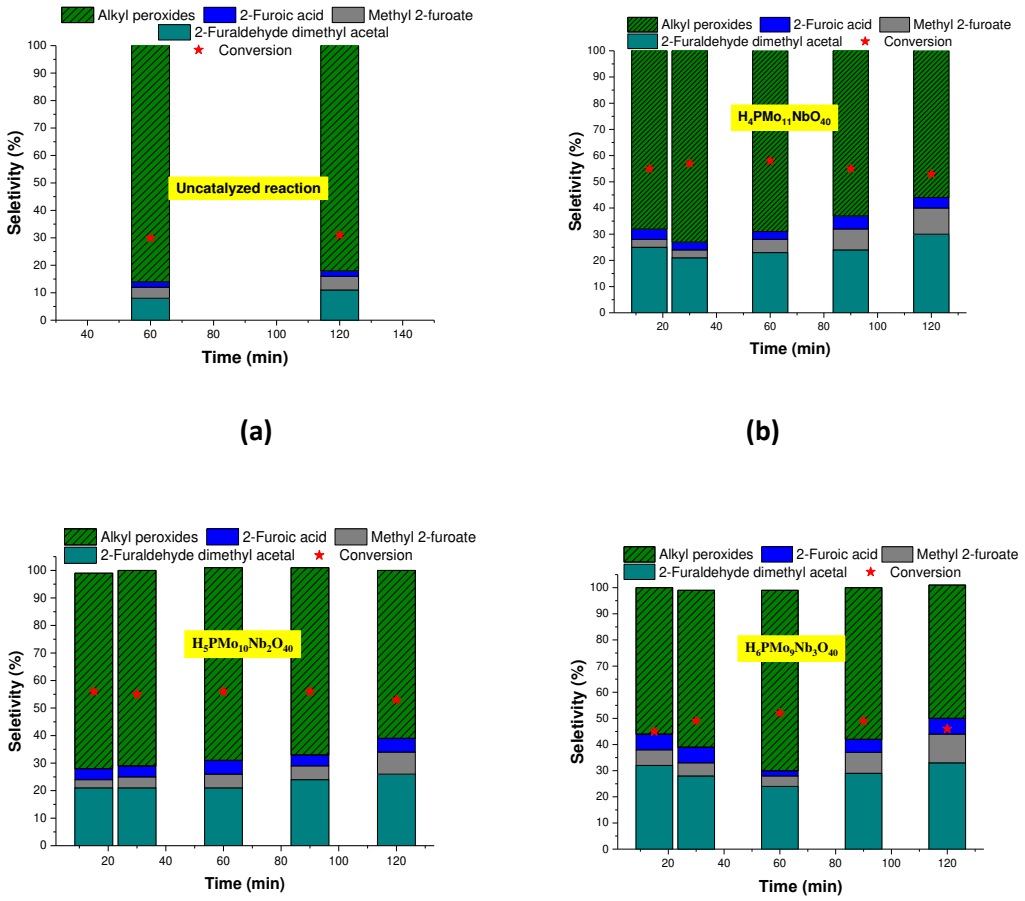

[a]Reaction conditions: (1:2) Furfural (2.5 mmol) and H_2O_2 (5 mmol), MeOH (9.37 mL), Toluene (internal stander), catalysts (1 mol%), temperature (60°C).

Furthermore, with the incorporation and increase in of the Niobium load, the selectivity remains the same, being the alkyl peroxides the main product and the 2-

furaldehyde dimethyl acetal as the secondary (Figure 33b, c, d). in all the cases minor quantity of furoic acid and methyl 2-furoate was formed.

Figure 34 shown the selectivity of the phosphomolybdic acid ($H_3PMo_{12}O_{40}$) in the esterificative oxidation reaction of furfural, when this catalyst was used, not oxidation product was formed, an 100% of the selectivity was for the condensation product.

Figure 34 - Effect of the phosphomolybdic acid as catalyst on the selectivity in the oxidation reactions of Furfural with H_2O_2.[a]

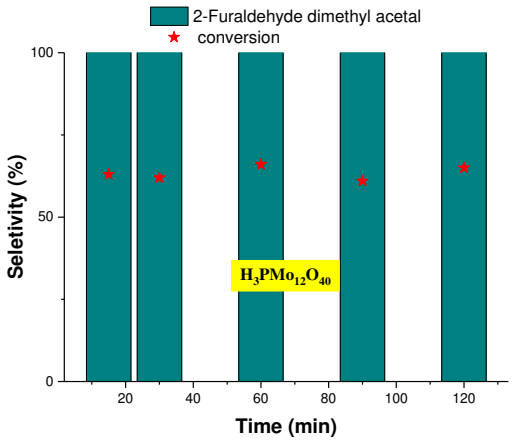

[a] Reaction conditions: (1:2) Furfural (2.5 mmol) and H_2O_2 (5 mmol), MeOH (9.37 mL), Toluene (internal stander), catalysts (1 mol%), temperature (60°C).

In previous report was found that these two competitive reactions, oligomerization and condensation of furfural with methyl alcohol, endanger the selectivity of the goal products (i.e., furoic acid and methyl furoate) (DA SILVA; RODRIGUES, 2020). The oligomerization is a common reaction experimented by furfural, in these reactions furan-base intermediates generated during the reaction are involved. This reactions is carried out more easily when H^+ and or peroxides

intermediates are present (DA SILVA; TEIXEIRA, 2018; TEIXEIRA; NATALINO; DA SILVA, 2020b) . In the same way, furfural condensation with alcohols is favored by H^+ ions. These ions are generated in the hydrolysis implying the water produced in the reaction and the Lewis acid metal cations (FUCHS; PIZZIO; BLANCO, 2008; DA SILVA; TEIXEIRA, 2018).

Taking into account the information in the literature and the results, which show that the performance of the Nb-doped phosphomolybdic acids as catalyst in the oxidative esterification is not sufficient and the selectivity toward the condensation products, we take the decision to teste our materials as possible catalysts in furfural acetalization reactions.

4.4. Niobium-Substituted Phosphomolybdate Acids as Catalysts for Furfural Acetalization

4.4.1 Effect of type of Nb-doped phosphomolybdic acid as catalyst in acetalization reaction of furfural

Furfural acetalization is a reaction in which acetal is generallt obtained as the main product. Although, the main product is the acetal, hemiacetals that are reaction intermediates could be obtained. However, as is descripted by (HRONEC et al., 2020) the stables hemiacetals can be only obtained as product when the catalyst is used with hydrogen and the basic catalysts. In addition, how this reaction is a reversible process, the more stable tetrahydrofurfuryl hemiacetal must be formed to achieve the equilibrium and the furfural acetal as main product.

To study the catalytic activity of Nb-doped phosphomolybdic acid in the furfural acetalization, the next catalytic tests were make, the initial reaction conditions were chosen taking as reference (DA SILVA; RODRIGUES, 2020),and previous tests in oxidative esterification reaction of furfural with the same catalyst, but in this case, hydrogen peroxide was not used.

When the furfural acetalization reaction with methanol was performed without catalyst a poor conversion was observed (omitted in Figure 35). Regardless of the alcohol excess.

Figure 35 - Effect of the catalyst on the conversion of acetalization reactions of Furfural.[a]

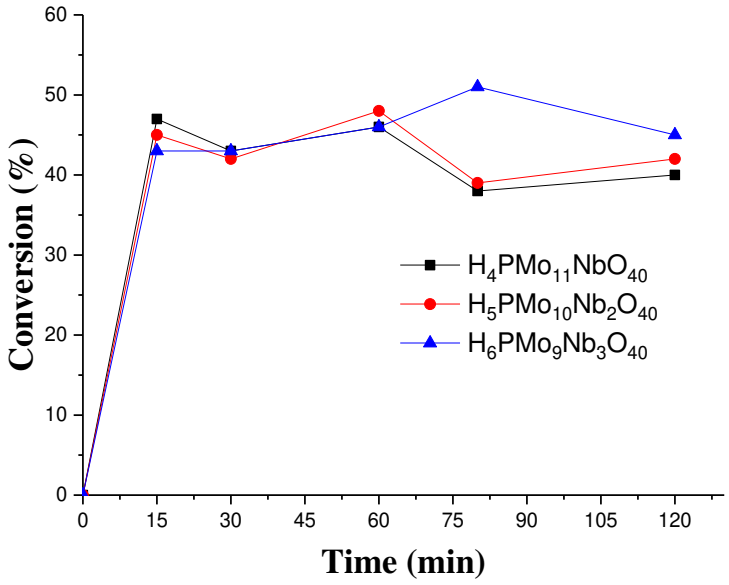

[a]Reaction conditions: Furfural (2.5 mmol), toluene (internal stander), temperature (50°C), MeOH (9,4 mL), Catalyst (1 mol %).

When the reaction was carried out in presence the catalyst a conversion improvement was observe (Figure 35). However, no significant difference was observing between catalysts with different Nb load and without Niobium (pristine $H_3PMo_{12}O_{40}$). All the catalyst shown conversion near 50% after the first hour of reaction. In addition, the $H_6PMo_9Nb_3O_{40}$ showed a slight enhancement in the conversion after one and half past hour of reaction. In all the runs, dimethyl acetal furfural was the only product.

The performance of the Niobium catalyst can be assigned to its strongest acidity; the catalyst acidity was previously estimated using potentiometric titration with n-butylamine (as reported in section 4.1.3), there is seem that all the catalyst presents almost the same acidity, it could be explaining the similar performance. Although, the acidy is a key factor to the success in the furfural acetalization reaction, the size of the

pore volume can also play an essential role in reaction (CLIMENT et al., 1998). Nevertheless, in our situation this explication is no useful due to the catalyst work in homogeneous phase.

The Brønsted and Lewis acid sites play the fundamental role of activate the carbon carbonylic of furfural, fostering its nucleophilic attack by the hydroxyl group of alcohol. This process can occur through the protonation step (i.e., Brønsted acidic site) or polarization (i.e., Lewis acidic site) of the furfural carbonyl group.

Taking as reference the slight in the conversion obtained in the reactions when the Nb_3-phosphomolybdic acid, was used, it was selected to evaluate the effect of the reaction parameters.

4.4.2 Effect of high concentration catalyst and low furfural load in acetalization reaction

To evaluate the effect in the catalyst and furfural load, the first test make was increase the catalytic concentration in the reaction. In the Figure 36, it is shown that when the catalyst load is high increased in the reaction conditions, the conversion of furfural in 2-furfuraldehyde-methylacetal (FMD) decrease. This effect was previous reported when acid catalyst where used in furfural acetalization, where it shows that when catalyst loading was further increase, the FMD conversion decreased, this behavior can be explained due to the equilibrium in the reaction is achieve faster with more acid sites and side reactions such as hydrolysis of furfural acetal could be occurring (KIM et al., 2018; SONG et al., 2021).

Figure 36 - - Effect of catalyst and furfural load on the conversion of acetalization reactions of Furfural.[a]

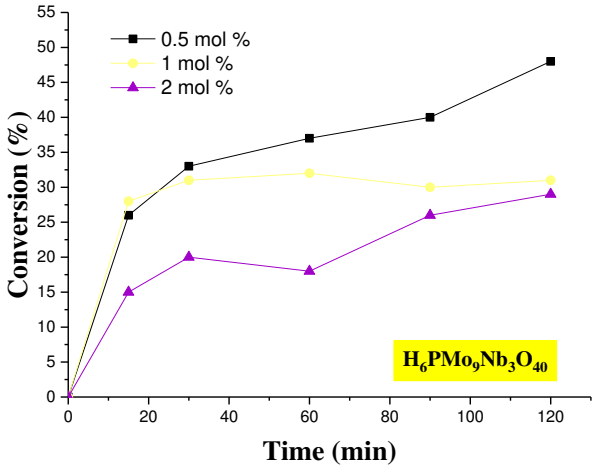

[a]Reaction conditions: Furfural (1,25 mmol), toluene (internal stander), temperature (50°C), MeOH (9,8 mL).

To evaluate, if the conversion was affected by the acidy or excess of catalyst, we decide to decrease the catalyst amount in the reaction conditions, Figure 37, allows to confirmed that and excess of catalyst and acidity sites was present in the initial reactions, in this is shown, that when a lower amount of catalyst was used, the catalytic conversion of furfural in FMD was enhance. It is shown that the best conversion was achieved when the catalyst load was 0.0312 mol %, reaching almost 55% of conversion in the first hour reaction.

Figure 37 - Effect of lower catalyst load on the conversion of acetalization reactions of Furfural.[a]

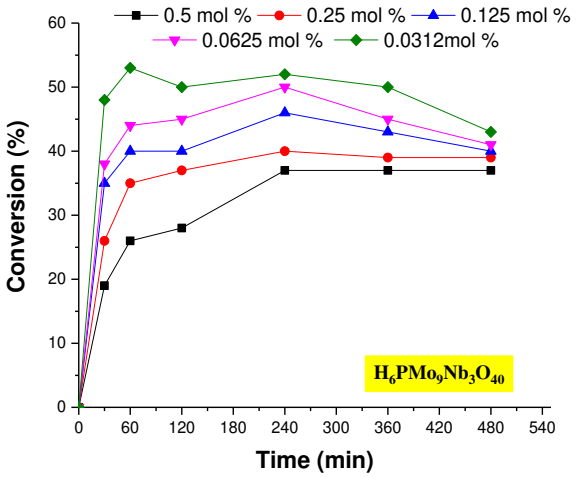

[a] Reaction conditions: Furfural (1,25 mmol), toluene (internal stander), temperature (50°C), MeOH (9,8 mL).

4.4.3 Effect of substrate and catalyst concentration furfural acetalization reaction: high substrate charge and catalyst load

It is known that furfural acetalization is a reversible reaction, and how was descripted by (MOREAU et al., 1997) the hydrolysis of acetals and thioacetal of furfural can be done in water and in the presence of strong Brønsted acid, through a pseudo-first order mechanism, the water produced in the acetalization reaction together with the Brønsted acid sites present in the Nb-doped phosphomolybdic acids, could hydrolyze the furfural dimethyl acetal to produce furfural in the reaction process (Figure 41).

For this, the furfural concentration in the reaction was varied, it was initially decrease from 2,5 mmol to 1,25 mmol as shown in Figures 36,37 and subsequently increase to 3,6 mmol (Figure 38), for this, the optimized conditions of catalyst load

used found in the section 4.4.2 were used. A similar study was previously conducted by (RUBIO-CABALLERO et al., 2014).

Figure 38 - Effect of high furfural charge and catalyst load on the conversion of furfural in acetalization reaction. [a]

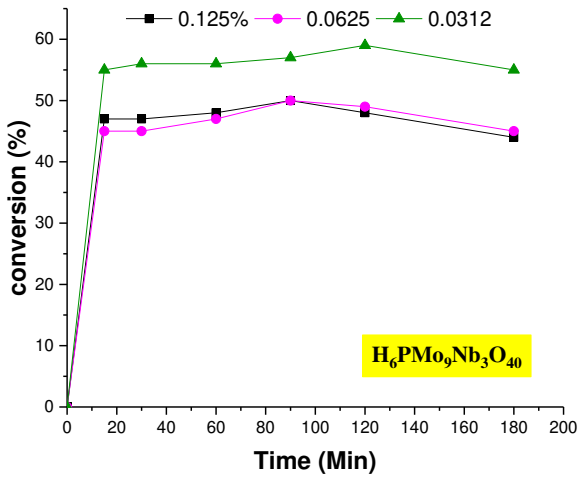

[a] Reaction conditions: Furfural (3,6mmol), toluene (internal stander), temperature 50°C), MeOH (9,6 mL).

Figure 38, shown that no matter the concentration of furfural the 2-furfuraldehyde-methylacetal yield remained almost unchanged, implying that the high or less amount quantity of furfural in the reaction is not a parameter that affects the selectivity. However, it is clear see that the maximum conversion is achieved in the first 15 minutes of reaction in all the situations. In addition, the catalyst loading seems to have the same effect regardless of the new reaction conditions.

4.4.4 Effect of high temperature and closed conditions in furfural Acetalization

To check the effect of temperature and the gas phase, the reaction was conducted in a reactor in close conditions, the temperature was elevated to 80°C under constant agitation.

Figure 39 - Effect of catalyst load, high temperature and closed conditions on the conversion of acetalization reactions of Furfural.[a]

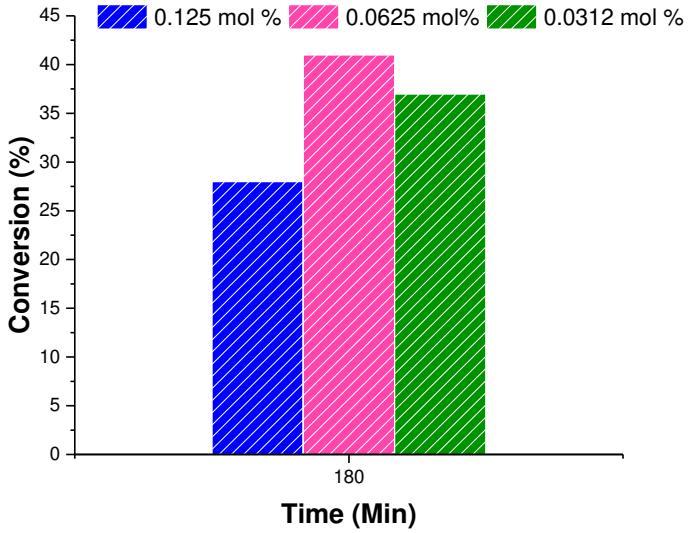

[a]Reaction conditions: Furfural (3,6mmol), toluene (internal stander), temperature (80°C), MeOH (9,6 mL), catalyst ($H_6PMo_9Nb_3O_{40}$).

Another effect, that can be study through this experience is check if any an oxidative route could be also occurring here. In the close conditions, with absence of atmospheric oxygen, the reaction seems to lees favorable and the furfural dimethyl acetal conversion decrease as is shown in the Figure 39. A difference in the catalytic behavior was observe when the catalytic load was change, it's possible to seem that

the concentration of 0.0625 mol% of catalyst achieve a better conversion in this situation.

As suggested by (DA SILVA; TEIXEIRA, 2018), the generation of H^+ cations in the reaction in close conditions can reduce the pH of reaction, it can be useful to explain the variation in the catalytic behavior. When the concentration of catalyst was 0.0312 mol %, the acidity was not enough to achieve the best performance, in the case where the catalytic concentration was 0.125 mol% may an excess of acidy was present, leaving as a result better performance when the catalyst load was 0.0625 mol%.

The increase in the temperature does not seem to improve the reaction performance, in addition, no oxidative route seems likely, since selectivity was maintained towards furfural dimethyl acetal.

4.4.5 Application of the optimized reaction conditions for acetalization of furfural using substituted Nb1,2,3 heteropoly acids

To ensure that under the optimized conditions, the best performances is achieved by the three Nb_3-doped phosphomolybdic acid, we decided to test the three synthesized catalyst (i.e.., $H_4PMo_{11}NbO_{40}$, $H_5PMo_{10}Nb_2O_{40}$, $H_6PMo_9Nb_3O_{40}$), the conditions test were 3.6 mmol of furfural, 9.6 mL of methanol, toluene as internal standard, 0.0312 mol % of catalyst and 50 °C, the reaction was carried out in a 25 mL three-necked glass reactor, equipped with a reflux condenser and sampling system, under magnetic stirring, the results are showed in Figure 40.

Figure 40 - Effect of type of catalyst in optimal conditions on the conversion of acetalization reactions of Furfural. [a]

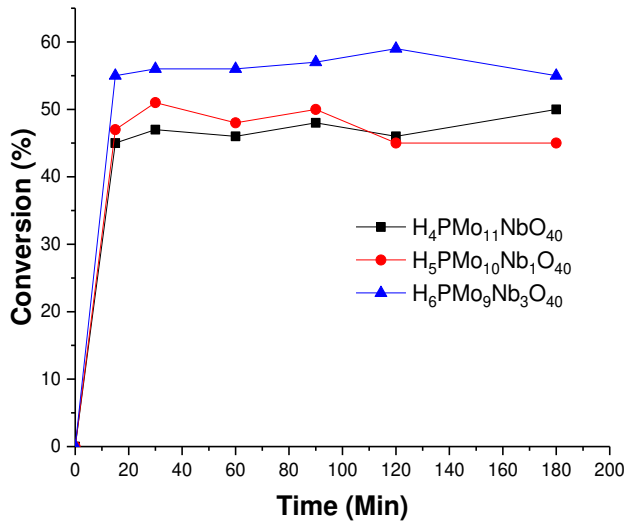

[a]Reaction conditions: Furfural (3,6mmol), toluene (internal stander), temperature (50°C), MeOH (9,6 mL), catalyst load (0.0312 mol %)

In the Figure 40, it is clear seem that the three catalyst present almost the same performance in the furfural acetalization reaction under the tested conditions. This allows us to infer that the catalysts have similar catalytic proprieties in the accomplished reaction.

4.4.6 Reaction mechanism proposal of the furfural acetalization with methanol in the presence of Nb-doped phosphomolybdic acid

Taking as reference results in the literature (RUBIO-CABALLERO et al., 2014; TEIXEIRA; NATALINO; DA SILVA, 2020b) we propose a mechanism involving cations H^+ present in the catalyst or generated in the reaction of the metals and methyl alcohol

(Figure 41). As was previous mentioned, the role of catalyst is to increment the electrophylicity of the carbonyl carbon of furfural and allow that the reaction proceed.

In according with the proposal mechanism in the Figure 41 taking the route (a), on the first step (I) occurs the formation of a protonated intermediate (II), which suffer a nucleophilic attack by the methyl alcohol molecule, generation a protonated tetrahedral intermediate that after being deprotonated, gives the hemiacetal (III), this hemiacetal is protonated and after that, result in the releasing of the water molecule (IV). The oxonium ion resulting (V) is attack by another methyl alcohol molecule giving the protonate acetal (VI), this final H^+ cation can start another catalytic cycle, leaving as result the 2-furfuraldehyde-dimethyl acetal.

As proposal by (DA SILVA; TEIXEIRA, 2018) we consider that the Brønsted acidity is not the only aspect to be considered, for us, it is possible think that Lewis acidity of the transition metals can be also important in acetilization reaction to active the aldehyde carbonyl group through polarization after coordination step (Figure 41b).

Figure 41 - Proposal reaction mechanism of furfural acetalization, a) H^+ catalyzed route, b) Metal catalyst route.

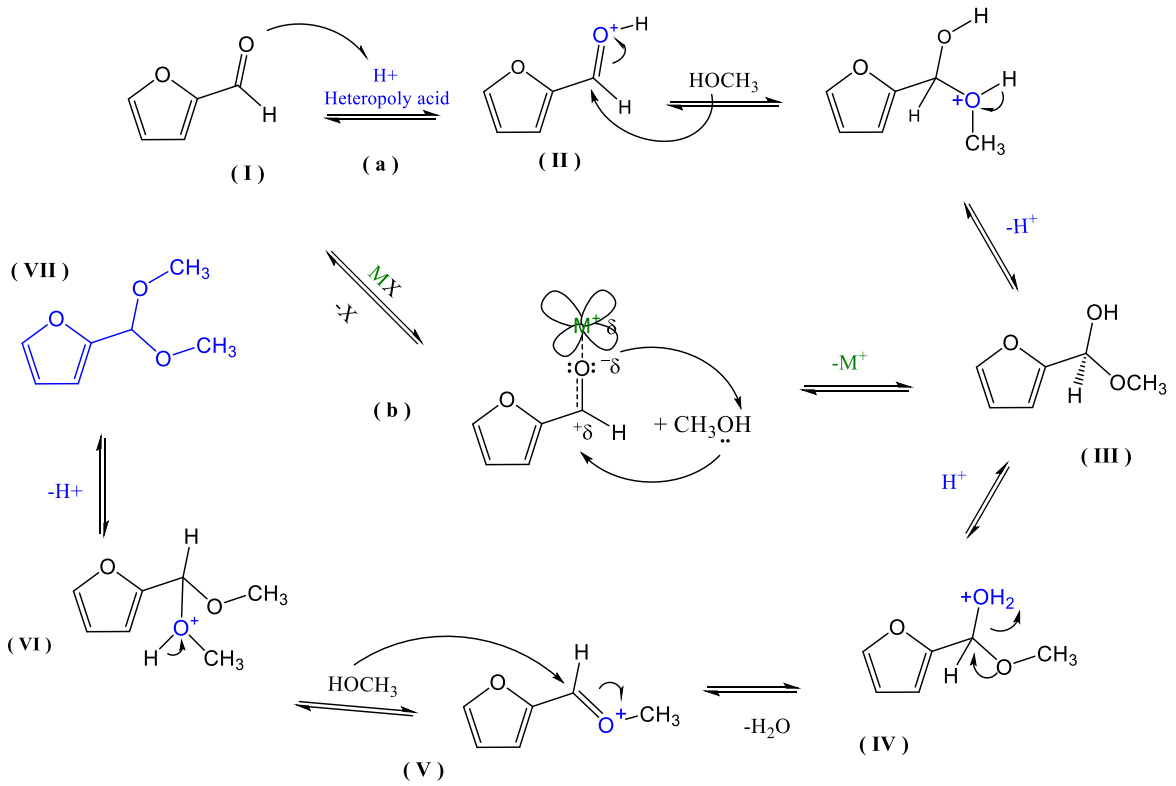

Adapted from: (RUBIO-CABALLERO et al., 2014; TEIXEIRA; NATALINO; DA SILVA, 2020b; DA SILVA; TEIXEIRA, 2018)

For Nb it is possible to propose that the interaction between of the HOMO orbitals of the metal (empty “d” orbitals of Niobium) and LUMO orbitals of the ligands (electrons of the carbonylic Oxygen), delocalize the electron density of the carbonyl carbon, allowing more easily the attack of the oxygen in the methyl alcohol (Figure 41b), it information is confirmed by (CLIMENT et al., 1998)(DA SILVA; TEIXEIRA; NATALINO, 2019) in other publications. Finally, metal cation such as Nb with Lewis acidity can interact with alcohols releasing H^+ in the alcohol, which can catalyze the

reaction (DA SILVA; CARARI; MANOEL DA SILVA, 2015)(DA SILVA; DE OLIVEIRA, 2021)

4.4.7 Effect of the aldehyde on the Nb-doped phosphomolybdic acid-catalyzed acetalization reaction of methyl alcohol

After having carried out the reaction of acetalization of furfural under the optimal conditions, we decided to assessment the efficiency of the three Nb-doped catalyst synthesized on the acetalization reaction with methanol of benzaldehyde, other aromatic aldehyde. The used conditions were the same as those used for furfural, in this situation the same amount in mL of aldehyde was used (e.i., 0,30 mL). trying to ensure that the new aldehyde was not in excess. In this reaction, benzaldehyde methyl acetal was the only product selectively formed. The results are showed in. Figure 42.

In the Figure 42, it is clear seem, that in the absence of catalyst the reaction does not proceed. When the different catalysts where used the reaction reached in all cases conversions greater than 55%. However, the type of catalyst did not show a significant difference in the behavior, in the used concentration range, the three catalyst showed close performance.

Figure 42 - Effect of type of catalyst in optimal conditions on the conversion of acetalization reactions of Benzaldehyde for comparison with Furfural reactions.[a]

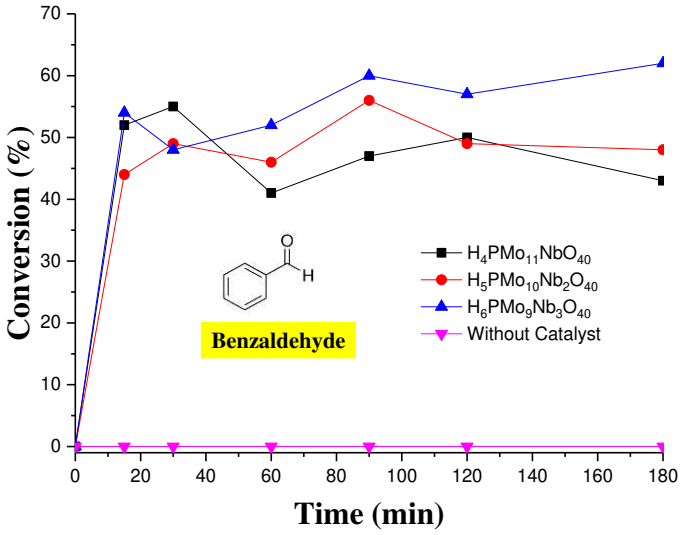

[a]Reaction conditions: Benzaldehyde (2,94 mmol), toluene (internal stander), temperature (50°C), MeOH (9,6 mL), catalyst load (0.0312 mol %).

As it was shown in the different experiments with furfural, there was a slight improvement in the conversion, when the Nb_3-doped catalyst was used. A same behavior was showed in previous research where benzaldehyde was used to study the effect of the aldehyde type being comparted to furfural(DA SILVA; TEIXEIRA; NATALINO, 2019)

5. CONCLUSION

In this work, phosphomolybdic acids doped with different Niobium loads were synthesized, characterized, and evaluated as catalysts in the oxidative esterification and acetalization of biomass aldehydes. In addition, the catalytic activity of Vanadium doped phosphomolybdic acids was assessed in the oxidation of terpene alcohols using hydrogen peroxide as a green oxidant, and CH_3CN as solvent. The Nb-doped phosphomolybdic acids were characterized by spectroscopy analyses in the infrared and UV-Vis, and powder X-ray diffraction patterns analyses, which allowed us to confirm that the synthesis of the three Nb-doped catalysts was successfully performed. Similarly, to the observed in Vanadium doped HPAs, the doping with Niobium did not affect the Keggin anion structure. When the Nb-doped HPAs and $H_3PMo_{12}O_{40}$ acid were tested as catalysts in the oxidative esterification of furfural in methanol, the best performance was achieved for $H_3PMo_{12}O_{40}$ acid, and the conversion became worse when the Nb loads increase. Indeed, when the Nb-doped acids were the catalysts the reaction selectivity was mainly toward the intermediated alkyl peroxides, suggesting that they were unable to convert these intermediates to desired oxidation products (i.e., acid and or ester). In addition, when the $H_3PMo_{12}O_{40}$ acid was tested, 100 % of the selectivity was toward 2-furfuraldehyde dimethyl acetal. Alternatively, the hydrogen peroxide was avoided, and these catalysts were also assessed in the acetalization reaction of furfural using methanol. When the reaction was carried out with the three Niobium catalysts no significant difference in the performance (i.e., conversion near to 50%, selectivity of 100% to acetal) was noticed. Only the $H_6PMo_9Nb_3O_{40}$ show a slight enhancement in the conversion, the catalytic activity of the catalyst was assigned to its strongest Brønsted acidity and the Lewis acidity that can play an important role. The effect of the main reaction variables was assessed using $H_6PMo_9Nb_3O_{40}$ as a catalyst,

obtained the lowest catalyst load as the best condition (i.e., 0.0312 mol%), confirming the strong acid force of the catalyst. Other studies are in development aiming to improve the performance of Niobium catalysts in furfural acetalization reactions. Finally, the reaction conditions were extended to the benzaldehyde showing almost the same behavior. The epoxidation of terpenic alcohols using Vanadium-doped phosphomolybdic acid was studied. The effect of the main reaction variables was assessed using geraniol as a model substrate. The best performance was achieved by $H_4PMo_{11}VO_{40}$ acid. The greatest catalytic capacity of the monosubstituted acid was assigned to two principal reasons; the highest reduction potential and the Brønsted acidity. In addition, compared with other Brønsted acids (i.e., sulfuric and p-toluene sulfonic acids) and even with the pristine phosphomolybdic acid, the Brønsted acidity, the Vanadium monosubstituted acid shows the best performance. It can be assigned to the Vanadium incorporation, which increases the potential reduction, accelerating the redox activity of the catalysts. Conversion higher than 90% and selectivity (80- 85 %) was achieved after the first reaction hour. When the reaction scope was extended to other terpene alcohols, we verified that this reaction is a hydroxyl group assisted reaction. Only geraniol and nerol that allylic alcohols were efficiently oxidized.

This was the first work in which phosphomolybdic acid catalysts containing Niobium were successfully synthesized, which opens new perspectives that they can be used in other reactions. In addition, it was the first time that Vanadium doped phosphomolybdic acid catalysts were used with success in terpene alcohol oxidations with hydrogen peroxide.

6. FUTURE PERSPECTIVES

As future perspectives of this research we have the following experiments:

- Use the different Nb-doped catalysts in reactions with others aldehydes
- Study of the redox properties of the different catalysts.
- Synthesize Sodium and Cesium salts from Nb-doped catalyst for homogeneous and heterogeneous studies, respectively.
- Synthesize Nb-doped phosphomolybdic lacunary salts as heterogeneous catalyst
- Characterize the strength of acidity of the Niobium and Vanadium phosphomolybdic acid catalysts NH_3 temperature-programmed desorption
- Use the Niobium and Vanadium catalysts in oxidation reactions of furfural and other derivatives substrates from biomass
- Used the Niobium and Vanadium catalyst in condensation reactions of biomass derivatives substrates

7. REFERENCES

ATKINS, P.; DE PAULA, J. Físico-Química. 9. ed. Rio de Janeiro: LTC, 2012.

AGRAWAL, M. K. ADIMURTHY, S. GHOSH, P. K. Oxidative esterification of benzaldehyde and deactivated aromatic aldehydes with N-bromosuccinimide-pyridine. Synthetic Communications, v. 42, n. 19, p. 2931–2936, 2012. DOI: 10.1080/00397911.2011.572219.

ALONSO-FAGÚNDEZ, N. GRANADOS, M. L. MARISCAL, R. OJEDA, M. Selective conversion of furfural to maleic anhydride and furan with VO x/Al_2O_3 catalysts. ChemSusChem, v. 5, n. 10, p. 1984–1990, 2012. DOI: 10.1002/cssc.201200167.

ALSALME, A. KOZHEVNIKOVA, E. F.KOZHEVNIKOV, I. V. Heteropoly acids as catalysts for liquid-phase esterification and transesterification. Applied Catalysis A: General, v. 349, n. 1–2, p. 170–176, 2008. DOI: 10.1016/j.apcata.2008.07.027.

ARCORIA, A. BALLISTRERI, F. P. TOMASELLI, G. A. FURIA, F. D. MODENA, G. Opposite Regioselectivity in the Epoxidation of Geraniol and Linalool with Molybdenum and Tungsten Peroxo Complexes. Journal of Organic Chemistry, v. 51, n. 12, p. 2374–2376, 1986. DOI: 10.1021/jo00362a037.

ARICHI, J. ETERNOT, M. LOUIS, B. Synthesis of V-containing Keggin polyoxometalates: Versatile catalysts for the synthesis of fine chemicals?, Catalysis Today, v. 138, n. 1–2, p. 117–122, 2008. DOI: 10.1016/j.cattod.2008.04.036.

AXELSSON, L. FRANZÉN, M. OSTWALD, M. BERNDES, G. LAKSHMI, G.; RAVINDRANATH, N. H. Perspective: Jatropha cultivation in southern India: Assessing farmers' experiences. Biofuels, Bioproducts and Biorefining, v. 6, n. 3, p. 246–256, 2012. DOI: 10.1002/bbb.

BAO, Q. QIAO, K. TOMIDA, D. YOKOYAMA, C.. Acetalization of carbonyl compounds catalyzed by $GaCl_3$ immobilized on imidazolium-styrene copolymers. Catalysis Communications, v. 10, n. 12, p. 1625–1628, 2009. DOI:

10.1016/j.catcom.2009.04.018.

BARDIN, B.B. BORDAWEKAR, S. V.; NEUROCK, M. DAVIS, R.J. Acidity of keggin-type heteropolycompounds evaluated by catalytic probe reactions, sorption microcalorimetry, and density functional quantum chemical calculations. Journal of Physical Chemistry B,v. 102, n. 52, p. 10817–10825, 1998. DOI: 10.1021/jp982345y.

BARLUENGA, J. GONZÁLEZ-BOBES, F. MURGUÍA, M. C.; ANANTHOJU, S. R. GONZÁLEZ, J. M. Bis(pyridine)iodonium tetrafluoroborate (IPy_2BF_4): A versatile oxidizing reagent. Chemistry - A European Journal, v. 10, n. 17, p. 4206–4213, 2004. DOI: 10.1002/chem.200400136.

BAROI, C. GAFFNEY, A. M.; FUSHIMI, Rebecca. Process economics and safety considerations for the oxidative dehydrogenation of ethane using the M1 catalyst. Catalysis Today, v. 298, n. April, p. 138–144, 2017. DOI: 10.1016/j.cattod.2017.05.041.

BARTEAU, K. P.; LYONS, J. E.; SONG, I. K.; BARTEAU, M. A. UV-visible spectroscopy as a probe of heteropolyacid redox properties: Application to liquid phase oxidations. Topics in Catalysis, v. 41, n. 1–4, p. 55–62, 2006. DOI: 10.1007/s11244-006-0094-6.

BECK, C.; MALLAT, T.; BAIKER, A. Epoxidation of allylic alcohols with TiO_2-SiO_2: Hydroxy-assisted mechanism and dynamic structural changes during reaction. Catalysis Letters, v. 88, n. 3–4, p. 203–209, 2003. DOI: 10.1023/A:1024074108874.

BELSITO, D. et al. A toxicologic and dermatologic assessment of cyclic and non-cyclic terpene alcohols when used as fragrance ingredients. Food and Chemical Toxicology, v. 46, n. 11 SUPPL., 2008. DOI: 10.1016/j.fct.2008.06.085.

BERNARDO-GUSMÃO, K. PERGHER, S. B. C.; DOS SANTOS, E. N. Um panorama da Catálise no Brasil nos últimos 40 anos. Quimica Nova, v. 40, n. 6, p. 650–655, 2017. DOI: 10.21577/0100-4042.20170083.

BIZZI, C. A.; SANTOS, D. SIEBEN, T. C.; MOTTA, G. V.; MELLO, Paola A.; FLORES, E. M. M. Furfural production from lignocellulosic biomass by ultrasound-assisted acid hydrolysis. Ultrasonics Sonochemistry, v. 51, p. 332–339, 2019. DOI: 10.1016/j.ultsonch.2018.09.011.

BIZZO, H. R.; ANA MARIA, C. H. REZENDE, C. M. Oleos essenciais no brasil: aspectos gerais, desenvolvimento e perspectivas. Quimica Nova, v. 32, n. 3, p. 588–594, 2009. DOI: 10.1590/S0100-40422009000300005.

BOTELLA, P. DEJOZ, A.ABELLO, M. C.; VÁZQUEZ, M. I.; ARRÚA, L.; LÓPEZ NIETO, J. M. Selective oxidation of ethane: Developing an orthorhombic phase in Mo-V-X (X = Nb, Sb, Te) mixed oxides. Catalysis Today, v. 142, n. 3–4, p. 272–277, 2009. DOI: 10.1016/j.cattod.2008.09.016.

CÁNEPA, A. L.; CHANQUÍA, C. M.; EIMER, G. A.; CASUSCELLI, S. G. Oxidation of olefins employing mesoporous molecular sieves modified with copper. Applied Catalysis A: General, v. 462–463, p. 8–14, 2013. DOI: 10.1016/j.apcata.2013.04.031.

CASARINI, D. CENTI, G. JÍRŮ, P. LENA, V. TVARŮŽKOVÁ, Z.. Reactivity of molybdovanadophosphoric acids: Influence of the presence of vanadium in the primary and secondary structureJournal of Catalysis, 1993. DOI: 10.1006/jcat.1993.1280.

CAVANI, F. BALLARINI, N. LUCIANI, S. Catalysis for society: Towards improved process efficiency in catalytic selective oxidations. Topics in Catalysis, v. 52, n. 8, p. 935–947, 2009. DOI: 10.1007/s11244-009-9244-y.

CHAVAN, S. P.; DANTALE, S. W.; GOVANDE, C. A.; VENKATRAMAN, M. S. PRAVEEN, C.. Titanosilicate (TS-1) catalyzed oxidation of aromatic aldehydes to esters. Synlett, n. 2, p. 267–268, 2002. DOI: 10.1055/s-2002-19744.

CHAVES, D. M. FERREIRA, S. O. CHAGAS DA SILVA, R. NATALINO, R. JOSÉ DA SILVA, M. Glycerol Esterification over Sn(II)-Exchanged Keggin Heteropoly Salt Catalysts: Effect of Thermal Treatment Temperature. Energy and Fuels, v. 33, n. 8, p. 7705–7716, 2019. DOI: 10.1021/acs.energyfuels.9b01583.

CHOUDHARY, H. NISHIMURA, S. EBITANI, K. Metal-free oxidative synthesis of succinic acid from biomass-derived furan compounds using a solid acid catalyst with hydrogen peroxide. Applied Catalysis A: General, v. 458, p. 55–62, 2013. DOI: 10.1016/j.apcata.2013.03.033.

CHOUDHARY, V. R.; DHAR, A. JANA, P. JHA, R. UPHADE, Balu S. A green process for chlorine-free benzaldehyde from the solvent-free oxidation of benzyl alcohol with molecular oxygen over a supported nano-size gold catalyst. Green Chemistry, v. 7, n. 11, p. 768–770, 2005. DOI: 10.1039/b509003b.

CHOUDHARY, V.R. DUMBRE, D. K.; BHARGAVA, S. K. Oxidation of benzyl alcohol to benzaldehyde by tert-butyl hydroperoxide over nanogold supported on TiO_2 and other transition and rare-earth metal oxides. Industrial and Engineering Chemistry Research, v. 48, n. 21, p. 9471–9478, 2009. DOI: 10.1021/ie801883d.

CLARK, J. H. Solid acids for green chemistry. Accounts of Chemical Research, v. 35, n. 9, p. 791–797, 2002. DOI: 10.1021/ar010072a.

CLIMENT, M. J.; CORMA, A.; GUIL-LÓPEZ, R.; IBORRA, S.; PRIMO, J. Use of mesoporous MCM-41 aluminosilicates as catalysts in the preparation of fine chemicals: A new route for the preparation of jasminaldehyde with high selectivity. Journal of Catalysis, *[S. l.]*, v. 175, n. 1, p. 70–79, 1998. DOI: 10.1006/jcat.1998.1970.

COLOMBO MIGLIORERO. B. PALERMO, V. ROMANELLI, G. P.; VÁZQUEZ, P. G. New niobium heteropolyacid included in a silica/alumina matrix: Application in selective sulfoxidation. Catalysis Today,. March, 2020. DOI: 10.1016/j.cattod.2020.10.034.

COLOMBO MIGLIORERO, M. B.; PALERMO, V. ROMANELLI, G. P.; VÁZQUEZ, P. G. New niobium heteropolyacid included in a silica/alumina matrix: Application in selective sulfoxidation. Catalysis Today, v. 372, n. October, p. 89–97, 2021. DOI: 10.1016/j.cattod.2020.10.034.

CORMA CANOS, A. IBORRA, S. VELTY, A. Chemical routes for the transformation of

biomass into chemicals. Chemical Reviews, v. 107, n. 6, p. 2411–2502, 2007. DOI: 10.1021/cr050989d.

CORONEL, N. C. DA SILVA, M. J.; FERREIRA, S. O.; DA SILVA, R. C.; NATALINO, Ricardo. $K_5PW_{11}NiO_{39}$-catalyzed oxidation of benzyl alcohol with hydrogen peroxide. ChemistrySelect, v. 4, n. 1, p. 302–310, 2019. DOI: 10.1002/slct.201802616.

CORONEL, N.C. DA SILVA, M. J. Lacunar Keggin Heteropolyacid Salts: Soluble, Solid and Solid-Supported Catalysts. Journal of Cluster Science, v. 29, n. 2, p. 195–205, 2018. DOI: 10.1007/s10876-018-1343-0.

DA CONCEIÇÃO, L.R. V. CARNEIRO, L. M. GIORDANI, D. S.; DE CASTRO, He.F. Synthesis of biodiesel from macaw palm oil using mesoporous solid catalyst comprising 12-molybdophosphoric acid and niobia. Renewable Energy, v. 113, p. 119–128, 2017. DOI: 10.1016/j.renene.2017.05.080.

DA SILVA, M. J.; CARARI, D. M.; MANOEL DA SILVA, A. Fe(III)-catalyzed α-terpinyl derivatives synthesis from β-pinene via reactions with hydrogen peroxide in alcoholic solutions. RSC Advances, v. 5, n. 14, p. 10529–10536, 2015. DOI: 10.1039/c4ra13112f.

DA SILVA, M. J.; JULIO, A. A.; DOS SANTOS, K. T. Sn(II)-catalyzed β-citronellol esterification: A Brønsted acid-free process for synthesis of fragrances at room temperature. Catalysis Science and Technology, v. 5, n. 2, p. 1261–1266, 2015. DOI: 10.1039/c4cy01069h.

DA SILVA, M. J.DA SILVA, G. R. N.; SAMPAIO, V. F. C.VILANCULO, C.B. FERNANDES, S. A.; TEIXEIRA, M. G. One-pot synthesis of benzaldehyde derivatives in $PdCl_2$-catalyzed reactions with H_2O_2 in alcoholic solutions. Chemical Papers, n. 0123456789, 2020. DOI: 10.1007/s11696-020-01408-7.

DA SILVA, M. J. DE ANDRADE LELES, L. C. FERREIRA, S. O. DA SILVA, R. C. DE V. VIVEIROS, K. CHAVES, D. M. PINHEIRO, P. F. A Rare Carbon Skeletal Oxidative Rearrangement of Camphene Catalyzed by Al-Exchanged Keggin Heteropolyacid

Salts. ChemistrySelect, v. 4, n. 26, p. 7665–7672, 2019. DOI: 10.1002/slct.201901025.

DA SILVA, M. J.RODRIGUES, A. A. Metal silicotungstate salts as catalysts in furfural oxidation reactions with hydrogen peroxide. Molecular Catalysis, v. 493, n. March, p. 111104, 2020. DOI: 10.1016/j.mcat.2020.111104.

DA SILVA, M. J.TEIXEIRA, R. R. CARARI, D.. $Pd(OAc)_2/M(NO_3)n$ (M = Cu(II), Fe(III); n = 2, 3): Kinetic investigations of an alternative Wacker system for the oxidation of natural olefins. Journal of Organometallic Chemistry, v. 694, n. 20, p. 3254–3261, 2009. DOI: 10.1016/j.jorganchem.2009.06.012.

DA SILVA, M. J.VIEIRA, L. M. M.OLIVEIRA, A. A. RIBEIRO, M. C. Novel effect of palladium catalysts on chemoselective oxidation of β-pinene by hydrogen peroxide. Monatshefte fur Chemie, v. 144, n. 3, p. 321–326, 2013. DOI: 10.1007/s00706-012-0875-5.

DA SILVA, M.J. DA SILVA ANDRADE, P. H. SAMPAIO, V. F.C.. Transition Metal-Substituted Potassium Silicotungstate Salts as Catalysts for Oxidation of Terpene Alcohols with Hydrogen Peroxide. Catalysis Letters,v. 151, n. 7, p. 2094–2106, 2021. DOI: 10.1007/s10562-020-03449-9.

DA SILVA, M. J. DE OLIVEIRA, C. . Catalysis by Keggin Heteropolyacid Salts. Current Catalysis, v. 7, n. 1, p. 26–34, 2017. a. DOI: 10.2174/2211544707666171219161414.

DA SILVA, M. J. DE OLIVEIRA, C. M. Catalysis by Keggin Heteropolyacid Salts. Current Catalysis, v. 7, n. 1, p. 26–34, 2017. b. DOI: 10.2174/2211544707666171219161414.

DA SILVA, M. J. DE OLIVEIRA, C. M. Metal nitrate-catalyzed one-pot oxidative esterification of benzaldehyde with hydrogen peroxide in alcoholic solutions at room temperature. New Journal of Chemistry, v. 45, n. 7, p. 3683–3691, 2021. DOI: 10.1039/d0nj05671e.

DA SILVA, M. J. LIBERTO, N. A. DE ANDRADE LELES, L. C. PEREIRA, Ulisses

Alves. $Fe_4(SiW_{12}O_{40})_3$-catalyzed glycerol acetylation: Synthesis of bioadditives by using highly active Lewis acid catalyst. Journal of Molecular Catalysis A: Chemical, v. 422, p. 69–83, 2016. DOI: 10.1016/j.molcata.2016.03.003.

DA SILVA, M. J.TEIXEIRA, M. G.. Assessment on the double role of the transition metal salts on the acetalization of furfural: Lewis and BrØnsted acid catalysts. Molecular Catalysis, v. 461, n. October, p. 40–47, 2018. DOI: 10.1016/j.mcat.2018.10.002.

DA SILVA, M. J.TEIXEIRA, M. G. NATALINO, R.. Highly selective synthesis under benign reaction conditions of furfural dialkyl acetal using $SnCl_2$ as a recyclable catalyst. New Journal of Chemistry, v. 43, n. 22, p. 8606–8612, 2019. DOI: 10.1039/c9nj01284b.

DASH, S. PATEL, S. MISHRA, B. K. Oxidation by permanganate: synthetic and mechanistic aspects. Tetrahedron, v. 65, n. 4, p. 707–739, 2009. DOI: 10.1016/j.tet.2008.10.038.

DEGENHARDT, J. KÖLLNER, T. G. GERSHENZON, J. Monoterpene and sesquiterpene synthases and the origin of terpene skeletal diversity in plants. Phytochemistry, v. 70, n. 15–16, p. 1621–1637, 2009. DOI: 10.1016/j.phytochem.2009.07.030.

DELLA PINA, C. FALLETTA, E. ROSSI, M. Highly selective oxidation of benzyl alcohol to benzaldehyde catalyzed by bimetallic gold-copper catalyst. Journal of Catalysis, v. 260, n. 2, p. 384–386, 2008. DOI: 10.1016/j.jcat.2008.10.003.

DENICOURT-NOWICKI; RAUCHDI; ALI; ROUCOUX. Catalytic Oxidation Processes for the Upgrading of Terpenes: State-of-the-Art and Future Trends. Catalysts, v. 9, n. 11, p. 893, 2019. DOI: 10.3390/catal9110893.

DEVARAJAN, C.VIJAYAKUMAR, V. RAMALINGAM, C.VIJAYARAGHAVAN, R. A simple, one-pot oxidative esterification of aryl aldehydes through dialkyl acetal using hydrogen peroxide. Research on Chemical Intermediates, v. 42, n. 6, p. 5849–5858,

2016. DOI: 10.1007/s11164-015-2408-4.

DUSI, M. MALLAT, T. BAIKER, A. Epoxidation of Functionalized Olefins over Solid Catalysts. Catalysis Reviews - Science and Engineering, v. 42, n. 1–2, p. 213–278, 2000. DOI: 10.1081/CR-100100262.

EVTUSHOK, V. Y. PODYACHEVA, O. Y. SUBOCH, Arina N.; MAKSIMCHUK, N. V.STONKUS, O. A.; KIBIS, L. S.KHOLDEEVA, O. A. H_2O_2-based selective oxidations by divanadium-substituted polyoxotungstate supported on nitrogen-doped carbon nanomaterials. Catalysis Today, v. 354, n. March, p. 196–203, 2020. DOI: 10.1016/j.cattod.2019.03.060.

FARSANI, M. R. JALILIAN, F. YADOLLAHI, B. RUDBARI, H. A. A comparative study on Keggin and Wells-Dawson sandwich type polyoxometallates in the oxidation of alcohols with 30% hydrogen peroxide. Polyhedron, v. 76, p. 102–107, 2014. DOI: 10.1016/j.poly.2014.03.060.

FOURNIER, M. FEUMI-JANTOU, C. RABIA, C. HERVÉ, G. LAUNAY, S. Polyoxometalates catalyst materials: X-ray thermal stability study of phosphorus-containing heteropolyacids $H_{3+x}PM_{12-x}V_xO_{40}\cdot 13\text{-}14H_2O$ (M=Mo,W; x=0-1). Journal of Materials Chemistry, v. 2, n. 9, p. 971–978, 1992. DOI: 10.1039/JM9920200971.

FUCHS, V. M. PIZZIO, L. R.; BLANCO, M. N. Hybrid materials based on aluminum tungstophosphate or tungstosilicate as catalysts in anisole acylation. Catalysis Today, v. 133–135, n. 1–4, p. 181–186, 2008. DOI: 10.1016/j.cattod.2007.12.047.

GALLEZOT, P. Catalytic routes from renewables to fine chemicals. Catalysis Today, v. 121, n. 1–2, p. 76–91, 2007. DOI: 10.1016/j.cattod.2006.11.019.

GARCÍA-LÓPEZ, E. I. MARCÌ, G. KRIVTSOV, I. CASADO ESPINA, J. LIOTTA, L. F. SERRANO, A. Local Structure of Supported Keggin and Wells-Dawson Heteropolyacids and Its Influence on the Catalytic Activity. Journal of Physical Chemistry C, v. 123, n. 32, p. 19513–19527, 2019. DOI: 10.1021/acs.jpcc.9b03659.

GOPINATH, R. PATEL, B. K. A catalytic oxidative esterification of aldehydes using V_2O_5-H_2O_2. Organic Letters, v. 2, n. 5, p. 577–578, 2000. DOI: 10.1021/ol990383+.

HERAVI, M. M.VAZIN FARD, M. FAGHIHI, Z. Heteropoly acids-catalyzed organic reactions in water: doubly green reactions. Green Chemistry Letters and Reviews, v. 6, n. 4, p. 282–300, 2013. DOI: 10.1080/17518253.2013.846415.

HILL, C. L.PROSSER-MCCARTHA, C. M. Homogeneous catalysis by transition metal oxygen anion clusters. Coordination Chemistry Reviews, v. 143, n. C, p. 407–455, 1995. DOI: 10.1016/0010-8545(95)01141-B.

HRONEC, M. FULAJTÁROVÁ, K. HORVÁTH, B. LIPTAJ, T. DOBROČKA, E. A facile conversion of furfural to novel tetrahydrofurfuryl hemiacetals. Applied Catalysis A: General, v. 594, n. December 2019, p. 117471, 2020. DOI: 10.1016/j.apcata.2020.117471.

HU, C. HASHIMOTO, M. OKUHARA, T. MISONO, M. Catalysis by heteropoly compounds: XXII. Reactions of esters and esterification catalyzed by heteropolyacids in a homogeneous liquid-phase effects of the central atom of heteropolyanions having tungsten as the addenda atomJournal of Catalysis, 1993. DOI: 10.1006/jcat.1993.1288.

IVANCHIKOVA, I. D. MAKSIMCHUK, N. V.SKOBELEV, I. Y.KAICHEV, V. V.KHOLDEEVA, O.A. Mesoporous niobium-silicates prepared by evaporation-induced self-assembly as catalysts for selective oxidations with aqueous H_2O_2. Journal of Catalysis, v. 332, p. 138–148, 2015. DOI: 10.1016/j.jcat.2015.10.003.

J. DA SILVA, M. A. LIBERTO, N.. Soluble and Solid Supported Keggin Heteropolyacids as Catalysts in Reactions for Biodiesel Production: Challenges and Recent Advances. Current Organic Chemistry, v. 20, n. 12, p. 1263–1283, 2015. DOI: 10.2174/1385272819666150907193100.

KABA, M. S. SONG, I. K.; BARTEAU, M. A. Investigation of framework and cation substitutions in Keggin-type heteropoly acids probed by scanning tunneling

microscopy and tunneling spectroscopy. Journal of Vacuum Science & Technology A: Vacuum, Surfaces, and Films, v. 15, n. 3, p. 1299–1304, 1997. DOI: 10.1116/1.580580.

KIM, M. SU, Y. FUKUOKA, A. HENSEN, E. J. M.; NAKAJIMA, K.. Aerobic Oxidation of 5-(Hydroxymethyl)furfural Cyclic Acetal Enables Selective Furan-2,5-dicarboxylic Acid Formation with CeO_2-Supported Gold Catalyst. Angewandte Chemie - International Edition, v. 57, n. 27, p. 8235–8239, 2018. DOI: 10.1002/anie.201805457.

KIRIHARA, M. YAMAMOTO, J. NOGUCHI, T. ITOU, A. NAITO, S. HIRAI, Y. Tantalum(V) or niobium(V) catalyzed oxidation of sulfides with 30% hydrogen peroxide. Tetrahedron, v. 65, n. 50, p. 10477–10484, 2009. DOI: 10.1016/j.tet.2009.10.007.

KNÖZINGER, H. KOCHLOEFL, K.. Heterogeneous Catalysis and Solid Catalysts. Ullmann's Encyclopedia of Industrial Chemistry, 2003. DOI: 10.1002/14356007.a05_313.

KOZHEVNIKOV, I. V. Catalysis by heteropoly acids and multicomponent polyoxometalates in liquid-phase reactions. Chemical Reviews, v. 98, n. 1, p. 171–198, 1998. DOI: 10.1021/cr960400y.

KUMAR, A. KUMAR, V. P. SRIKANTH, A. VISHWANATHAN, V. CHARY, K. V. R. Vapor Phase Oxidation of Benzyl Alcohol over Nano Au/SBA-15 Catalysts: Effect of Preparation Methods. Catalysis Letters,v. 146, n. 1, p. 35–46, 2016. DOI: 10.1007/s10562-015-1656-7.

LEE, D. W. LEE, K. Y. Heterogeneous Solid Acid Catalysts for Esterification of Free Fatty Acids. Catalysis Surveys from Asia, v. 18, n. 2–3, p. 55–74, 2014. DOI: 10.1007/s10563-014-9166-y.

LEE, S. A. KIM, Y. M. LEE, J. C. Oxidative esterification of aldehydes with urea hydrogen peroxide catalyzed by aluminum chloride hexahydrate. Bulletin of the Korean Chemical Society, v. 37, n. 8, p. 1368–1370, 2016. DOI: 10.1002/bkcs.10851.

LI, G. ZHAO, H. HONG, J. QUAN, K. YUAN, Q. WANG, X.. Antifungal graphene oxide-borneol composite. Colloids and Surfaces B: Biointerfaces, v. 160, p. 220–227, 2017. a. DOI: 10.1016/j.colsurfb.2017.09.023.

LI, J. LIANG, X. Magnetic solid acid catalyst for biodiesel synthesis from waste oil. Energy Conversion and Management, v. 141, p. 126–132, 2017. DOI: 10.1016/j.enconman.2016.06.072.

LI, X. HO, B. LIM, D. S. W.; ZHANG, Y. Highly efficient formic acid-mediated oxidation of renewable furfural to maleic acid with H_2O_2. Green Chemistry,v. 19, n. 4, p. 914–918, 2017. b. DOI: 10.1039/c6gc03020c.

LI, X. HO, B. ZHANG, Y.. Selective aerobic oxidation of furfural to maleic anhydride with heterogeneous Mo-V-O catalysts. Green Chemistry, v. 18, n. 10, p. 2976–2980, 2016. DOI: 10.1039/c6gc00508j.

LINDE, G. A. COLAUTO, N. B. ALBERTÓ, E. GAZIM, Z. C. Quimiotipos, extração, composição e uso do óleo essencial de Lippia alba. Revista Brasileira de Plantas Medicinais,v. 18, n. 1, p. 191–200, 2016. DOI: 10.1590/1983-084X/15_037.

LIU, R. LIANG, X. DONG, Ch. HU, X. Transition-Metal-Free: A Highly Efficient Catalytic Aerobic Alcohol Oxidation Process. Journal of the American Chemical Society, v. 126, n. 13, p. 4112–4113, 2004. DOI: 10.1021/ja031765k.

LONG, D. L.TSUNASHIMA, R. CRONIN, L. Polyoxometalates: Building blocks for functional nanoscale systems. Angewandte Chemie - International Edition,v. 49, n. 10, p. 1736–1758, 2010. DOI: 10.1002/anie.200902483.

MA, S. GAO, W. YANG, Z. LIN, R. WANG, X. ZHU, X. JIANG, Y. Superior Ce–Nb–Ti oxide catalysts for selective catalytic reduction of NO with NH_3. Journal of the Energy Institute, v. 94, p. 73–84, 2021. DOI: 10.1016/j.joei.2020.11.001.

MAESTRE, J. M. LOPEZ, X. BO, C. POBLET, J. M. CASAÑ-PASTOR, N. Electronic and magnetic properties of α-Keggin anions: A DFT study of $[XM_{12}O_{40}]n-$, (M = W, Mo; X = $A1^{III}$, Si^{IV}, P^{V}, Fe^{III}, Co^{II}, Co^{III}) and $[SiM_{11}VO_{40}]^{m-}$ (M = Mo and W). Journal of the American Chemical Society, v. 123, n. 16, p. 3749–3758, 2001. DOI: 10.1021/ja003563j.

MAROSI, L.PLATERO, E. E. CIFRE, J. AREAN, C. O. Thermal dehydration of $H_{(3+x)}PV_{(x)}M_{(12-x)}O_{(40)}\cdot yH_2O$ Keggin type heteropolyacids; Formation, thermal stability and structure of the anhydrous acids $H_3PM_{(12)}O_{(40)}$, of the corresponding anhydrides $PM_{(12)}O_{(38.5)}$ and of a novel trihydrate $H3PW_{(12)}O_{(40)}\cdot 3H_2O$. Journal of Materials Chemistry, v. 10, n. 8, p. 1949–1955, 2000. DOI: 10.1039/b001476l.

MATKOVIC, S. R. VALLE, G. M. BRIAND, L. E. Optimization of the operative conditions for heteropolyacids synthesis through ion exchange. Materials Research, v. 8, n. 3, p. 351–355, 2005. DOI: 10.1590/S1516-14392005000300022.

MCKENDRY, P. Energy production from biomass (part 1): Overview of biomass. Bioresource Technology, v. 83, n. 1, p. 37–46, 2002. DOI: 10.1016/S0960-8524(01)00118-3.

MICEK-ILNICKA, A. The role of water in the catalysis on solid heteropolyacids. Journal of Molecular Catalysis A: Chemical, v. 308, n. 1–2, p. 1–14, 2009. DOI: 10.1016/j.molcata.2009.04.003.

MILLER, R. A. HOERRNER, R. S. Iodine as a chemoselective reoxidant of TEMPO: Application to the oxidation of alcohols to aldehydes and ketones. Organic Letters, v. 5, n. 3, p. 285–287, 2003. DOI: 10.1021/ol0272444.

MISONO, M. Unique acid catalysis of heteropoly compounds (heteropolyoxometalates) in the solid state. Chemical Communications, v. 1, n. 13, p. 1141–1153, 2001. DOI: 10.1039/b102573m.

MIZUNO, N. Modern Heterogeneous Oxidation Catalysis: Design, Reactions and Characterization. DOI: 10.1002/9783527627547.

MOFFAT, J. B. Implicit and explicit microporosity in heteropoly oxometalates. Journal of Molecular Catalysis, v. 52, n. 1, p. 169–191, 1989. DOI: 10.1016/0304-5102(89)80088-4.

MOREAU, C. LECOMTE, J. MSEDDI, S. ZMIMITA, N. Stereoelectronic effects in hydrolysis and hydrogenolysis of acetals and thioacetals in the presence of heterogeneous catalysts. Journal of Molecular Catalysis A: Chemical, v. 125, n. 2–3, p. 143–149, 1997. DOI: 10.1016/S1381-1169(97)00083-6.

MOTHÉ-ESTEVES, P. MACIEL PEREIRA, M.ARICHI, J. LOUIS, B. How Keggin-type polyoxometalates self-organize into crystals. Crystal Growth and Design, v. 10, n. 1, p. 371–378, 2010. DOI: 10.1021/cg900984z.

NARKHEDE, N. SINGH, S. PATEL, A. Recent progress on supported polyoxometalates for biodiesel synthesis via esterification and transesterification. Green Chemistry, v. 17, n. 1, p. 89–107, 2015. DOI: 10.1039/c4gc01743a.

NDOLOMINGO, M. J. MEIJBOOM, R. Selective liquid phase oxidation of benzyl alcohol to benzaldehyde by tert-butyl hydroperoxide over γ-Al $_2$ O $_3$ supported copper and gold nanoparticles. Applied Surface Science, v. 398, p. 19–32, 2017. DOI: 10.1016/j.apsusc.2016.12.020.

NOMIYA, K. MATSUOKA, S. HASEGAWA, T. NEMOTO, Y. Benzene hydroxylation with hydrogen peroxide catalyzed by vanadium(V)- substituted polyoxomolybdates. Journal of Molecular Catalysis A: Chemical, v. 156, n. 1–2, p. 143–152, 2000. DOI: 10.1016/S1381-1169(99)00430-6.

ODYAKOV, V. F. ZHIZHINA, E. G. RODIKOVA, Y. A.; GOGIN, Leonid L. Mo-V-Phosphoric Heteropoly Acids and Their Salts: Aqueous Solution Preparation - Challenges and Perspectives. European Journal of Inorganic Chemistry, v. 2015, n. 22, p. 3618–3631, 2015. DOI: 10.1002/ejic.201500359.

OKUMURA, K. YAMASHITA, K. YAMADA, K. NIWA, M. Studies on the identification

of the heteropoly acid generated in the H_3PO_4-WO_3-Nb_2O_5 catalyst and its thermal transformation process. Journal of Catalysis, v. 245, n. 1, p. 75–83, 2007. DOI: 10.1016/j.jcat.2006.09.021

.

OMWOMA, S. GORE, C. T. JI, Y.HU, C. SONG, Yu Fei. Environmentally benign polyoxometalate materials. Coordination Chemistry Reviews, v. 286, p. 17–29, 2015. DOI: 10.1016/j.ccr.2014.11.013.

PALERMO, V. SATHICQ, Á. CONSTANTIEUX, T. RODRÍGUEZ, J. VÁZQUEZ, P. ROMANELLI, G.. New Vanadium Keggin Heteropolyacids Encapsulated in a Silica Framework: Recyclable Catalysts for the Synthesis of Highly Substituted Hexahydropyrimidines Under Suitable Conditions. Catalysis Letters,v. 145, n. 4, p. 1022–1032, 2015. DOI: 10.1007/s10562-015-1498-3.

PALERMO, V. SATHICQ, Á. CONSTANTIEUX, T. RODRÍGUEZ, J. VÁZQUEZ, P.G. ROMANELLI, G. P. First Report About the Use of Micellar Keggin Heteropolyacids as Catalysts in the Green Multicomponent Synthesis of Nifedipine Derivatives. Catalysis Letters,v. 146, n. 9, p. 1634–1647, 2016. DOI: 10.1007/s10562-016-1784-8.

PALERMO, V. SATHICQ, Á. G.; VÁZQUEZ, P.G.; THOMAS, H. J.; ROMANELLI, Gustavo P. Doped Keggin heteropolyacids as catalysts in sulfide oxidation. Reaction Kinetics, Mechanisms and Catalysis, v. 104, n. 1, p. 181–195, 2011. DOI: 10.1007/s11144-011-0341-0.

PAQUIN, F. RIVNAY, J. SALLEO, A. STINGELIN, N. SILVA, C. Multi-phase semicrystalline microstructures drive exciton dissociation in neat plastic semiconductors. J. Mater. Chem. C, v. 3, p. 10715–10722, 2015. DOI: 10.1039/b000000x.

PARK, D. R. CHOI, J. H. PARK, S. SONG, I. K.. Reduction potential, UV-visible absorption edge energy, and oxidation catalysis of niobium-containing $H_{3+x}PW_{12-x}Nb_xO_{40}$ Keggin and $H_{6+x}P_2W_{18-x}Nb_xO_{62}$ Wells-Dawson heteropolyacid catalysts. Applied Catalysis A: General, v. 394, n. 1–2, p. 201–208, 2011. DOI: 10.1016/j.apcata.2010.12.042.

PARK, D. R. PARK, S. BANG, Y. SONG, I. K. Redox properties and oxidation catalysis of group 5 metal (V, Nb, Ta)-containing Keggin and Wells-Dawson heteropolyacid (HPA) catalysts. Applied Catalysis A: General, *[S. l.]*, v. 373, n. 1–2, p. 201–207, 2010. a. DOI: 10.1016/j.apcata.2009.11.018.

PARK, D R. PARK, S. CHOI, J. H. SONG, I. K. Acidity of group 5 metal (V, Nb, Ta)-substituted keggin and wells-dawson heteropolyacid (HPA) catalysts and their application to esterification of acetic acid with ethanol. Catalysis Letters, v. 135, n. 3–4, p. 269–274, 2010. b. DOI: 10.1007/s10562-010-0299-y.

PARK, D. R. SONG, S. H. HONG, U. G. SEO, J. G. JUNG, J. C. SONG, I. K. Redox properties and catalytic oxidation activities of polyatom-substituted H n $PW_{11}M_1O_{40}$ (M = V, Nb, Ta, and W) keggin heteropolyacid catalysts. Catalysis Letters, v. 132, n. 3–4, p. 363–369, 2009. DOI: 10.1007/s10562-009-0114-9.

PATEL, A. NARKHEDE, N. SINGH, S. PATHAN, S. Keggin-type lacunary and transition metal substituted polyoxometalates as heterogeneous catalysts: A recent progress. Catalysis Reviews - Science and Engineering, v. 58, n. 3, p. 337–370, 2016. DOI: 10.1080/01614940.2016.1171606.

PELETEIRO, S. RIVAS, S. ALONSO, J. L. SANTOS, V. PARAJÓ, J. C. Furfural production using ionic liquids: A review. Bioresource Technology, v. 202, p. 181–191, 2016. DOI: 10.1016/j.biortech.2015.12.017.

ILLINGWORTH. J. W. Keggin J. F. Identification of 12-heteropoly-acids and theris salts by means of , X-ray Powder phptpgraphs. 1935 1 2 7.

PILLAI, U. R. SAHLE-DEMESSIE, E. Selective oxidation of alcohols over vanadium phosphorus oxide catalyst using hydrogen peroxide. Applied Catalysis A: General, v. 276, n. 1–2, p. 139–144, 2004. DOI: 10.1016/j.apcata.2004.07.052.

PIZZIO, L. R.VÁZQUEZ, P. G CÁCERES, C. V. BLANCO, M. N. Supported Keggin type heteropolycompounds for ecofriendly reactions. Applied Catalysis A: General, v.

256, n. 1–2, p. 125–139, 2003. DOI: 10.1016/S0926-860X(03)00394-6.

RABINDRAN JERMY, B. PANDURANGAN, A. Efficient synthesis of diacetal of pentaerythritol under microwave irradiation using heteropoly acid $H_3PW_{12}O_{40}$. Catalysis Communications, v. 7, n. 12, p. 921–925, 2006. DOI: 10.1016/j.catcom.2006.03.021.

RAO, P. S. N. PARAMESWARAM, G.RAO, A. V. P.LINGAIAH, N. Influence of cesium and vanadium contents on the oxidation functionalities of heteropoly molybdate catalysts. Elsevier B.V., 2015. v. 399 DOI: 10.1016/j.molcata.2015.01.023.

RAVAT, V. NONGWE, I. MEIJBOOM, R. BEPETE, G. COVILLE, N. J. Pd on boron-doped hollow carbon spheres - PdO particle size and support effects. Journal of Catalysis, v. 305, p. 36–45, 2013. DOI: 10.1016/j.jcat.2013.04.018.

REDDY, K. m. LINGAIAH, N. SAI PRASAD, P. S. SURYANARAYANA, I. Acidity constants of supported salts of heteropoly acids using a methodology related to the potentiometric mass titration technique. Journal of Solution Chemistry, v. 35, n. 3, p. 407–423, 2006. DOI: 10.1007/s10953-006-9025-1.

REED, N. R.; KWOK, E. S. C. Furfural. Encyclopedia of Toxicology: Third Edition, v. d, p. 685–688, 2014. DOI: 10.1016/B978-0-12-386454-3.00147-0.

ROCCHICCIOLI-DELTCHEFF, C. FOURNIER, M. Catalysis by polyoxometalates. Part 3. - Influence of vanadium(V) on the thermal stability of 12-metallophosphoric acids from in situ infrared studies. Journal of the Chemical Society, Faraday Transactions, v. 87, n. 24, p. 3913–3920, 1991. DOI: 10.1039/FT9918703913.

RODRIGUES, A. A. Esterificação do furfural e centralização do glicerol catalisadas pelo ácido silicotúbgstico e seus sais metálicos. 118f. Dissertação (Mestrado em Agroquímica) - Universidade Federal de Viçosa, UFV, Viçosa. 2020

ROMANELLI, G.P.; AUTINO, J. C. BLANCO, M. N. PIZZIO, L. R. Tungstosilicate salts as catalysts in phenol tetrahydropyranylation and depyranylation. Applied Catalysis A: General, v. 295, n. 2, p. 209–215, 2005. DOI: 10.1016/j.apcata.2005.08.019.

RUBIO-CABALLERO, J. M. SARAVANAMURUGAN, S. MAIRELES-TORRES, P. RIISAGER, A. Acetalization of furfural with zeolites under benign reaction conditions. Catalysis Today, v. 234, p. 233–236, 2014. DOI: 10.1016/j.cattod.2014.03.004.

.

RUIZ, V. R. VELTY, A. SANTOS, L. L.LEYVA-PÉREZ, A. SABATER, M. J. IBORRA, S. CORMA, A. Gold catalysts and solid catalysts for biomass transformations: Valorization of glycerol and glycerol-water mixtures through formation of cyclic acetals. Journal of Catalysis, v. 271, n. 2, p. 351–357, 2010. DOI: 10.1016/j.jcat.2010.02.023.

SANCHEZ-MARTINEZ, J. D. BUENO, M. ALVAREZ-RIVERA, G. TUDELA, J. IBANEZ, E. CIFUENTES, A. In vitro neuroprotective potential of terpenes from industrial orange juice by-products. Food and Function, v. 12, n. 1, p. 302–314, 2021. DOI: 10.1039/d0fo02809f.

SCHLÖGL, R. Heterogeneous catalysis. Angewandte Chemie - International Edition, v. 54, n. 11, p. 3465–3520, 2015. DOI: 10.1002/anie.201410738.

SCHOBERT, H. Chemistry of fossil fuels and biofuels. Chemistry of Fossil Fuels and Biofuels, v. 9780521114, p. 1–480, 2010. DOI: 10.1017/CBO9780511844188.

SCHULTZ, M. J. ADLER, R. S.ZIERKIEWICZ, W. PRIVALOV, T. SIGMAN, M. S. Using mechanistic and computational studies to explain ligand effects in the palladium-catalyzed aerobic oxidation of alcohols. Journal of the American Chemical Society, v. 127, n. 23, p. 8499–8507, 2005. DOI: 10.1021/ja050949r.

SHEN, L. YIN, H. WANG, A. FENG, Y. SHEN, Y. WU, Z. JIANG, T.. Liquid phase dehydration of glycerol to acrolein catalyzed by silicotungstic, phosphotungstic, and phosphomolybdic acids. Chemical Engineering Journal,v. 180, p. 277–283, 2012. DOI: 10.1016/j.cej.2011.11.058.

SING, K. S. W. Reporting physisorption data for gas / solid systems with Special Reference to the Determination of S. Pure & Appl. Chem., v. 54, n. 11, p. 2201–2218, 1982.

SONG, H. JIN, F. LIU, Q. LIU, H. Zeolite-catalyzed acetalization reaction of furfural with alcohol under solvent-free conditions. Molecular Catalysis, v. 513, n. June, p. 111752, 2021. DOI: 10.1016/j.mcat.2021.111752.

SONG, I K. BARTEAU, M. A. Redox properties of Keggin-type heteropolyacid (HPA) catalysts: Effect of counter-cation, heteroatom, and polyatom substitution. Journal of Molecular Catalysis A: Chemical, v. 212, n. 1–2, p. 229–236, 2004. DOI: 10.1016/j.molcata.2003.10.040.

STEPAN, Emil et al. A versatile method for obtaining new oxygenated fuel components from biomass. Industrial Crops and Products,v. 113, n. July 2017, p. 288–297, 2018. DOI: 10.1016/j.indcrop.2018.01.059.

SUN, M. ZHANG, J. CAO, C. ZHANG, Q. WANG, Y.WAN, Huilin. Significant effect of acidity on catalytic behaviors of Cs-substituted polyoxometalates for oxidative dehydrogenation of propane. Applied Catalysis A: General, v. 349, n. 1–2, p. 212–221, 2008. DOI: 10.1016/j.apcata.2008.07.035.

TAGUSAGAWA, C. TAKAGAKI, A. HAYASHI, S. DOMEN, K. Efficient utilization of nanospace of layered transition metal oxide $HNbMoO_6$ as a strong, water-tolerant solid acid catalyst. Journal of the American Chemical Society, v. 130, n. 23, p. 7230–7231, 2008. DOI: 10.1021/ja802478d.

TAGUSAGAWA, C. TAKAGAKI, A. TAKANABE, K. EBITANI, K. HAYASHI, S. DOMEN, K. Effects of transition-metal composition of protonated, layered nonstoichiometric oxides $H_{1-x}Nb_{1-x}Mo_{1+x}O_6$ on heterogeneous acid catalysis. Journal of Physical Chemistry C, v. 113, n. 40, p. 17421–17427, 2009. DOI: 10.1021/jp906628k.

TANABE, K. Catalytic application of niobium compounds. Catalysis Today, v. 78, n. 1-

4 SPEC., p. 65–77, 2003. DOI: 10.1016/S0920-5861(02)00343-7.

TANG, Y. ZHANG, J. Direct oxidation of benzene to phenol catalyzed by vanadium substituted heteropolymolybdic acid. Transition Metal Chemistry, v. 31, n. 3, p. 299–305, 2006. DOI: 10.1007/s11243-005-6412-1.

TEIXEIRA, M. G. NATALINO, R. DA SILVA, M. J. A kinetic study of heteropolyacid-catalyzed furfural acetalization with methanol at room temperature via ultraviolet spectroscopy. Catalysis Today, v. 344, n. May, p. 143–149, 2020. a. DOI: 10.1016/j.cattod.2018.11.071.

TEIXEIRA, M. G. NATALINO, R. DA SILVA, M. J. A kinetic study of heteropolyacid-catalyzed furfural acetalization with methanol at room temperature via ultraviolet spectroscopy. Catalysis Today,v. 344, n. November, p. 143–149, 2020. b. DOI: 10.1016/j.cattod.2018.11.071.

TEIXEIRA, V. G. COUTINHO, F. M. B.; GOMES, A. S. Principais métodos de caracterização da porosidade de resinas à base de divinilbenzeno. Quimica Nova,v. 24, n. 6, p. 808–818, 2001. DOI: 10.1590/s0100-40422001000600019.

TEJEDOR, D. PRIETO-RAMÍREZ, M. C. INGOLD, M. CHICÓN, M. GARCÍA-TELLADO, F. Synthesis of Polysubstituted Benzoic Esters from 1,2-Dihydropyridines and Its Application to the Synthesis of Fluorenones. Organic Letters, v. 18, n. 11, p. 2770–2773, 2016. DOI: 10.1021/acs.orglett.6b01260.

THOMMES, M. KANEKO, K. NEIMARK, A. V.; OLIVIER, J. P.; RODRIGUEZ-REINOSO, F. ROUQUEROL, J. SING, K. S. W. Physisorption of gases, with special reference to the evaluation of surface area and pore size distribution (IUPAC Technical Report). Pure and Applied Chemistry, v. 87, n. 9–10, p. 1051–1069, 2015. DOI: 10.1515/pac-2014-1117.

TIMOFEEVA, M. N. Acid catalysis by heteropoly acids. Applied Catalysis A: General, v. 256, n. 1–2, p. 19–35, 2003. DOI: 10.1016/S0926-860X(03)00386-7.

TONIATO, A. VAUCHER, A. C. Jo u rn a l P re of. Catalysis Today, 2021. DOI: 10.1016/j.cattod.2021.10.001.

TURSI,A. A review on biomass: Importance, chemistry, classification, and conversion. Biofuel Research Journal, v. 6, n. 2, p. 962–979, 2019. DOI: 10.18331/BRJ2019.6.2.3.

VIANA, L A S. DA SILVA, G. R.N. DA SILVA, M.J. A Highly Selective Na_2WO_4-Catalyzed Oxidation of Terpenic Alcohols by Hydrogen Peroxide. Catalysis Letters, v. 148, n. 1, p. 374–382, 2018. DOI: 10.1007/s10562-017-2246-7.

.

VILANCULO, C. B. DA SILVA, M. J. Can Brønsted acids catalyze the epoxidation of allylic alcohols with H_2O_2? With a little help from the proton, the $H_3PMo_{12}O_{40}$ acid did it and well. Molecular Catalysis, v. 512, n. April, 2021. DOI: 10.1016/j.mcat.2021.111780.

VILANCULO, C. B. DA SILVA, M.J.OLAVO FERREIRA, S. TEIXEIRA, M.G.A rare oxidation of camphene to acid and aldehyde in the presence of Lacunar Keggin heteropoly salts. Molecular Catalysis, v. 478, n. July, p. 110589, 2019. DOI: 10.1016/j.mcat.2019.110589.

VILANCULO, C. B. DA SILVA, M. J.RODRIGUES, Al. A. FERREIRA, S. O. DA SILVA, R. C. Vanadium-doped sodium phosphomolybdate salts as catalysts in the terpene alcohols oxidation with hydrogen peroxide. RSC Advances, v. 11, n. 39, p. 24072–24085, 2021. DOI: 10.1039/d1ra04191f.

VILLABRILLE, P. ROMANELLI, G. VÁZQUEZ, P.CÁCERES, C. Vanadium-substituted Keggin heteropolycompounds as catalysts for ecofriendly liquid phase oxidation of 2,6-dimethylphenol to 2,6-dimethyl-1,4- benzoquinone. Applied Catalysis A: General, v. 270, n. 1–2, p. 101–111, 2004. DOI: 10.1016/j.apcata.2004.04.028.

VILLABRILLE, P. VÁZQUEZ, P. BLANCO, M.CÁCERES, C. Equilibrium adsorption of molybdosilicic acid solutions on carbon and silica: Basic studies for the preparation of ecofriendly acidic catalysts. Journal of Colloid and Interface Science, v. 251, n. 1, p. 151–159, 2002. DOI: 10.1006/jcis.2002.8391.

WANG, S. S. YANG, G. Y. Recent Advances in Polyoxometalate-Catalyzed Reactions. Chemical Reviews, v. 115, n. 11, p. 4893–4962, 2015. DOI: 10.1021/cr500390v.

WEINGARTEN, R. CHO, J.CONNER, W. C. HUBER, G.W. Kinetics of furfural production by dehydration of xylose in a biphasic reactor with microwave heating. Green Chemistry, v. 12, n. 8, p. 1423–1429, 2010. DOI: 10.1039/c003459b.

WEINSTOCK, I. A. SCHREIBER, R.E.; NEUMANN, Ronny. Dioxygen in Polyoxometalate Mediated Reactions. Chemical Reviews, v. 118, n. 5, p. 2680–2717, 2018. DOI: 10.1021/acs.chemrev.7b00444.

WEN, Li; LI, Q. LI, Wei. CAI, Qiao. CAI, Yong Ming. A QSAR Study Based on SVM for the Compound of Hydroxyl Benzoic Esters. Bioinorganic Chemistry and Applications, v. 2017, 2017. DOI: 10.1155/2017/4914272.

WU, H. ZHOU, M.QU, Y. LI, H. YIN, H. Preparation and Characterization of Tungsten-substituted Molybdophosphoric Acids and Catalytic Cyclodehydration of. Chinese Journal of Chemical Engineering, v. 17, n. 2, p. 200–206, 2009. DOI: 10.1016/S1004-9541(08)60194-9.

WU, X. F.. Zinc-catalyzed oxidative esterification of aromatic aldehydes. Tetrahedron Letters, v. 53, n. 26, p. 3397–3399, 2012. DOI: 10.1016/j.tetlet.2012.04.111.

XIAN-E, C. DAICHUN, D. JIANPING, N. YOUMING, J. JING, Z. YIXIANG, Q.. Enthalpies of formation and DSC and TG results of heteropoly acids containing tungsten and molybdenum. Thermochimica Acta, v. 292, n. 1–2, p. 45–50, 1997. DOI: 10.1016/S0040-6031(96)03094-8.

YANG, F. TANG, J. OU, R. GUO, Z. GAO, S. WANG, Y. WANG, X. CHEN, L. YUAN, A. Fully catalytic upgrading synthesis of 5-Ethoxymethylfurfural from biomass-derived 5-Hydroxymethylfurfural over recyclable layered-niobium-molybdate solid acid. Applied Catalysis B: Environmental, v. 256, n. May, 2019. DOI: 10.1016/j.apcatb.2019.117786.

YANG, H. BAI, Y. OUYANG, D. WANG, F. LIU, D. ZHAO, X. Coupling biomass pretreatment for enzymatic hydrolysis and direct biomass-to-electricity conversion with molybdovanadophosphoric heteropolyacids as anode electron transfer carriers. Journal of Energy Chemistry, v. 58, p. 133–146, 2021. DOI: 10.1016/j.jechem.2020.09.009.

YOO, S. K. DAY, D. F. Bacterial metabolism of α- and β-pinene and related monoterpenes by Pseudomonas sp. strain PIN. Process Biochemistry, v. 37, n. 7, p. 739–745, 2002. DOI: 10.1016/S0032-9592(01)00262-X.

YUE, L. LI, J. CHEN, W. LIU, X. JIANG, Q. XIA, W. Geraniol grafted chitosan oligosaccharide as a potential antibacterial agent. Carbohydrate Polymers, v. 176, p. 356–364, 2017. DOI: 10.1016/j.carbpol.2017.07.043.

YUSUF, M. SITEPU, D. E.Br. Computational calculation of acetalization of benzaldehyde using acid catalysts (HCl) with computational method (Ab-Initio). AIP Conference Proceedings, v. 1803, p. 1–6, 2017. DOI: 10.1063/1.4973182.

ZIOLEK, M.. Niobium-containing catalysts - The state of the art. Catalysis Today, v. 78, n. 1- 4 SPEC., p. 47–64, 2003. DOI: 10.1016/S0920-5861(02)00340-1.

ZIOLEK, M. SOBCZAK, I. The role of niobium component in heterogeneous catalysts. Catalysis Today, v. 285, p. 211–225, 2017. DOI: 10.1016/j.cattod.2016.12.013.

8. ATTACHMENTS

Attachment 1 - Chromatogram of geraniol oxidation with hydrogen peroxide.

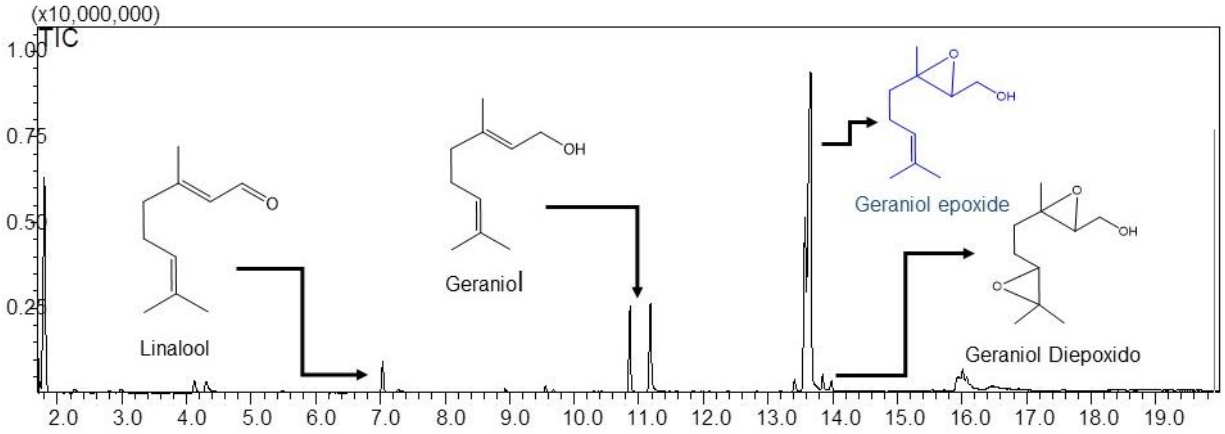

Attachment 1.1 – Mass spectrum of geraniol

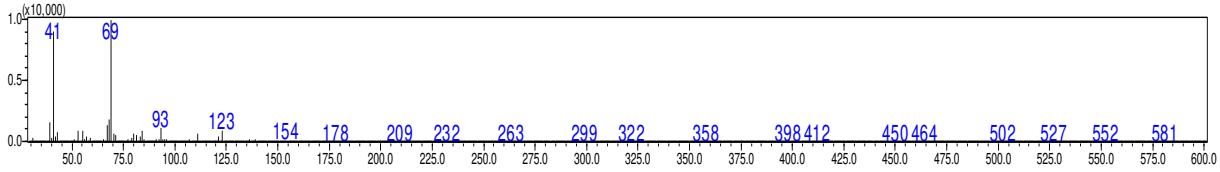

Attachment 1.2 – Mass spectrum of geraniol epoxide

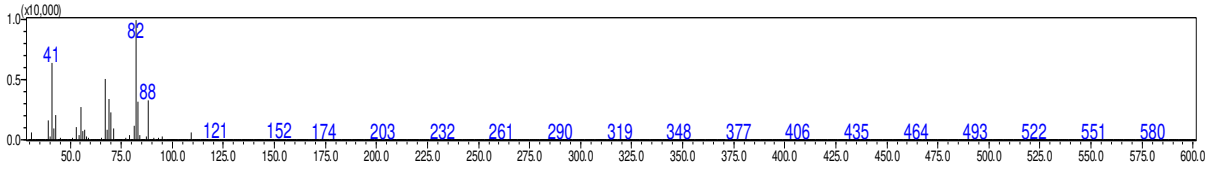

Attachment 1.3 – Mass spectrum of geraniol diepoxido

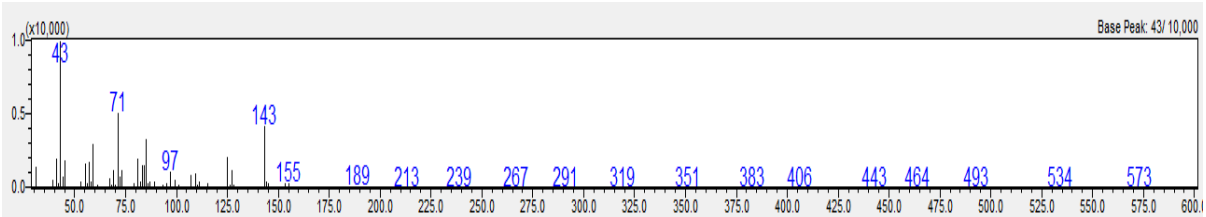

Attachment 1.4 – Mass spectrum of linalool

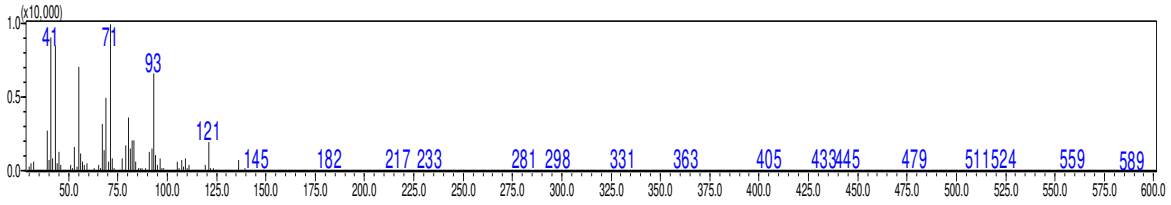

Attachment 2 - Chromatogram of furfural oxidative reaction with methanol and hydrogen peroxide.

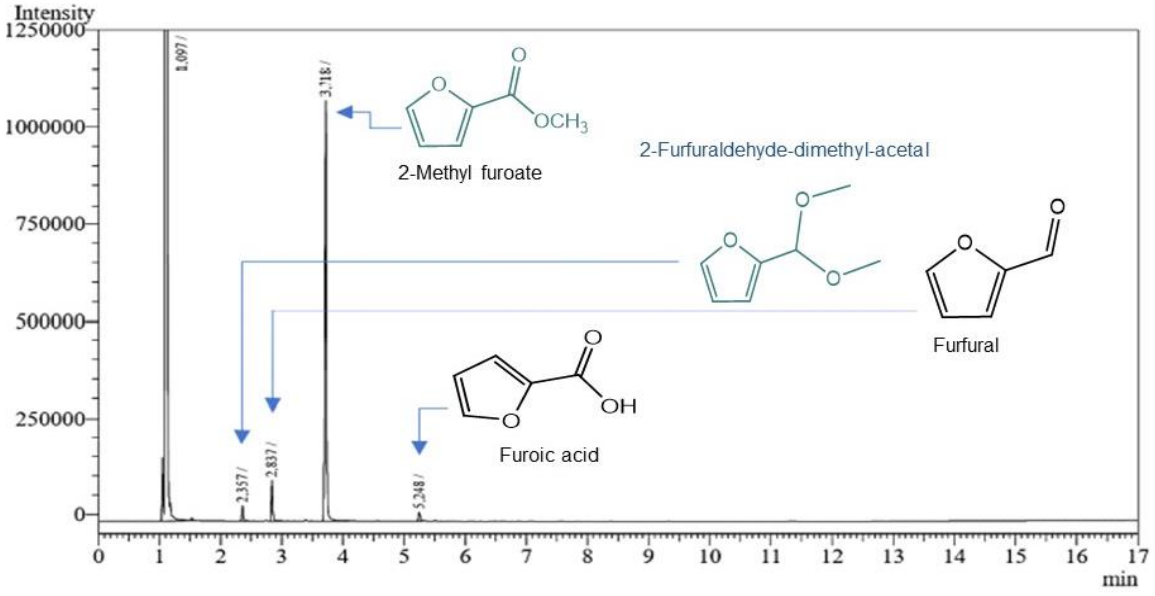

Attachment 3 - Chromatogram of furfural acetalization with methanol.

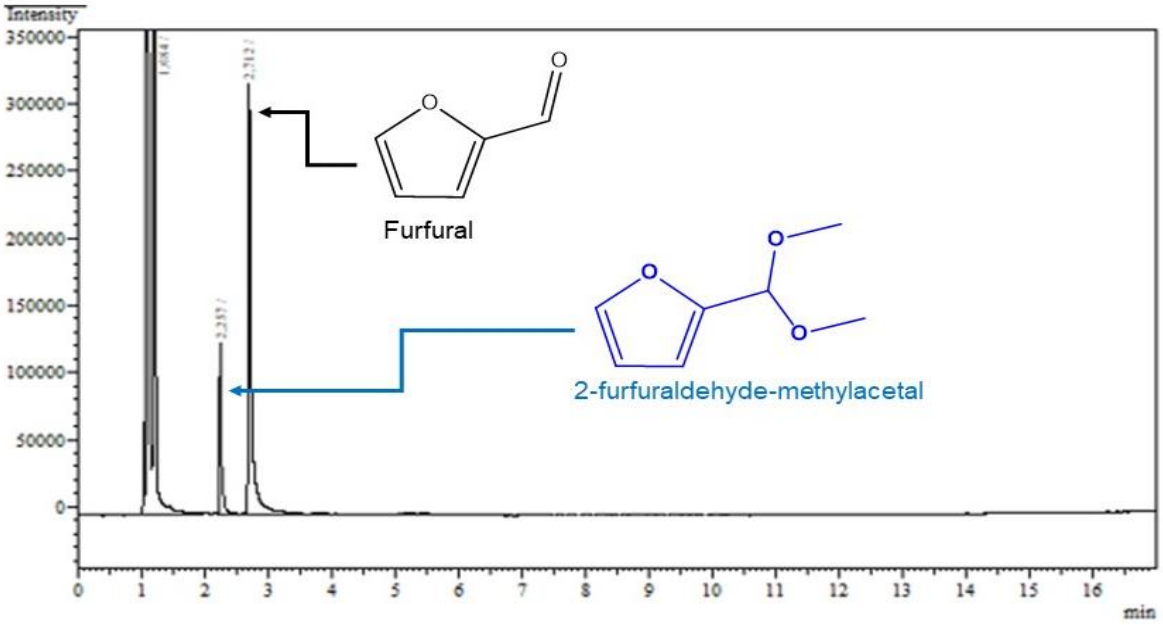

Attachment 3.1 – Mass spectrum of furfural.

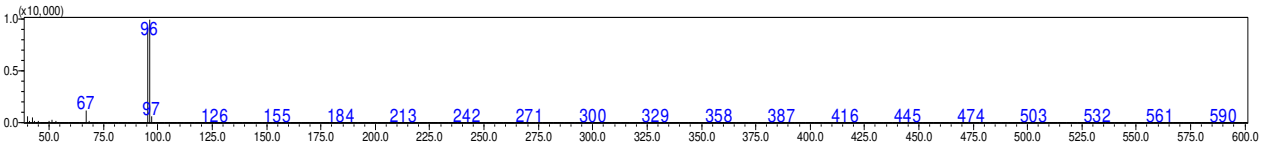

Attachment 3.2 – Mass spectrum of 2-furfuraldehyde-methylacetal

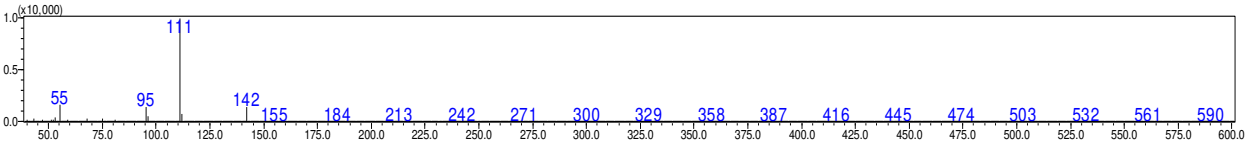

Attachment 4 - Chromatogram of benzaldehyde acetalization with methanol.

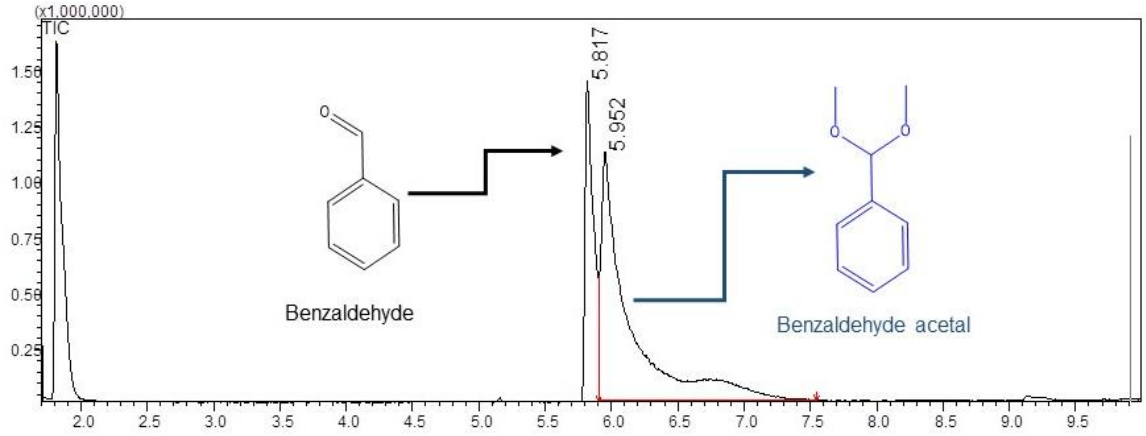

Attachment 4.1 – Mass spectrum of benzaldehyde.

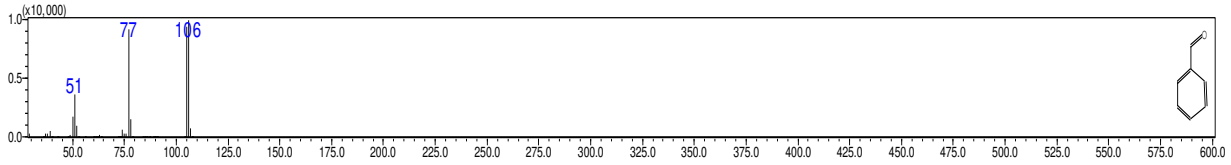

Attachment 4.2 – Mass spectrum of benzaldehyde acetal.

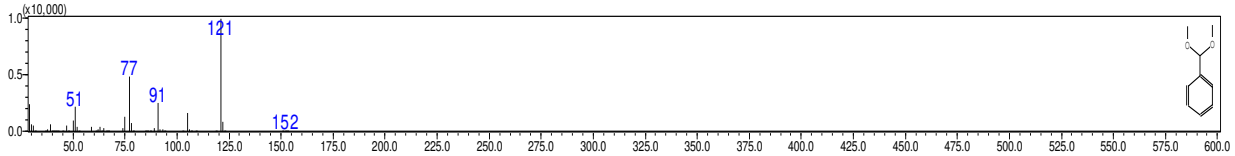

Attachment 5 - Submitted article N° 1

FURFURAL CONDENSATION WITH ALKYL ALCOHOLS OVER NIOBIUM CATALYSTS AT ROOM TEMPERATURE

--Manuscript Draft--

Manuscript Number:		
Full Title:	FURFURAL CONDENSATION WITH ALKYL ALCOHOLS OVER NIOBIUM CATALYSTS AT ROOM TEMPERATURE	
Article Type:	Original Paper	
Section/Category:	Catalysis and Reaction Engineering	
Funding Information:	Coordenação de Aperfeiçoamento de Pessoal de Nível Superior (001)	Dr Marcio Jose da Silva
Abstract:	Several platform molecules like furfural are easily obtained from lignocellulose hydrolysis and it has highlighted because can be used as raw material in biorefinery processes to produce biofuels and fine chemicals. We have developed a process to synthesize furfural acetals at room temperature, using simple commercial Niobium catalysts. Niobium pentoxide and phosphate were evaluated before and after being treated with hydrogen peroxide. All the catalysts were characterized by physical adsorption/ desorption of nitrogen, infrared and Raman spectroscopies, scanning electron microscopy, powder X-ray diffraction analyses, NH3-Temperature Programmed Desorption and pyridine-FTIR. The effects of the main reaction parameters were assessed. Untreated commercial Niobium phosphate was the most active catalyst, converting almost all the furfural to acetal in methanol. The use of a highly active commercially affordable solid catalyst was the key aspect of this process.	
Corresponding Author:	Marcio Jose da Silva Universidade Federal de Viçosa Vicosa, **Please Select** BRAZIL	
Corresponding Author Secondary Information:		
Corresponding Author's Institution:	Universidade Federal de Viçosa	
Corresponding Author's Secondary Institution:		
First Author:	Marcio Jose da Silva	
First Author Secondary Information:		
Order of Authors:	Marcio Jose da Silva	
	Carlos Giovani Oliveira Bruziquesi	
	Daniel Carreira Batalha, Ds	
	John Alexander Vergara Torres, Master	
	José Balena G. Filho, Master	
	Daniele C. Ferreira, Master	
	Luiz Carlos A. Oliveira, Ds	
Order of Authors Secondary Information:		

Attachment 6 - Submitted article N° 2

Catalysis Letters

Springer

Impacts of Vanadium doping on the activity of phosphomolybdic acid catalysts in oxidation reactions of geraniol with hydrogen peroxide

Journal:	*Catalysis Letters*
Manuscript ID	CATLET-2021-1201
Manuscript Type:	Original Manuscript
Date Submitted by the Author:	01-Dec-2021
Complete List of Authors:	da Silva, Marcio; Federal University of Vicosa, Chemistry Torres, John; Federal University of Vicosa, Chemistry Vilanculo, Castelo; Teacher Training University, Chemistry;
Keywords:	Homogeneous catalysis < Catalysis, Epoxidation < Mainly Organic Chemicals and Reactions, Heteropoly acids < Preparation and Materials, terpene alcohols